Technical Medicine Master of Science Thesis
January 19, 2018

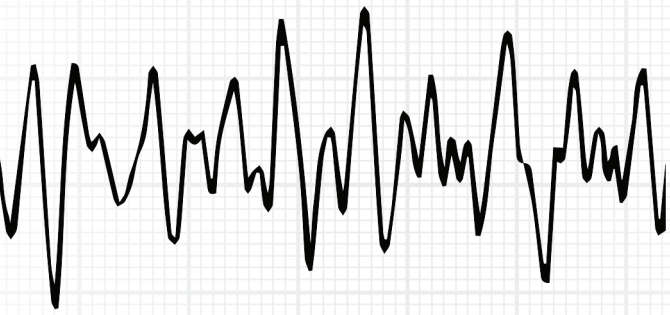

The effect of cardiopulmonary resuscitation on ventricular fibrillation waveform measures: a new tool to optimize infield identification of an acute coronary occlusion during cardiac arrest

Author:
Jeanne van der Waal, BSc.

Supervisors:
Prof. dr. H.J. Zwart
Dr. M.A. Brouwer
Dr. ir. C. Meinsma
J. Nas, MSc.
J. Thannhauser, MSc.
Drs. P.A. van Katwijk

General information

Thesis title	The effect of cardiopulmonary resuscitation on ventricular fibrillation waveform measures: a new tool to optimize in-field identification of an acute coronary occlusion during cardiac arrest
Author	Jeanne van der Waal, BSc.
Email	jeannevanderwaal@outlook.com

Organization

Address	Radboud University Medical Centre Geert Grooteplein-zuid 10 6525 GA Nijmegen
Department	Department of Cardiology

Institution

Address	University of Twente Drienerlolaan 5 Postbus 217 7500 AE Enschede
Faculty	Faculty of Science and Technology
Program	Technical Medicine
Master	Medical Sensing and Stimulation

Committee

Chairman	Prof. dr. H.J. Zwart
Medical supervisor	Dr. M.A. Brouwer
Technical supervisor	Dr. ir. G. Meinsma
Process supervisor	Drs. P.A. van Katwijk
External member	M.C. Hermans, MSc.
Additional member	J. Nas, MSc.

January 19, 2018

Radboudumc

UNIVERSITY OF TWENTE.

Summary

The effect of cardiopulmonary resuscitation on ventricular fibrillation waveform measures: a new tool to optimize in-field identification of an acute coronary occlusion during cardiac arrest

by Jeanne van der Waal

Since the ventricular fibrillation (VF) waveform has been shown to decrease over time, it has been regarded as marker of arrest duration and has been investigated to predict defibrillation success. However, exact prediction of arrest duration is complicated by other factors also influencing the VF waveform. The VF waveform has been shown to increase with uninterrupted chest compressions, and decrease with pauses in chest compressions. Animal and human studies have also shown that myocardial infarction (MI) affects VF, and animal studies suggest that the change in VF waveform in response to cardiopulmonary resuscitation (CPR) may be altered in the presence of an acute coronary occlusion (ACO). This study investigated the change in VF waveform characteristics in relation to CPR quality, whether this is altered in the presence of an ACO, and whether this information can help in identifying these patients during out-of-hospital cardiac arrest (OHCA).

For the change in VF characteristics in response to CPR, we compared this change between patients with and without adequate CPR (defined as chest compression fraction (CCF) $\geq$ or $<$ 0.6) between the first and second defibrillation. In a sub analysis we investigated this change in characteristics in a sub population of patients with and without ACO. In patients with CCF$\geq$0.6 (n=90), an increase in all VF amplitude characteristics was detected, while this did not occur in patients with CCF<0.6 (n=48). Furthermore, this numeric increase was significantly higher in patients with CCF$\geq$0.6 compared to patients with CCF<0.6. The sub analysis showed a difference in change in VF amplitude characteristics between CCF$\geq$0.6 and CCF<0.6 in patients without ACO (n=22), whereas this difference was not found in patients with ACO (n=38).

Next the VF waveform parameters were investigated to determine their ability to predict the presence of an ACO. In patients with an underlying ACO (n=62), the VF amplitude characteristics were significantly lower when compared to patients without an underlying ACO (n=40), showing a limited discriminative ability with an AUC of 0.66. Combining the VF waveform parameter with the change in that parameter in response to CPR using binary logistic regression led to an improved discriminative ability, with an AUC of 0.75.

These findings suggest that the VF waveform parameters and their change in response to CPR can be used to provide additional information to ensure correct and early triage of patients to the cardiac catheterization laboratory. Further studies are needed to determine if the combination of waveform parameters and their change in response to CPR can predict the presence of an ACO in a prospective fashion, and whether this results in improved survival after OHCA.

Acknowledgements

In the period of September to November 2016 I did the last of my 10-week internships in the second year of the Master Technical Medicine at the Cardiology department of the Radboudumc. This confirmed my interest in cardiology in general, and more specifically for the electrophysiological aspects. Since there was a very good work atmosphere at the research department, I was glad that I could stay there to start my graduation internship in February 2017. Here, I would like to take the opportunity to thank the people that made this possible.

I would like to thank Joris Nas for guiding me throughout the year, for helping me with research questions, the explanation of some (for me) complicated statistical concepts and the critical revisions of the manuscript. For critical revisions of the manuscript I would also like to thank Jos Thannhauser, who provided a fresh set of eyes to further improve the research and the writing. I would like to thank Marc Brouwer for the opportunity to do my graduation internship at the cardiology department. Even though our contact during the project was limited, I was amazed by your ability to read people.

I would like to thank Gjerrit Meinsma for investing time and helping me construct the Detrended Fluctuation Analysis chapter. I would like to thank Paul van Katwijk for being my mentor for the past two years and asking difficult questions that made me think about who I am and who I want to be. Furthermore I would like to thank Hans Zwart for being the chairman in the committee, and Mathilde Hermans for also taking place in the committee.

Thanks to all my colleagues for the nice collaboration and making me feel welcome, and a special thanks to the PhD candidates for the frequent educational moments. Thanks to all fellow students in the research department during this internship, for always filling my mug of tea without complaining. Also thanks for some great times, I hope the bucket list keeps growing and also keeps getting checked off.

Thanks to my fellow 'kerels', for a wonderful time during the years of studying (and hopefully beyond of course). Very special thanks go to Rogier and my family, thank you for your support and for always believing in me.

Contents

List of Abbreviations

ACO	Acute Coronary Occlusion
AED	Automated External Defibrillator
AMI	Acute Myocardial Infarction
AMSA	Amplitude Spectrum Area
AP	Action potential
AV	Atrioventricular
AUC	Area under the curve
BLS	Basic Life Support
CABG	Coronary artery bypass graft
CAG	Coronary angiography
CCF	Chest Compression Fraction
COP	Cardioversion Outcome Predictor
CPR	Cardiopulmonary resuscitation
CWT	Continuous Wavelet Transform
DF	Dominant Frequency
DFA	Detrended Fluctuation Analysis
ECC	Extracorporeal Circulation
ECG	Electrocardiogram
ED	Emergency Department
EMS	Emergency Medical Services
FFT	Fast Fourier Transform
FR	Frequency Ratio
ICD	Implantable Cardioverter Defibrillator
LAD	Left anterior descending artery
LBBB	Left bundle branch block
LCA	Left coronary artery
MAA	Mean Absolute Amplitude
MdF	Median Frequency
MdS	Median Slope

MI	Myocardial Infarction
OHCA	Out-of-hospital cardiac arrest
PCI	Percutaneous Coronary Intervention
PDA	Posterior descending artery
PEA	Pulseless electrical activity
PSA	Power Spectrum Area
PSD	Power Spectral Density
PVC	Premature Ventricular Complex
PVT	Pulseless Ventricular Tachycardia
RCA	Right coronary artery
RCx	Ramus circumflex artery
RMS	Root-mean-square
ROC	Receiver Operating Characteristic
ROOR	Return of Organized Rhythm
ROSC	Return of Spontaneous Circulation
SA	Sinoatrial
SDW	Scale Distribution Width
STEMI	ST-elevation myocardial infarction
TTI	Transthoracic Impedance
VF	Ventricular Fibrillation
VS	Variance of Slope
VT	Ventricular Tachycardia
WFP	Waveform parameter

1 Introduction

Ventricular fibrillation (VF) is the first observed cardiac rhythm in about 20-50% of out-of-hospital cardiac arrests (OHCAs) [1, 2]. Survival after OHCA is poor, although VF as first observed rhythm has a better outcome in terms of survival to hospital discharge (15-40%) when compared to non-shockable rhythms (2-8%) [2–5]. Still, VF will gradually deteriorate into asystole with passage of time and this will consequently decrease chance of survival [6, 7]. Defibrillation is considered the only therapy to establish return of spontaneous circulation (ROSC) in patients with ventricular fibrillation [8]. Therefore, the guidelines for cardiopulmonary resuscitation (CPR) recommend immediate defibrillation as soon as a defibrillator is made available [9]. However, if the myocardial metabolic state is compromised, success rates of defibrillation are poorer [8, 10]. Additionally, defibrillation can also have the adverse effect of producing asystole [11].

In absence of an automated external defibrillator (AED) or in between defibrillations, chest compressions and ventilations can be administered to keep oxygenated blood flowing to the brain and other vital organs. Studies have shown that CPR does not only slow the deterioration of myocardial cells, but also increases the chances of survival [9, 12, 13]. Therefore, it has been suggested that for VF of longer duration, withholding defibrillation in order to apply CPR might increase myocardial readiness for defibrillation and increase chances of successful defibrillation [14, 15]. This was shown in two studies where patients with ambulance response time of more than four to five minutes showed increased rates of ROSC and survival if 1.5 or 3 minutes of CPR was administered by ambulance personnel before defibrillation [16, 17]. Unfortunately, the onset time of VF is (especially in the out-of-hospital setting) rarely known, making it difficult to determine the priority of CPR intervention based on the duration of the untreated cardiac arrest. In this light, the VF waveform on the electrocardiogram (ECG) has been investigated for its ability to reflect myocardial metabolic state.

However, the application of VF waveform to guide initial therapy may be complicated by the largely unknown effect of factors influencing the VF waveform. The VF waveform deteriorates after an episode without CPR [18, 19], accompanied by a decrease in survival chances. Since VF characteristics are associated with shock success and long-term outcome [20–23], and CPR improves the chance of ROSC [13, 16, 17], VF characteristics are also likely to be affected by CPR. In addition, VF characteristics have shown to be influenced by the presence of myocardial ischemia. Animal studies have indicated that VF characteristics were lower in the presence of an induced myocardial infarction (MI) [24–26]. Similarly, in human studies lower VF characteristics were found in patients with acute MI as underlying aetiology of VF [27], as well as in patients with a previous MI where VF was induced during ICD-testing [28, 29]. One animal study also shows that the reaction of the VF waveform on CPR may be altered in the presence of acute coronary occlusion [30].

In light of the above, VF waveform may give an indication of the effectiveness of CPR, and thus might also provide an indication for myocardial readiness for defibrillation. In addition, the presence of ischemia may also alter the VF waveform and its reaction on CPR, yet the etiology of the OHCA is often unknown. In this context, we investigated the response of VF waveform characteristics to CPR, and whether this is altered in the presence of myocardial ischemia. In addition, we investigated whether (a combination of) VF waveform characteristics are able to discriminate between patients with and without coronary occlusion as underlying cause of OHCA.

2 Background

2.1 Anatomy and physiology of the heart

The heart is a pump, allowing blood to flow through the body. The right side of the heart contributes to the pulmonary circulation, and the left side of the heart contributes to the systemic circulation. The flow through the heart is schematically illustrated in Figure 2.1. In the pulmonary circulation, deoxygenated blood enters the right atrium and continues to flow to the right ventricle. The right ventricle pumps the blood towards the lungs via the pulmonary arteries. In the lungs exchange of oxygen and carbon dioxide occurs, after which oxygen enriched blood is transported from the lungs to the left atrium via the pulmonary veins. In the systemic circulation, the oxygenated blood travels from the left atrium to the left ventricle. Through forceful contraction of the left ventricle, the blood is pumped into the aorta, via which the blood is distributed towards the organs and tissues. After supplying the tissue with oxygen the blood is returned to the right atrium via the superior and inferior vena cava [31, 32].

A cardiac cycle, defined as all cardiac events from the beginning of one heartbeat to the beginning of the next, consists of two phases: the diastole and the systole. In the diastole the ventricles are relaxed, allowing blood to flow from the atria to the ventricles. By the end

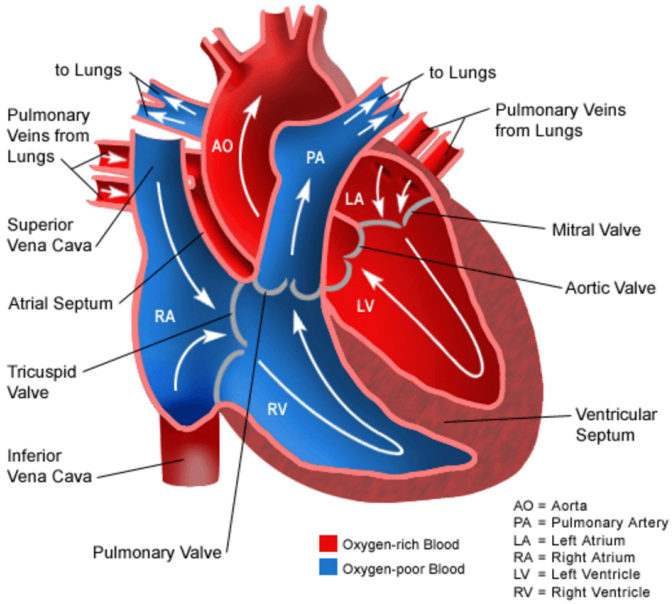

FIGURE 2.1: Blood flow through the heart. The right atrium receives blood via the superior vena cava and inferior vena cava and the right ventricle pumps blood via the pulmonary artery to the lungs. The left atrium receives blood from the lungs and the left ventricle pumps blood into the aorta, for distribution to the organs. Backflow of blood from the ventricles to the atria is prevented by the atrioventricular valves (i.e. the tricuspid and mitral valve), and backflow from the pulmonary artery and aorta is prevented by the semilunar valves (i.e. the pulmonary and aortic valve). Reproduced from [33].

of the diastole, the atria contract to pump the remaining volume of blood to the ventricles. During relaxation of the ventricles, backflow of blood from the pulmonary artery and aorta is prevented by the pulmonary valve and aortic valve respectively (see Figure 2.1). After the diastole, the systole starts by isovolumetric contraction, i.e. contraction without a change in volume, of both ventricles simultaneously. When the pressure in the ventricle exceeds the pressure in the associated outflow tract, the aortic and pulmonary valve are forced to open and bood starts flowing out. During contraction of the ventricles, backflow of blood from the ventricles to the atria is prevented by the atrioventricular valves, with the tricuspid valve between the right atrium and ventricle and the mitral valve between the left atrium and ventricle (see Figure 2.1). After the blood is ejected in the pulmonary artery and aorta, the diastole starts with isovolumetric relaxation until the pressure in the ventricles drops below the atrial pressure, after which the ventricles are filled with blood again and the cycle repeats [31, 32].

To be able to provide the oxygen-rich blood to the body tissues, the heart itself also needs a steady oxygen supply. This is provided through the coronary arteries, originating from the root of the aorta (Figure 2.2). The left coronary artery (LCA) bifurcates into the left anterior descending artery (LAD) and the ramus circumflex artery (RCx). The LAD descends into the anterior inter-ventricular groove, where its branches mainly supply the anterior wall of the left ventricle, the inter-ventricular septum and parts of the conduction system. The RCx travels in the left atrioventricular groove, where it supplies most of the left atrium and the posterolateral wall of the left ventricle. The right coronary artery (RCA) runs through the right atrioventricular groove, and distributes blood to the right atrium, the right ventricle, and parts of the conduction system of the heart. The inferior wall of the heart is provided with blood by the posterior descending artery (PDA), which originates either from the RCA (in 85% of people) or from the RCx (in 15% of people) [32, 34].

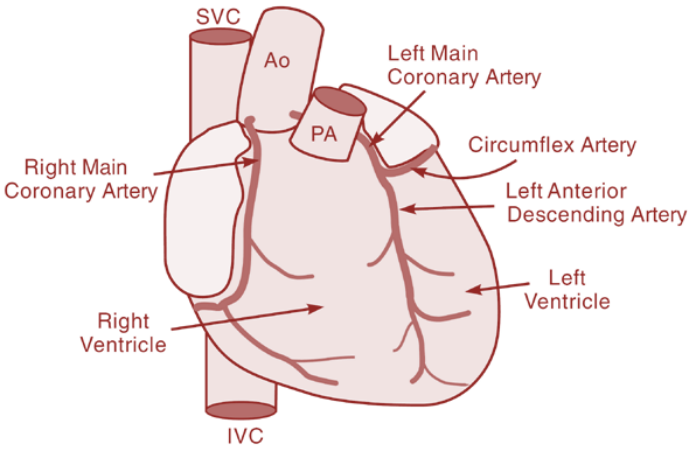

FIGURE 2.2: Anterior view of the heart showing the main coronary arteries. The left main coronary artery bifurcates into the left anterior descending artery, descending into the anterior interventricular groove, and the ramus circumflex artery, running in the left atrioventricular groove. The right coronary artery runs through the right atrioventricular groove towards the posterior region of the heart. SVC = Superior vena cava, Ao = Aorta, PA = Pulmonary artery, IVC = Inferior vena cava. Adapted from [32].

2.2 Electrical activity in the heart

The contraction of the myocardium is controlled by the cardiac conduction system. It consists of cardiac muscle cells and conducting fibers that are specialized for initiating impulses and conducting them rapidly through the heart. There are two types of cells found in the

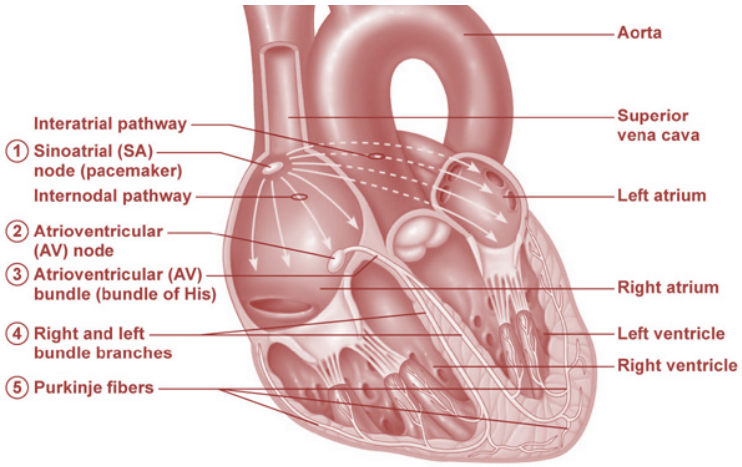

FIGURE 2.3: Electrical conduction system of the heart. The impulse originates from the sinoatrial node, travels through the atria toward the atrioventricular node. After a short delay it is conducted trough the bundle of His to the Purkinje fibers, resulting in depolarization of the ventricles. Adapted from [39].

heart: pacemaker cells that have the ability to generate electrical impulses and cardiomyocytes which can only conduct an impulse. Normally, the electrical impulse originates from a group of pacemaker cells that is located in the high right atrium near the superior vena cava, called the sinoatrial (SA) node (Figure 2.3) [35]. The impulse propagates through neighbouring cells in the atria and stimulates the myocardium of the atria for contraction. When it reaches the atrioventricular (AV) groove, a fibrous structure which is electrically inert disables conduction directly from the atria to the ventricles. Therefore, conduction from the atria to the ventricles is only possible through the AV node, located close to the tricuspid valve in the interatrial septum. The AV node has specific electrophysiologic properties, which slows the conduction velocity. This results in a delay in conduction between the atria and ventricles, allowing sufficient emptying of the atria. When leaving the AV node, the impulse enters the bundle of His, which penetrates the fibrous tissue to allow conduction toward the ventricles. The His bundle branches into the right and left bundle branches, and the rapidly conducting Purkinje fibers reaching to the more distal and lateral parts of the ventricular myocardium ensure an almost simultaneous depolarization of the ventricles [32, 35–38].

The generation of the electrical impulse can be explained by the electrical potential across the cell membrane of the cardiomyocytes. The inside of the cell has a negative electrical charge compared to the outside of the cell, resulting from a different concentration of ions present. The resting transmembrane potential of a cardiac cell is around -90 mV. Changes in cell membrane permeability (i.e. opening of specific ion gates) allows ion to travel across the cell membrane, which gives rise to the action potential (AP). The cardiac AP of a myocyte can be divided into several phases involving the sodium, potassium and calcium ion currents (see Figure 2.4). The first phase in generating the action potential is the opening of the rapid sodium channels (phase 0). This causes a rush of sodium ions into the cell, leading to a positively directed change in the transmembrane potential. This is called the depolarization of the cell. The voltage spike causes the sodium channels in the neighbouring cells to open, leading to a propagation of the action potential. Once a cell is depolarized, it cannot be depolarized again until the ionic fluxes are reversed. This is called repolarization. The repolarization starts at phase 1 with an outward current of potassium and the inactivation of the sodium channels. In phase 2 the outward current of potassium still occurs, but a plateau arises due to the slow inflow of calcium ions. The end of phase 2 is initiated by inactivation of the calcium channels. This results to the persistent outflow of potassium exceeding the calcium inflow, bringing the transmembrane potential back towards the resting potential of -90 mV. This happens in phase 3. Phase 4 is the resting phase, where the sodium and calcium channels are closed and the potential is maintained at -90 mV due to a constant outward leak of potassium [32, 35, 36].

2.2.1 The electrocardiogram

The cardiac action potential represents the electrical activity of a single cardiac cell, which cannot be measured from the outside. To find information about the electrical properties of the heart, a surface electrocardiogram (ECG) can be measured. Tissues surrounding the heart are able to conduct electrical currents, allowing these currents to be detected at the body surface by an array of electrodes. This ECG represents the sum of electrical activity in the heart, which is measured as voltage changes from a baseline voltage. A normal rhythm consists of a P wave, a QRS complex and a T wave, as seen in Figure 2.5. The P wave represents the depolarization wave spreading through the atria. The conduction delay in the AV node as discussed earlier leads to a brief isoelectric (i.e. zero voltage) period. The fast ventricular depolarization results in the QRS complex, only lasting about 0.06 to 0.1 seconds. The isoelectric ST segment is the period at which the entire ventricle is depolarized. It roughly corresponds to the plateau phase of the ventricular action potential as seen in Figure 2.4. The T wave represents repolarization of the ventricles (phase 3 of the action potential) [32, 35].

The height and direction of the different deflections of the ECG is dependent on the recording direction. The ECG is measured as a potential difference between a positive and a negative electrode. A wave of depolarization travelling toward a positive electrode will result in a positive deflection in the ECG trace. A wave of depolarization or repolarization oriented perpendicular to an electrode axis produces no net deflection (i.e. equally positive and negative voltages). Therefore, the ECG is conventionally measured in 12 directions, i.e. leads, using 10 electrodes. Four electrodes are placed on each arm and leg and six electrodes are placed at defined locations on the chest. The electrodes on the left arm, right arm and left leg together compose the triangle of Einthoven, and form the three bipolar limb leads I, II and III (see Figure 2.6). With the same three electrodes, augmented limb leads (aVR, aVL, aVF) are measured by using a single positive electrode referenced against a combination of the other two electrodes. These limb leads record the ECG in the frontal plane. The same three electrodes are used as a combined negative electrode to the positive precordial electrodes. The resulting precordial leads (V1-V6) record electrical activity in the horizontal plane, perpendicular to the frontal plane in which the limb leads record. A visualization of the different recording directions is given on the right side of Figure 2.6 [32, 35–37].

An ECG gives diagnostic information about a possible underlying condition of the heart. It can be used to determine the heart rate and rhythm, and therefore also detects if the rhythm does not follow the usual conduction pathway as described above. Furthermore, the shape

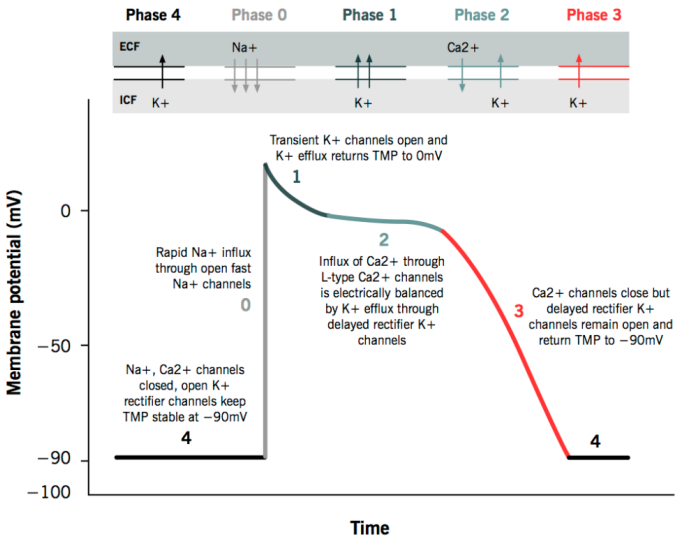

FIGURE 2.4: The five phases of an action potential in a (non-pacemaker) myocardial cell. Reproduced from [40].

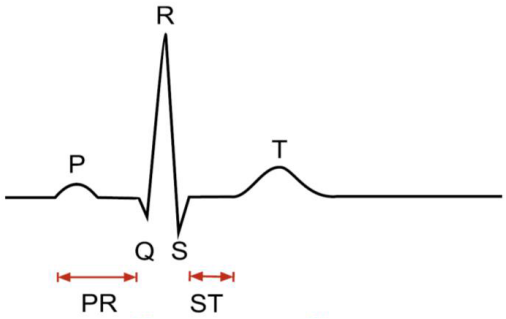

FIGURE 2.5: Electrocardiogram of a normal cardiac cycle. P-wave: atrial depolarization, QRS-complex: ventricular depolarization, T-wave: ventricular repolarization.The PR interval is the time from the onset of atrial depolarization to the time from the onset of ventricular depolarization. The ST segment represents the isoelectric period when the entire ventricle is depolarized. Reproduced from [32].

of the P wave can give information about the size of the atria, whereas the height of the R wave (in the precordial leads) can give an indication for left ventricular wall thickening. Events of ischemia of the heart can be detected on the ECG by looking for elevated or depressed ST segments, inverted T waves or deep Q waves [35, 37].

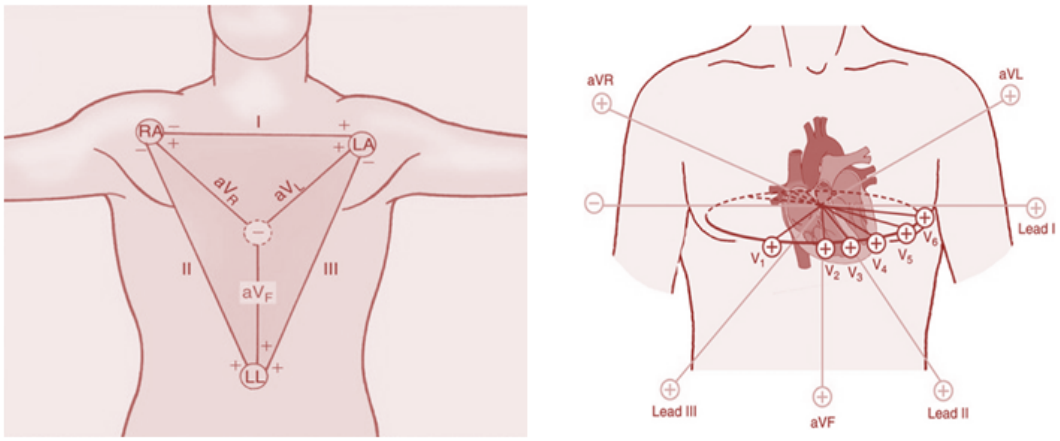

FIGURE 2.6: Left: Triangle of Einthoven. Right: Recording directions of the 12 leads of the electrocardiogram.

2.3 Myocardial infarction

Myocardial infarction (MI) is a major cause of death and disability worldwide. It is defined as a clinical event caused by myocardial ischemia in which there is evidence of myocardial injury or necrosis [41]. Cell death is reached when ischemia exceeds a critical threshold, as a result of decreased delivery of oxygen via the coronary arteries, increased myocardial metabolic demand or a combination of both.

Decreased delivery of oxygen is most commonly caused by severe atherosclerosis, a condition in which plaque (made up of fat, cholesterol, calcium and other substances) builds up in the inner layer of the arteries (intima). When a plaque occupies more than 75% of the coronary lumen, increased metabolic demand can easily cause myocardial ischemia [42]. Also, the intima separates the blood in the arteries from potentially thrombogenic components of the medial arterial layer. The presence of plaque stretches this layer, increasing the chance of a rupture. This disruption allows blood to come in contract with the thrombogenic components, leading to intraluminal thrombus formation. This thrombus superimposed over the

disrupted plaque can cause an (almost) complete occlusion of the coronary artery [43–45]. However, occlusion of a coronary artery can also occur due to a blood clot without underlying plaque (although less frequently). Conditions associated with increased myocardial metabolic demand include physical activity, severe hypertension, hypertrophic cardiomyopathy and severe aortic valve stenosis [31, 32].

Acute MI can have different manifestations in individual patients. The most characteristic symptoms are chest pain described as a pressure sensation or squeezing of the thorax, radiation of chest pain into jaw, shoulder, arm and/or back, shortness of breath, nausea, syncope or near syncope and (excessive) sweating [41, 42].

MIs can be subcategorized on the basis of diagnostic clinical information, meaning symptoms, myocardial biomarkers, ECG findings and imaging techniques. Two types of acute MIs are commonly distinguished by a classification scheme based on ECG findings: (1) MI with ST-segment elevation in at least two contiguous leads (STEMI) and (2) MI without ST-segment elevation (non-STEMI) [41]. In case of a STEMI, the ECG leads with ST elevation give an indication of the localization of the MI [35].

Treatment of MI consist of three main options: (1) With percutaneous coronary intervention (PCI) a catheter is used to place a stent over the obstructed lumen to reinstate blood flow, (2) coronary artery bypass grafting (CABG) provides an alternative route for the blood via a bypass vein or artery, thereby circumventing the obstructed coronary artery and (3) conservative treatment with pharmacological therapy. In STEMI, one of the first two treatments is essential to restore coronary blood flow. Non-STEMI on the other hand can sometimes initially also be treated conservatively, while planning a PCI or CABG in the non-acute setting [42, 46].

Ischemia is a common cause of premature ventricular contractions (PVC's), which in turn can trigger ventricular arrhythmias. This mechanism and different kinds of arrhythmias are discussed in the next section.

2.4 Ventricular arrhythmias

Abnormal rhythms (arrhythmias) can be caused by abnormal formation of an action potential. They are generally divided into two categories based on the origin of the action potential: Supraventricular and ventricular arrhythmia. Supraventricular arrhythmias initiate in the area above the ventricles (i.e. atria or AV-node), whereas ventricular arrhythmias initiate in the ventricles. In ventricular arrhythmias, depolarization does not follow the normal conduction pathways, which in combination with an increased heartbeat (tachycardia) results in inefficient filling and contraction of the heart. This in turn causes a decrease in cardiac output, therefore insufficient oxygen supply to the body tissues, eventually leading to death. Two important/well-known ventricular arrhythmias are ventricular tachycardia (VT) and ventricular fibrillation (VF) (Figure 2.7).

Ventricular tachycardia

VT is defined as a regular tachycardia of >120 bpm solely originating in ventricular tissue, therefore exhibiting dissociation between atrial and ventricular electrical activity [47]. There are several mechanisms of initiation for a VT. Sometimes a cell (or group of cells) in the ventricle can act as a pacemaker cell and fire at the 'wrong' time. The effect of such an impulse depends on the surrounding tissue properties. When the surrounding tissue is homogeneous, the depolarization wave radiates out, which causes a premature ventricular contraction (PVC). This is relatively benign, though can be triggered by more structurally abnormal or ischemic hearts. In heterogeneous tissue, neighbouring cells have different properties, i.e. conduction velocity and refractory time. The depolarization wave will not be distributed evenly over the surrounding tissue, but can start to curve. It can even curve so much that it circles back to the start and initiate another depolarization. This can lead to even more depolarization circles and result in a functional re-entry [48]. Another mechanism of re-entry

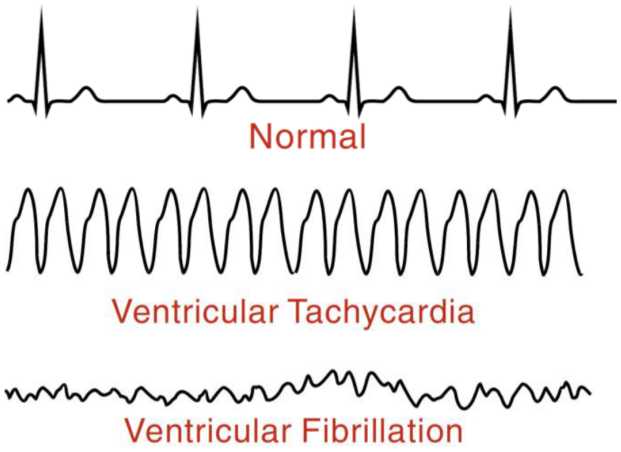

FIGURE 2.7: ECG examples of a normal sinus rhythm and the abnormal rhythms ventricular tachycardia and ventricular fibrillation. Reproduced from [32]

is an anatomical re-entry. This is the case when depolarization waves circle around (non-conducting) scar tissue and initiates re-entry. These mechanism are illustrated in Figure 2.8.

As a result of the fast ventricular rhythm, the ventricles are continuously in motion and therefore do not pump efficiently. This can cause symptoms such as palpitations, dyspnea and dizziness, but could lead to sudden cardiac death [47]. Therefore it requires immediate attention to convert to sinus rhythm. A VT can eventually evolve into VF [48].

Ventricular fibrillation

VF has been defined as turbulent cardiac electrical activity with varying frequency and amplitude, indicating a large amount of irregularity in the depolarization waves causing the ventricular excitation [50]. During VF, there is no efficient contraction of the ventricles, resulting in an inadequate cardiac output [32].

Despite a lot of investigation, the exact mechanism of VF remains unknown. The two principal proposed mechanisms are mother rotors and multiple wavelets. The mother rotors theory hypothesizes that VF is maintained by a single, stable re-entrant circuit, i.e. the mother rotor, which gives rise to variable daughter wavelets that spread through the remainder of the ventricular myocardium [50–52]. The multiple wavelet theory also indicates initiation of VF by a re-entrant circuit, but it hypothesizes that this circuit breaks into other wavelet circuits. These 'wandering wavelets' follow constantly changing pathways and are easily terminated. However, these wavelets create new re-entry circuits, allowing the fibrillation

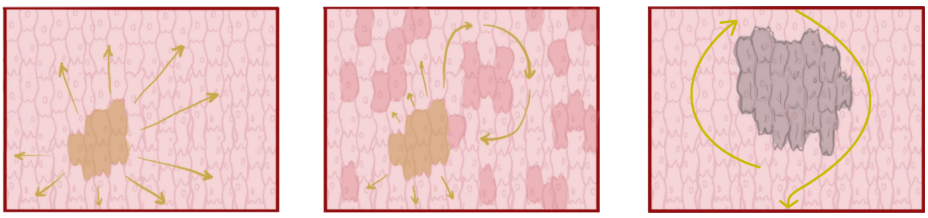

(a) PVC **(b)** Functional re-entry **(c)** Anatomical re-entry

FIGURE 2.8: Examples of initiation mechanisms of ventricular tachycardia: (a) Premature ventricular contraction (PVC); (b) functional re-entry due to heterogeneity of the myocardial cells; (c) anatomical re-entry due to scar tissue. Reproduced from [49].

to be sustained [50, 51, 53]. Both theories remain under investigation, and studies have provided evidence for (a combination of) both mechanisms [54–56].

Since VF results in a cardiac output decreasing to zero, it requires immediate attention to convert to a normal (perfusing) rhythm. VF is the most commonly identified rhythm in out-of-hospital cardiac arrest (OHCA) [3], and can be caused by several diseases. Here, we will focus on underlying cardiovascular diseases. The most common cause of VF, and therefore also the most common cardiovascular cause, is coronary artery disease [57]. This can be due to either acute MI (75%) or scarring from a previous MI (25%) [58]. (Acute) MI causes increased extracellular potassium concentration, and this causes a disruption of the normal repolarization. This causes heterogeneity in conductive properties and therefore could give rise to an arrhythmia [59]. Other (less common) cardiovascular causes are cardiomyopathy, ion-channel abnormalities or congenital heart disease.

2.5 Out-of-hospital cardiac arrest therapy

A cardiac arrest is defined as sudden cessation of cardiac mechanical activity, leading to the absence of signs of circulation (pulse) [60]. Several initial cardiac rhythms can occur during this cardiac arrest, which can be divided in shockable and non-shockable rhythms. Shockable rhythms include pulseless ventricular tachycardia (PVT) and ventricular fibrillation (VF), whereas non-shockable rhythms are pulseless electrical activity (PEA) and asystole. Early recognition and immediate cardiopulmonary resuscitation (CPR) are important determinants of survival. Therefore, the first steps of the American Heart Association guidelines for OHCAs are recognition of the arrest, calling for help and initiating chest compressions and ventilations. In the shockable rhythms, defibrillation of the heart can be achieved with application of an electrical shock. The goal of an electrical defibrillation is to depolarize all myocardial cells at the same time. This could result in the extinction of the propagating wavefronts that preserve VF, so that a natural pacemaker cell (e.g. SA or AV node) can take over again [61]. This defibrillation can be performed by lay rescuers when an automated external defibrillator (AED) is available. When a team of professionally trained emergency medical service providers take over responsibility, intravenous access can be acquired to administer drugs, and the patient can be transported to an emergency department and/or cardiac catheterization lab. OHCA with VF as initially observed rhythm has a survival rate of 19-22% [2, 3], but early initiation of CPR combined with defibrillation can double or quadruple chances of survival [62].

2.6 Ventricular fibrillation waveform analysis

Although the importance of early electric defibrillation for treatment of VF has been well established, the efficacy of defibrillation for prolonged VF is considered questionable as the probability of defibrillation success declines with increasing arrest duration [6, 63]. In the last decade researchers hypothesized that CPR before defibrillation would improve defibrillation success and outcome for prolonged OHCA patients with a shockable rhythm. This theory is explained by a model of the pathophysiology of VF by Weisfeldt and Becker [14]. They hypothesize that VF consists of three phases, which require time-specific interventions. The first phase is the *electrical* phase (0-4 min), in which the myocardial cells should be defibrillated as soon as possible. The second phase is the *circulatory* phase (4-10 min), in which the outcome may improve by performing a period of CPR before defibrillation. The third phase is the *metabolic* phase, in which irreversible damage of the myocardial cells occurs due to depletion of energy substrate [14]. This model is supported by findings of Cobb et al. and Wik et al., who demonstrated that performing CPR before defibrillation when onset of VF is more than 4 or 5 minutes respectively improves the likelihood of return of spontaneous circulation (ROSC) and survival [16, 17]. Unfortunately, this time-based approach is complicated by the fact that the exact duration of the arrest is unknown in most out-of-hospital resuscitations.

Over time studies have focused on several methods to find non-invasive markers of myocardial metabolic state that allow prediction of whether or not a shock would achieve ROSC [22, 63–65]. Measurement of the VF waveform from the ECG offers a non-invasive, real-time analysis of the myocardial cells, with a deteriorating VF waveform over time indicating a worse prognosis [6, 66, 67]. There is evidence that this decrease is related to a depletion of myocardial energy phosphates during untreated VF [68], therefore the VF waveform gives an indication of the metabolic state of the myocardium. A frequently investigated parameter is amplitude spectrum area (AMSA), which comprises information on both the amplitude and the frequency of the VF waveform. This is considered a promising outcome predictor, with studies showing that a high AMSA correlates with defibrillation success and long-term outcome [21, 23, 64, 69]. Additionally, the change in AMSA throughout the first three shock sequences was associated with the likelihood of survival [70, 71]. Because of these relationships, VF waveform analysis has been proposed to guide the priority of interventions and to predict the best timing for defibrillation delivery, thereby reducing the number of failed defibrillation attempts and CPR interruptions.

To investigate this new approach, in 2013 a randomized controlled trial was conducted using a VF waveform analysis based algorithm to guide initial treatment of OHCA patients. Unfortunately, this study did not find improved survival rates [72]. A possible explanation for this is that recent studies showed that altered VF waveforms are also influenced by the underlying aetiology of the arrhythmia, especially by the presence of myocardial ischemia [25, 27, 28, 73]. Therefore, low VF waveform characteristics may not only be caused by longer arrest duration, indicating a smaller chance of defibrillation success, but could also be an expression of myocardial ischemia in a patients with a short arrest duration, with possibly a better chance of successful defibrillation.

Calculation of VF waveform parameters

During resuscitation the two paddles of a defibrillator record the ECG signal as well as the transthoracic impedance (TTI) data. As often with physiological signals, the raw ECG can be noisy, containing low-frequency baseline drift and high-frequency noise. This can be removed by pre-processing the signal using a bandpass filter, which removes frequencies below and above the lower and higher cut-off frequency (i.e. 2 and 48 Hz in VF analysis). To cancel out the phase shift that is introduced by filtering, the filter is applied once forward and once backward. Furthermore, the ECG also contains artefacts induced by chest compressions. Due to variations in the rate (i.e. frequency) of chest compressions, complete removal of these artefacts by filtering is difficult. Therefore, only chest compression free segments of the ECG can be used for VF analysis. The presence of chest compressions is identified with the TTI data, which shows peaks for each chest compression. To assure inter- and intra-patient comparability, a VF period of equal length needs to be selected. After selecting and pre-processing the VF segments, several parameters can be calculated. The parameters investigated in this study are described below.

First parameters are calculated from the ECG segment in the time domain. The mean absolute amplitude (MAA) represents the mean absolute deviation (i.e. amplitude) of the mean of the waveform, and the median slope (MdS) is the median steepness of the waveform [25]. The variance of the slope (VS) gives an indication about the diversity of the slope in the segment. Then, the VF segment is transformed to the frequency domain using the Fast Fourier Transform (FFT). From this signal the amplitude spectrum area (AMSA) is computed as the summed product of individual frequencies and their corresponding amplitudes [19, 22, 64, 74]. From the Fourier transform of the original VF signal, the power spectral density (PSD) is estimated as $PSD_k = \frac{2}{N \cdot f_s} \cdot |FFT_k|^2$, in which N is the number of samples, k is the specific sample and f_s is the sampling frequency. This power spectrum gives information about the frequency components composing the original VF signal, with the area under the curve representing the total power of the signal. The dominant frequency (DF) is the frequency with the highest power, whereas the median frequency (MdF) is the frequency at which the power spectrum is divided into two regions with equal power [29, 65, 75]. The frequency ratio (FR) is calculated as the summed power in the high-frequency band (8-24 Hz) divided

TABLE 2.1: Mathematical description of VF waveform characteristics

Parameter	Mathematical definition	Units
Mean absolute amplitude	$MAA = \frac{1}{N}\sum_{i=0}^{N-1}\lvert x_i\rvert$	mV
Median Slope	$MdS = \text{median}(\lvert x_1 - x_0\rvert, \ldots, \lvert x_{N-1} - x_{N-2}\rvert) \cdot f_s$	mV/s
Variance of Slope	$VS = \text{var}(\lvert x_1 - x_0\rvert, \ldots, \lvert x_{N-1} - x_{N-2}\rvert) \cdot f_s$	mV^2/s
Amplitude spectrum area	$AMSA = \frac{2}{N}\sum_{4\leq f_k\leq 48}\lvert\hat{x}_k\rvert \cdot f_k$	mV·Hz
Power spectrum area	$PSA = \frac{f_s}{N}\sum_{4\leq f_k\leq 48} PSD_k \cdot f_k$	mV^2·Hz
Dominant frequency	$DF = \text{argmax}_{f_k}\, PSD_k$	Hz
Median frequency	$MdF = f_m$ with m minimal sample number at which the trapezoidal integral approximation $\left(\sum_{k=0}^{m} PSD_k\right) - (PSD_0 + PSD_m)/2$ is closest to 50% of the total trapezoidal $\left(\sum_{k=0}^{N-1} PSD_k\right) - (PSD_0 + PSD_{N-1})/2$	Hz
Frequency ratio	$FR = \sum_{8\leq f_k\leq 24} PSD_k \,/\, \sum_{3\leq f_k\leq 5} PSD_k$	

$x_i (i = 0, 1, 2, \ldots, N-1)$ are the samples of the ECG segment $x(t)$ in time domain with sampling rate f_s. Amplitude $|\hat{x}_k|$ indicates the amplitude of Fourier transform of x_i at frequency f_k, and PSD_k indicates the power of the PSD at frequency f_k. The frequency f_k is equal to $\frac{k}{N} f_s$. $\sum_{4\leq f_k\leq 48}$ indicates the sum over the indices k for which the frequency f_k is between 4 and 48 Hz.

by the summed power in the low-frequency band (3-5 Hz) [76]. These frequency parameters give information about the power distribution of the VF signal. The power spectrum area (PSA) describes the area under the curve from the power frequency spectrum, as the summed product of individual frequencies and corresponding powers [65]. In this study, the AMSA and PSA were calculated between the frequency of 4 and 48 Hz. The mathematical descriptions of these characteristics can be seen in Table 2.1.

Unfortunately, the amplitude and frequency measures also have disadvantages. Amplitude measures are very sensitive for recording conditions, e.g. skin resistance, size and position of electrodes. Fourier analysis is most suitable for a stationary signal, which means that statistical properties such as mean and standard deviation remain the same throughout the period of recording. However, it is indicated that VF is a non-stationary, complex process, suggesting that it is generated by multiple interacting systems within the heart [77]. Therefore, a method which could simultaneously describe local and temporal spectral information from a signal might be more appropriate for the analysis of transient, aperiodic and other non-stationary signal features. This can be done with a scaling analysis approach. In this study, two different techniques for scaling analysis were used.

The first method is detrended fluctuation analysis (DFA). This method gives information about the complexity of the VF waveform morphology [78, 79]. Computation of detrended fluctuation analysis is as follows [80]: First the global constant trend of the original time series is eliminated by subtracting the mean of the signal. This signal is subsequently integrated by taking the cumulative sum of the signal (Figure 2.9a). The resulting signal is divided into equal boxes of length *n*, for various values of *n*. In each box the local linear trend is calculated and subtracted from the integrated time series. Of this detrended signal the root mean square (RMS) is calculated representing the fluctuation in that box size (Figure 2.9b). This is repeated for several box sizes *n* (different scales) (Figure 2.9c). A relationship between *F(n)*, the fluctuation as a function of box size, and the box size *n* (i.e. the number of samples in a box) is plotted on logarithmic axes. The DFA scaling exponent α is the slope of the trend line of this function estimated using linear regression (see Figure 2.10).

This α can be estimated in different time ranges of interest, providing information about organisation within a time scale. In this study, two different slopes are determined: 1) the slope on small time scales, i.e. 0.032 to 0.4 seconds (DFAα_1) and 2) the slope on larger time scales, i.e. 0.4 to 3.0 seconds (DFAα_2). A more detailed description of the calculation of DFA, its application on different signals and the interpretation of the scaling exponent α is given

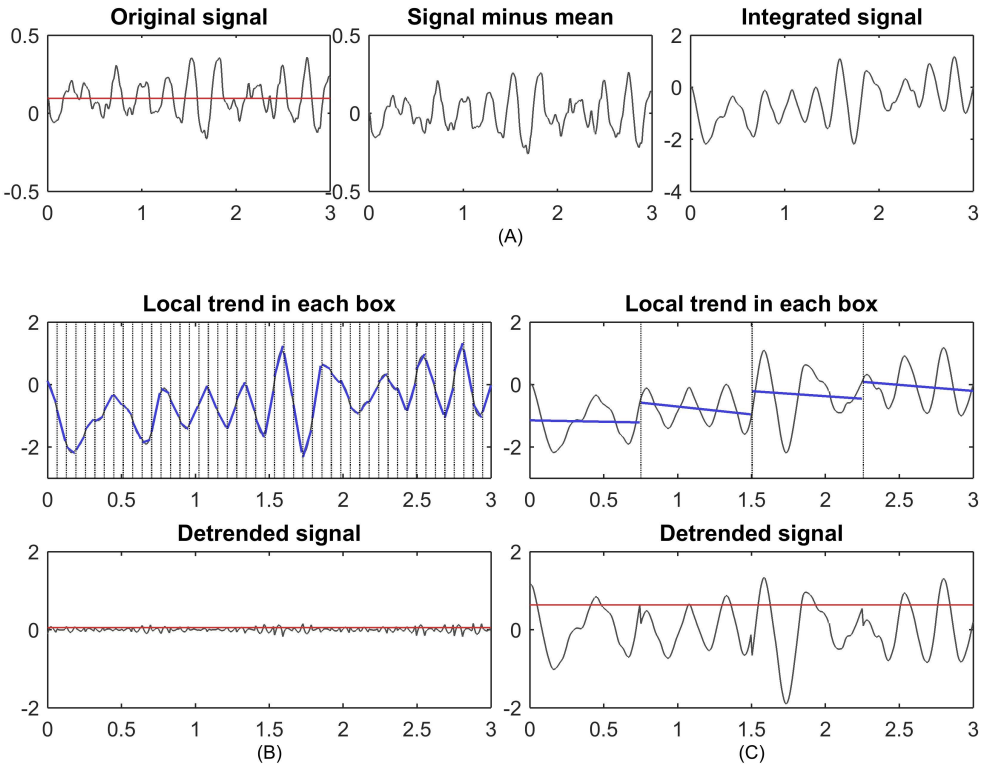

FIGURE 2.9: Step-wise explanation of Detrended Fluctuation Analysis. In panel A, the mean is subtracted from an example VF signal sampled at 125 Hz with a duration of 3 seconds (left and middle plot). The right plot shows the resulting integrated signal. In panel B, the local trends of the integrated signal from panel A are calculated (blue lines) and subtracted (bottom plot) for box size≈0.2 s (20 samples). In panel C this is shown for box size=0.8 s (100 samples). In the bottom plots of B and C, the root-mean-square of the detrended signal is presented as the red line.

in Appendix A. A short summary: The α_1 approaches the value of 2 for smooth functions on small box sizes, and will be lower if the signal is more noisy or is more complex on a smaller level. The α_2 will approach zero for a harmonic oscillating smooth signal (i.e. sine wave), but a more complex or varying oscillating signal the α_2 will be larger than zero.

The second method using a signal analysis approach is wavelet analysis. Wavelet analysis uses a continuous wavelet transform (CWT), in which a signal $x(t)$ is modelled using all possible translated and dilated versions of a mother wavelet $\psi_{a,b}$ (where a and b are the dilational (or scale) and translational (or position) parameters). It is given by:

$$CWT_x(a,b) = \frac{1}{\sqrt{a}} \int_{-\infty}^{\infty} x(t)\psi^*(\frac{t-b}{a})dt$$

The mother wavelet used in this study is the Symlet wavelet. Initial analysis showed that this wavelet yielded better results compared to other wavelets (Gaussian and Morlet). Applying this CWT to a signal leads to a set of wavelet decomposition coefficients, representing the distribution of energy over the time and scales. An example of such an energy distribution can be seen in Figure 2.11. The energy distribution over the range of scales varies depending upon the signal composition (i.e. morphology) of the VF waveform. In other words, the analyzing wavelet captured different amounts of signal energy at each scale a, depending on the signal characteristics. The waveform parameter scale distribution width (SDW) is based on this principle. The signal energy is summed along the time-axis to represent the entire segment, resulting in a 2D-signal as shown in Figure 2.12. The SDW is then calculated as the width of the energy distribution at half the height of its peak. It is hypothesized that a VF waveform that is very regular, the distribution will be a sharp and tall peak indicating that

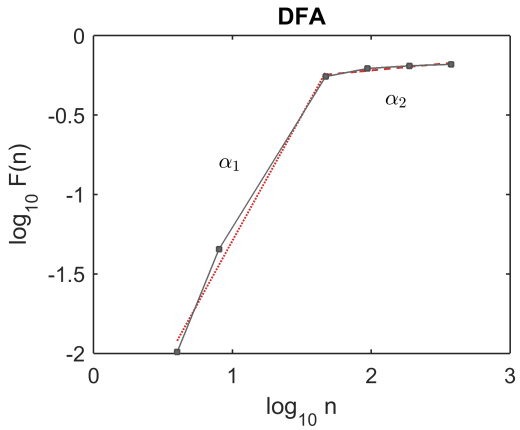

FIGURE 2.10: DFA on the example VF signal of Figure 2.9. In this example, the α_1 is 1.58 and α_2 is 0.08 (red lines).

very few scales were required to model most of the signal energy [81]. This could serve as an indicator of the morphology and complexity of the VF signal, which might give information about the status of the myocardium.

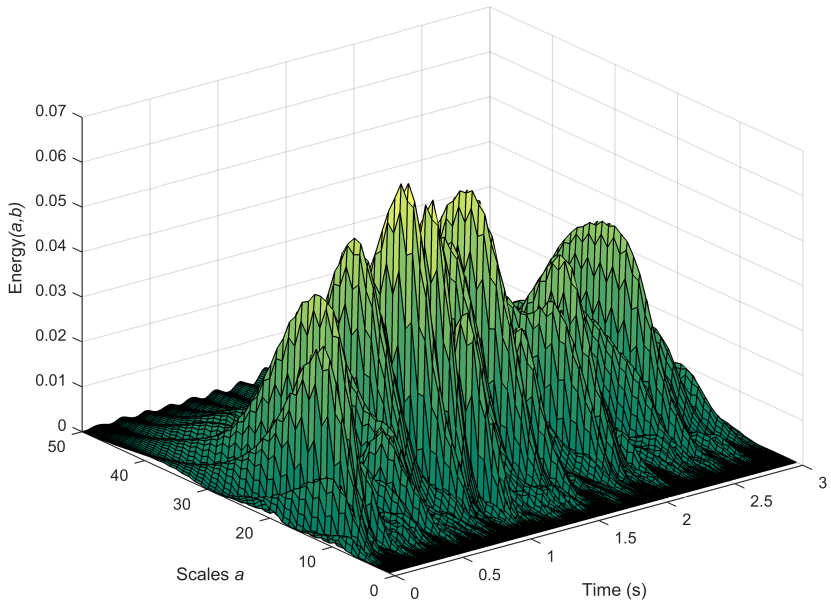

FIGURE 2.11: The energy per scale a per translation b (time), plotted against the scales and time.

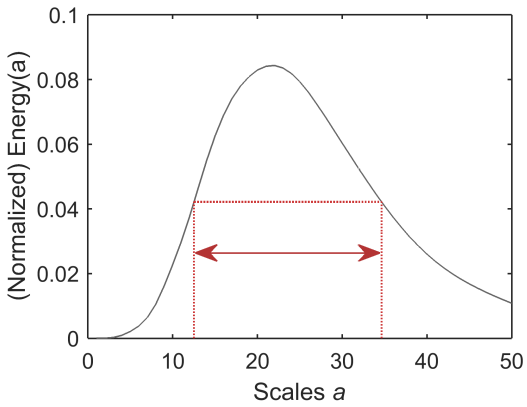

FIGURE 2.12: Calculation of Scale Distribution Width. The width of the energy signal is defined at half the height of the peak energy (red line).

3 The effect cardiopulmonary resuscitation on ventricular fibrillation waveform measures: The role of CPR quality and underlying acute coronary occlusions

3.1 Introduction

The initially recorded rhythm in 20-40% of out-of-hospital cardiac arrests (OHCAs) is ventricular fibrillation (VF), with better survival rates than other presenting rhythms [1–4, 82]. However, the chance of survival decreases with longer duration of VF. Since the electrocardiographic VF waveform also decreases over time, it is thought to reflect the myocardial metabolic state [6, 7, 75]. Therefore, the VF waveform has been investigated for some time now, and found to be associated with defibrillation success and long-term outcome [20, 22, 23, 83].

More recently, it has been shown that not only the absolute value of the VF waveform, but also the change in these parameters is associated with outcome. An increase in VF characteristics during the course of resuscitation is associated with a better chance of survival [71, 84, 85]. However, the determinants of these changes in VF characteristics are largely unknown. Earlier data have shown that uninterrupted chest compressions increase VF parameters [15] and pauses in chest compressions decrease these measures [18, 19]. The ratio of uninterrupted chest compressions and pauses might therefore be a determinant of in- or decrease in VF parameters. A measure for this ratio is the amount of time in which compressions are given divided by the total time, i.e. chest compression fraction (CCF). A CCF of higher than 0.6 has been associated with higher survival rates [13], and has therefore also been adopted as a recommendation in the guidelines for cardiopulmonary resuscitation (CPR) [9].

In addition, evidence from an animal study suggests that in animals with an acute coronary occlusion (ACO) VF parameters did not increase as much in response to CPR as in animals without an ACO [30]. This is of particular importance since ACO is the most common cause of VF OHCA [57, 86]. In humans it has been shown that ischemic heart disease indeed affects the appearance of the VF waveform [27, 29], but the influence of ischemia on the change in VF waveform in relation to CPR quality has never been investigated.

An altered response of VF waveform characteristics to CPR in patients with ACO could potentially provide a method to identify these patients in an early phase. However, to be able to investigate this, first the increase in VF parameters needs to be confirmed in the common human OHCA setting, where periods of uninterrupted chest compressions are alternated with pauses for e.g. intubation attempts and shock application. Therefore, we aim to investigate the association between CPR quality and change in VF characteristics. This is done by comparing the change in VF characteristics between two groups based on whether or not

the guideline-prescribed CCF of 0.6 has been achieved. As a sub-analysis, we investigated if there is a difference in the reaction on CPR between patients with and without an ACO.

3.2 Methods

3.2.1 Patient population

All consecutive out-of-hospital cardiac arrest patients who where resuscitated by the emergency medical services (EMS) in the region of Nijmegen (Gelderland-Zuid, the Netherlands) between November 2005 and January 2011 are identified. For the present study inclusion criteria are: available paddle ECG tracings, VF as first observed cardiac rhythm and at least two shocks applied by EMS. Exclusion criteria are: age < 18 years, traumatic arrest (including hanging and drowning), AED shocks before EMS arrival and prematurely stopped resuscitations (due to 'do not resuscitate order' or terminal illness). Given the observational design of the study, written informed consent is not necessary to obtain according to the Dutch Act on Medical Research involving Human Subjects.

Gelderland-Zuid has a population of about 540,000 residents and covers 1,040 square kilometers, including urban, suburban and rural areas. The EMS system in Gelderland-Zuid is a one-tier system that is activated by calling 112. Paramedics will give instructions to the caller to initiate basic life support (BLS), and at least one, but usually two ambulances are dispatched to the location of the emergency. A mechanical chest compression device (Autopulse) was part of the standard EMS-equipment, but not routinely used. During the study period, CPR was performed according to the guidelines of the European Resuscitation Council of 2005. EMS staff were not instructed to withhold chest compressions in order to acquire artefact-free ECG recordings.

3.2.2 Data collection

Demographic, clinical and arrest characteristics were defined according to the Utstein style definitions [60] and collected using EMS and hospital records. During resuscitation, ECG tracings and transthoracic impedance (TTI) data were recorded with the two paddles of the LIFEPAK Biphasic Defibrillator (Physio-Control, Redmond, WA, USA) at a sample frequency of 125 Hz and 61 Hz respectively. A MATLAB (version 2014b, Mathworks, Natick, MA, USA) programmed Graphical User Interface was used for the annotation of chest compressions in the tracings.

3.2.3 VF waveform characteristics

Analysis of the VF waveform was performed using MATLAB. The ECG recordings were processed by twice applying fourth-order Butterworth bandpass filter with cut-off frequencies of 2 and 48 Hz for elimination of non-physiological low and high frequency noise. Three-second chest compression free segments of pre-shock VF (i.e. the chest compression free segment of the ECG tracing closest before the shock) before the first and second shock were selected for further analysis.

From the selected ECG signal in the time domain, the mean absolute amplitude (MAA) was computed as the mean absolute deviation (i.e. amplitude) from the mean of the waveform and the median slope (MdS) was computed as the median value of all amplitude differences, describing the median steepness of the waveform [25, 65]. The variance of the slope (VS) gives an indication about the diversity of the slope in the segment, and is computed as the variance of all amplitude differences. The VF segment was then transformed to the frequency domain using the Fast Fourier Transform (FFT). From this signal the amplitude spectrum area (AMSA) is computed as the summed product of individual frequencies and their corresponding amplitudes [19, 64, 65, 69]. From the signal's power spectrum (estimated

by squaring the Fourier transform of the original VF signal) we calculated the dominant frequency, which is the frequency where the power spectrum attains its maximum [22, 75] and the median frequency, the frequency at which the power spectrum is divided into two regions with equal power [29, 75]. Furthermore, we calculated the power spectrum area (PSA) as the summed product of individual frequencies and corresponding powers [65]. A detailed description and mathematical formulation of these characteristics was presented in Chapter 2.

In addition, two parameters were determined using a scaling analysis approach. The first is detrended fluctuation analysis (DFA), which is used to describe the underlying structure of non-stationary data [78]. DFA is calculated to give information about the complexity of the VF waveform morphology [78, 79]. The method of DFA and an extensive investigation on applying this method to different kinds of signals is presented in Appendix A. The other scaling analysis approach is wavelet analysis, based on continuous wavelet transform. The scale distribution width (SDW) is the width of the distribution of wavelet energy among scales, and gives a measure for the degree of organization of the signal [87, 88]. A more extensive explanation of the use of wavelet analysis to calculate SDW can be found in Chapter 2.

The reaction of the waveform parameters on CPR was determined as the change in the parameter between the first and second shock, calculated as ΔWFP = WFP_2 - WFP_1. The WFP_1 is the investigated waveform parameter before the first shock and WFP_2 before the second shock. Since some patients received resuscitation according to an old protocol, where up to three stacked shocks were given [89], these delta characteristics were only taken into account if the period between the two segments was more than 30 seconds.

3.2.4 CPR quality

Chest compressions were identified as spikes in the transthoracic impedance (TTI) data. These were automatically detected through an algorithm, but manually checked on accuracy. Based on the literature, chest compressions separated by not more than 1.5 seconds were considered consecutive [90–92], resulting in a lower limit of chest compression rate of 40 beats per minute. The effective chest compression time (CC_{time}) was defined as the total time of the period in which compressions are given. The chest compression fraction (CCF) is the proportion of time in which compressions are given [13, 93]. This is calculated with the following equation:

$$CCF = \frac{CC_{time}}{Total\ time}.$$

In our study, the CCF is calculated between the two VF segments, and the total time is defined as the beginning of the first VF segment to the end of the second VF segment. Therefore, due to the chest compression free periods of rhythm analysis before shock and shock delivery, the CCF can by definition never be 1 in this study.

3.2.5 Patient classification

The patients were divided into two groups: patients that received CPR with a chest compression fraction greater than or equal to 0.6 between the VF segments (CCF$\geq$0.6) and patients that received CPR with a chest compression fraction lower than 0.6 (CCF<0.6). The chest compression fraction is calculated as the amount of time in which compressions are given divided by the total time between the segments [13, 93], and the cut-off value of 0.6 is based on the recommendation in the 2010 CPR Guidelines [9].

For the secondary analysis, the presence or absence of a localised myocardial infarction related to an ACO as underlying cause of VF was determined on a case-by-case basis. For each patient, records of symptoms, cardiac biomarkers, 12-leads ECG in the emergency department (ED), echocardiography, coronary angiography (CAG) and autopsy reports were investigated. Categorization was based on the criteria of the third universal definition of

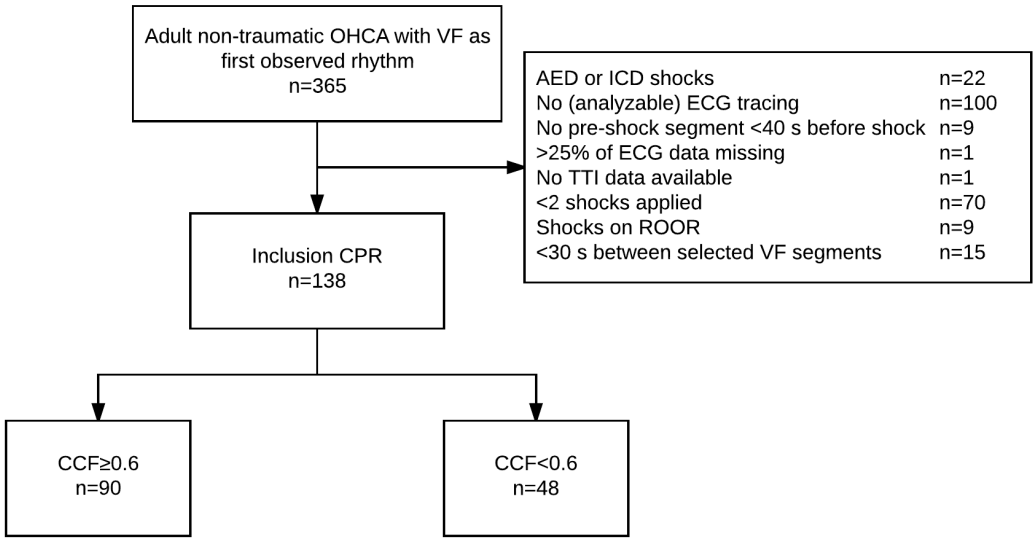

FIGURE 3.1: Flowchart of patient inclusion. OHCA = Out-of-hospital cardiac arrest, VF = Ventricular fibrillation, AED = Automated external defibrillator, ICD = Implantable cardioverter defibrillator, ECG = Electrocardiogram, ROOR = Return of Organized rhythm, CPR = Cardiopulmonary resuscitation, CCF = Chest compression fraction.

myocardial infarction (MI) and criteria for ACO (i.e. ACO on CAG or autopsy and/or ST-segment elevation in accordance with an acute localized MI) [41]. Subjects without sufficient clinical information were excluded. Patients that met both the universal definition of MI as well as the criteria for ACO were categorised in the ACO group. Patients that did not meet the universal definition of MI and/or the criteria for ACO, were categorised in the non-ACO group. An extensive description of study group categorisation regarding ACO can be found in Appendix B.

3.2.6 Outcome measures

The primary outcome measures were the changes in the VF waveform parameters between the first and second shock, as described above. These characteristics were compared between the two main study groups (CCF$\geq$0.6 vs. CCF<0.6). Secondly, as a sub-analysis, analyses were stratified according to ACO status.

3.2.7 Statistical analysis

Statistical analysis was performed using IBM SPSS Statistics software (version 22, IBM Corp., Armon, NY, USA). Categorical data were expressed as frequencies (percentages) and continuous data as medians (interquartile ranges). In case of missing data, proportions were calculated using the available data as denominator. For comparison of baseline variables between the groups, the Chi-square test was used for categorical data and the Mann-Whitney U test was used for continuous data. The difference of the VF waveform characteristics between the two segments within each group was compared using a Wilcoxon signed rank test. The changes in VF waveform characteristics (ΔWFP) were compared between the groups using a Mann-Whitney U test. In the sub-analysis, pairwise comparisons were performed using the Mann-Whitney U test to check for differences between the groups. A p-value of <0.05 was considered statistically significant for all tests.

TABLE 3.1: Baseline characteristics of OHCA-patients with CCF≥0.6 and CCF<0.6

Variable	All (n=138)	CCF≥0.6 (n=90)	CCF<0.6 (n=48)	p-value
Age (n=138)	63 (53.75 - 73)	63 (54 – 72.25)	62 (51.25 - 73)	0.684
Male gender (n=138)	107 (77.5)	73 (81.1)	34 (70.8)	0.168
Public location arrest (n=102)	43 (42.2)	29 (46.0)	14 (35.9)	0.314
Witnessed arrest (n=99)	79 (79.8)	48 (78.7)	31 (81.6)	0.728
- Bystander witnessed	75 (75.8)	45 (73.8)	30 (78.9)	0.559
- EMS witnessed	5 (5.1)	4 (6.6)	1 (2.6)	0.646
Bystander CPR (n=98)	54 (55.1)	34 (50.8)	23 (62.2)	0.302
Autopulse used (n=135)	54 (40.0)	43 (48.9)	11 (23.4)	0.004
Response time (n=121)	8 (6 - 10)	8 (6 - 11)	7.5 (5 - 10)	0.229
Shocks delivered by EMS (n=129)	4 (3 - 7)	5 (3 - 7.25)	4 (3 - 7)	0.413
Amiodarone (n=122)	95 (77.9)	63 (79.7)	32 (74.4)	0.498
Epinephrine (n=124)	115 (92.7)	78 (96.3)	37 (86.0)	0.063
Atropine (n=123)	52 (42.3)	37 (46.3)	15 (34.9)	0.224
First shock success (n=135)	40 (29.6)	19 (21.8)	21 (43.8)	0.008

Values are given in numbers (%) or medians (interquartile ranges). P-values are calculated for comparisons between patients with CCF≥0.6 and CCF<0.6. OHCA = Out-of-hospital cardiac arrest, CCF = Chest compression fraction, EMS = Emergency medical services, CPR = Cardiopulmonary resuscitation.

3.3 Results

3.3.1 Study population

In the study period of November 2005 and January 2011, 138 patients were included. Main reasons for exclusion were AED shocks before EMS arrival (6%), no available or analyzable ECG tracing (27%) and less than two shocks applied (19%). Details regarding in- and exclusion can be found in Figure 3.1.

Of these included patients, median age was 63 years (54-74) and 78% was male. 80% of patients had a witnessed arrest, either by bystanders (76%) or EMS (5%). Bystander CPR was delivered in 55% of the patients. The median EMS response time was 8 minutes (6-10) and median number of shocks delivered by the EMS was 4 (3-7). Baseline characteristics did not differ between the two groups, except for use of Autopulse and first shock success. In the CCF≥0.6 group, more patients received chest compression with the Autopulse than in the CCF<0.6 group (49% vs. 23% respectively, p=0.005). First shock success occurred more often in the CCF<0.6 group than in the CCF≥0.6 group (44% vs. 22%, p=0.010). The baseline characteristics for all patients and comparisons between the groups are presented in Table 3.1.

3.3.2 VF waveform characteristics

In all amplitude characteristics, a significant increase between the two VF segments was found in the CCF≥0.6 group, while no difference was found in the CCF<0.6 group (Table 3.2). The delta amplitude characteristics ΔAMSA, ΔMAA and ΔPSA were significantly higher in patients that received CPR with CCF≥0.6 compared to patients that received CPR with CCF<0.6, while ΔVS showed a trend towards higher values in the CCF≥0.6 group (p=0.06).

In the frequency characteristics, a significant increase between the two VF segments was found for MdF in the CCF≥0.6 group, while DF and FR showed a significant increase in the CCF<0.6 group. The delta frequency characteristics showed no differences between the two groups.

TABLE 3.2: Change in VF waveform parameters of OHCA-patients after a period with CCF≥0.6 and CCF<0.6

WFP	CCF group	VF_1	VF_2	p_1	Δ WFP	p_2
		Amplitude characteristics				
AMSA	CCF≥0.6	7.94 (5.70 – 10.43)	9.46 (6.64 – 13.39)	<0.001	1.29 (-0.73 – 4.00)	0.029
	CCF<0.6	8.78 (5.40 – 13.66)	9.51 (5.37 – 13.37)	0.720	0.07 (-1.02 – 1.23)	
MAA	CCF≥0.6	0.09 (0.07 – 0.12)	0.10 (0.07 – 0.13)	0.002	0.01 (-0.01 – 0.04)	0.038
	CCF<0.6	0.11 (0.08 – 0.15)	0.12 (0.07 – 0.15)	0.814	0.00 (-0.03 – 0.02)	
MdS	CCF≥0.6	2.72 (1.94 – 3.98)	3.27 (2.26 – 4.83)	<0.001	0.65 (-0.40 – 1.36)	0.110
	CCF<0.6	3.14 (2.04 – 4.91)	3.59 (2.05 – 5.19)	0.272	0.07 (-0.54 – 0.84)	
PSA	CCF≥0.6	0.05 (0.02 – 0.10)	0.08 (0.03 – 0.14)	<0.001	0.02 (-0.01 – 0.07)	0.029
	CCF<0.6	0.06 (0.03 – 0.16)	0.07 (0.02 – 0.19)	0.704	0.00 (-0.02 – 0.03)	
VS	CCF≥0.6	0.05 (0.03 – 0.12)	0.08 (0.04 – 0.16)	<0.001	0.02 (-0.02 – 0.07)	0.057
	CCF<0.6	0.08 (0.03 – 0.17)	0.09 (0.03 – 0.17)	0.806	0.00 (-0.02 – 0.03)	
		Frequency characteristics				
DF	CCF≥0.6	3.66 (2.99 – 5.40)	4.99 (3.32 – 5.98)	0.068	0.33 (-1.00 – 1.66)	0.987
	CCF<0.6	3.99 (3.41 – 5.32)	4.32 (3.32 – 5.98)	0.042	0.33 (-0.33 – 1.00)	
MdF	CCF≥0.6	4.65 (3.66 – 5.65)	4.99 (3.99 – 5.98)	0.032	0.33 (-0.66 – 1.08)	0.531
	CCF<0.6	4.32 (3.99 – 5.32)	4.65 (3.32 – 5.98)	0.280	0.00 (-0.58 – 1.00)	
FR	CCF≥0.6	0.32 (0.16 – 0.62)	0.40 (0.17 – 0.91)	0.439	0.03 (-0.22 – 0.28)	0.270
	CCF<0.6	0.22 (0.11 – 0.45)	0.27 (0.13 – 0.70)	0.040	0.07 (-0.13 – 0.53)	
		Scaling analysis characteristics				
DFAα_1	CCF≥0.6	1.41 (1.26 – 1.51)	1.35 (1.22 – 1.47)	0.009	-0.05 (-0.14 – 0.06)	0.236
	CCF<0.6	1.42 (1.28 – 1.50)	1.39 (1.21 – 1.54)	0.573	-0.01 (-0.13 – 0.10)	
DFAα_2	CCF≥0.6	0.08 (0.05 – 0.10)	0.07 (0.04 – 0.10)	0.203	-0.01 (-0.03 – 0.02)	0.855
	CCF<0.6	0.06 (0.04 – 0.09)	0.05 (0.04 – 0.07)	0.255	-0.01 (-0.03 – 0.02)	
SDW	CCF≥0.6	24.6 (19.4 – 29.7)	20.0 (15.5 – 28.8)	0.032	-2.04 (-9.25 – 6.47)	0.270
	CCF<0.6	21.9 (18.3 – 25.9)	20.5 (15.1 – 25.3)	0.367	-1.11 (-6.28 – 4.17)	

Values are given in medians (interquartile ranges). VF = Ventricular fibrillation, OHCA = Out-of-hospital cardiac arrest, CCF = Chest compression fraction, WFP = Waveform parameter. 90 patients were included in the CCF≥0.6 group, versus 48 in the CCF<0.6 group. p_1 is the difference between the related samples within the groups and p_2 is the difference in the delta characteristics between the groups. AMSA = Amplitude spectrum area, MAA = Mean absolute amplitude, MdS = Median slope, PSA = Power spectrum area, VS = Variance of slope, DF = Dominant frequency, MdF = Median frequency, FR = frequency ratio, DFA = Detrended fluctuation analysis, SDW = Scale distribution width.

In the scaling analysis characteristics, DFAα_1 and SDW showed a significant decrease in the CCF≥0.6 group, while no differences in scaling analysis characteristics were found in the CCF<0.6 group. The delta scaling analysis characteristics showed no differences between the two groups.

Sub analysis: ΔWFP after CPR in patients with ACO

Of the 138 patients included in this study, 60 patients (43%) were included for sub-analysis (CCF≥0.6: 19 ACO and 14 non-ACO; CCF<0.6: 19 ACO and 8 non-ACO). For details regarding in- and exclusion, see Appendix C. Pairwise comparisons showed significant differences in all amplitude characteristics in the non-ACO group between CPR with CCF≥0.6 and CCF<0.6, while no differences were seen in the ACO group between CPR with CCF≥0.6 and CCF<0.6. Pairwise comparison within the CCF≥0.6 group showed significant differences between the ACO and non-ACO group for ΔMAA and ΔMdS. These results are presented in Figure 3.2.

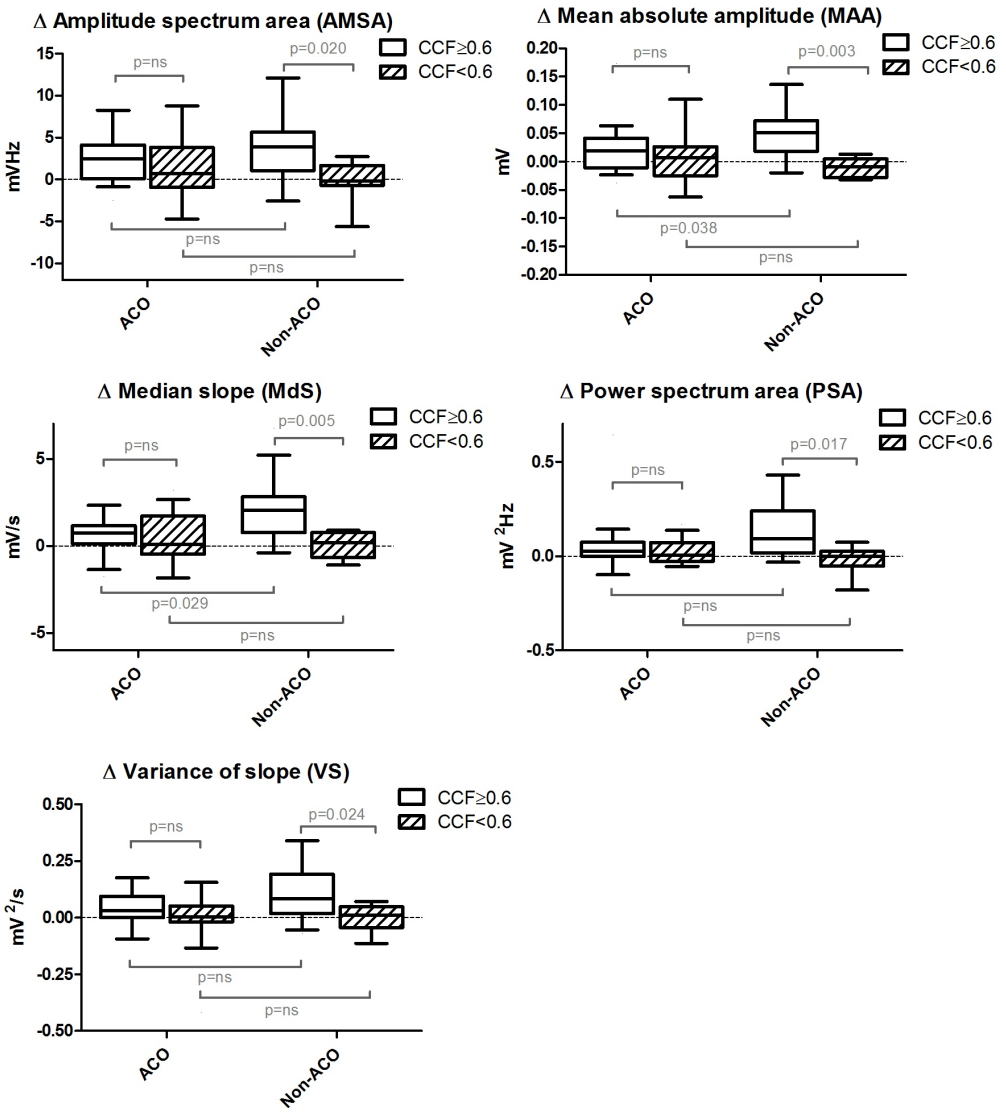

FIGURE 3.2: Differences in the change in VF amplitude parameters for CCF≥0.6 and CCF<0.6, divided in subgroups of patients with and without acute coronary occlusion (ACO). p-values are presented for significant differences (p<0.05). VF = Ventricular fibrillation, CCF = Chest compression fraction.

3.4 Discussion

This is the first human study investigating the reaction of VF waveform characteristics to CPR considering the common situation where chest compressions need to be interrupted for rhythm analysis, shock delivery or application of ventilations. In patients where these interruptions were kept to a minimum, resulting in a CCF of 0.6 or higher, an increase in all amplitude characteristics and a decrease in most scaling analysis characteristics was detected. For the amplitude characteristics MAA, PSA and AMSA, this numeric increase was significantly higher in patients with CCF≥0.6 compared to patients with CCF<0.6. Secondary analysis also revealed a difference in the response of VF characteristics to CPR between patients with and without an ACO, with a larger increase in VF characteristics in patients without ACO compared to patients with ACO after adequate CPR (i.e. CCF ≥0.6). These findings confirm the increase of waveform parameters with CPR, once again emphasizing the need for high-quality chest compressions with minimal interruptions. Furthermore, the difference in response of VF characteristics to CPR between patients with and without myocardial substrate may offer a method for early distinction of acute coronary occlusion.

3.4.1 Response of VF waveform characteristics to CPR

Animal studies

Several studies investigating the use of VF waveform analysis to guide therapy also describe the reaction of the waveform parameter to CPR, with many studies relying on the controllability of the cardiac arrest setting attainable in animal studies. Our results are consistent with results from swine and rat studies by Marn-Parnat et al., Achleitner et al. and Kolarova et al., showing an increasing amplitude and AMSA (or AMSA correspondent) with increased CPR duration [74, 94, 95]. Marn-Pernat et al. also reported more successful defibrillation with increasing AMSA, while Kolarova et al. only reported increased shock success after 6 minutes of CPR. In the guidelines for cardiopulmonary resuscitation, a CPR time of 2 minutes between shocks is advised [9], therefore only a few patients included in our study received CPR of more than 6 minutes between the two shocks. In the study by Achleitner, VF frequency characteristics were even more increased after CPR than amplitude characteristics [95], similarly to two studies by Berg et al. [96, 97]. This is in contrast with the results from our studies, suggesting a bigger increase in amplitude characteristics. However, we did find an increase in VF median frequency in the CCF$\geq$0.6 group, corresponding to the findings by Achleitner and Berg.

A study by Li et al. in swine found that the increase in AMSA was also related to the depth of chest compressions, with AMSA increasing with adequate compression depth but remaining equal with shallow compressions [98]. Unfortunately, TTI data cannot provide reliable information on the compression depth [99], therefore the adequacy of this depth could not be taken into account in our study.

Human studies

Since in human studies the setting during out-of-hospital cardiac arrest cannot be controlled, the change of the VF waveform in response to CPR is less documented in humans. A study by Eftestøl et al. investigated the effect of varying durations of CPR sequences on VF waveform parameters. In their study, uninterrupted CPR increased the centroid frequency (corresponding to median frequency) and AMSA after a sequence of 0-1 minute, then staying at the same level. Only AMSA showed further increase after CPR sequence of more than 3 minutes [15]. Our results correspond with these findings, showing an increase in AMSA and MdF even when CPR sequences are interrupted, as long as these interruptions are kept to a minimum (CCF$\geq$0.6). In addition, that the increase in AMSA (and other amplitude characteristics) was higher in patients with CCF$\geq$0.6 compared to patients with CCF<0.6 adds more strength to the findings of Eftestøl.

A study of Box et al. compared reaction of VF waveform on CPR for two different types of CPR, i.e manual and mechanical CPR. They found an increase in the mean of cardioversion outcome predictor (COP), which is a parameter based on wavelet transform signal processing, for both types of CPR. However, the increase in COP was only significant for the automated CPR. The authors speculate this to be the result of possibly more hands-off time in the manual CPR group for longer CPR periods. Unfortunately, (difference in) chest compression fractions were not calculated [100]. In our study, we found a decrease in the wavelet analysis marker SDW (smaller SDW means more regular/organized VF, see Chapter 2) in the CCF$\geq$0.6 groups, while this decrease is not seen in the CCF<0.6 group. In our study population, mechanical CPR was also administered with the Autopulse, which occurred more in the CCF$\geq$0.6 group. However, this was only given in 49% of the patients in this group, and therefore it can be assumed that mechanical CPR cannot be solely responsible for the increase in VF waveform characteristics in this group.

3.4.2 Differences in the response of VF waveform characteristics to CPR in the presence of ACO

The effect of CPR on VF waveform parameters in the presence of myocardial ischemia is even less widely investigated. A swine study of Ristagno et al. showed that when the left anterior descending coronary artery (LAD) contained an occlusion of approximately 75%, AMSA was significantly lower after 2 minutes of CPR compared to an ischemia model without an occluded LAD [30], while AMSA values before initiation of CPR were similar. In a more recent study, Indik et al. compared change in AMSA and slope after CPR between swine with a coronary occlusion, a previous MI and control swine. They found that both AMSA and slope were significantly higher after 2 minutes of CPR in the control and previous MI swine than in the swine with acute coronary occlusion, while the initial values of waveform characteristics were similar between the groups [101].

In these animal studies, the cardiac arrest setting was controlled and therefore, adequate CPR was administered. In our study, we investigated the difference between patients with CCF$\geq$0.6 and CCF<0.6, and found that the increase in waveform parameter was larger in the CCF$\geq$0.6 group when looking at non-ACO patients, but this difference did not occur in ACO patients. Additionally, in the patients with CCF$\geq$0.6 there was a significantly larger increase in amplitude and median slope in non-ACO patients compared to ACO patients. This agrees with the results from Indik et al., showing an increase in waveform characteristics in swine with ACO after CPR, but an even larger increase in waveform characteristics in swine without ischemic injury [101].

There is also one human study by Hidano et al. that investigated if the VF waveform characteristics after CPR differed according to the aetiology of the arrest. Contrastingly to our results, they did not find a difference between patients with STEMI, non-STEMI and patients without ischemic cause of VF [102]. This may be caused by a difference in study groups. With stratification of patients based on the presence of ST-elevation on the ECG, patients with coronary artery disease without a total occlusion might also be stratified in the ischemia groups, while in our study those are stratified in the non-ACO group. Therefore, the difference between the result of our study and the study by Hidano et al. might be due to different responses of VF waveform characteristics to CPR for subtotal and total occlusion of the coronary artery.

Interestingly, in our study the ΔAMSA was not significantly different between ACO and non-ACO patients in the CCF$\geq$0.6 group, while in many studies the AMSA is a good predictor of shock success [20–23, 83] and it is lowered in the presence of myocardial ischemia [25–27, 29]. One explanation for this could be that the frequency content is less affected by CPR, leading to no significant in- or decrease in frequency characteristics in any of the subgroups (results not shown). Furthermore, since VF waveform characteristics also have been shown to differ according to the localisation of the infarction [29], the effect of CPR on the VF waveform characteristics may be dependent on the localisation of the coronary occlusion. Unfortunately, subdividing the ACO group according to localisation would result in groups too small for comparison (11 inferior, 6 anterior and 2 posterior coronary occlusions).

3.4.3 Initial value of VF waveform parameter

In this study, a difference was found in the amount of first shock success, with more shock success occurring in the CCF<0.6 group. Since waveform parameters are associated with defibrillation outcome, one might expect higher values of the initial waveform parameter in this group. Upon further analysis, the parameters MAA and SDW showed a significant difference in WFP_1 between the groups. A lower value for MAA in the CCF≥0.6 group might lead to the parameter increasing 'more easily' than in the CCF<0.6 group, where higher values are noted for WFP_1. A sub analysis dividing the waveform parameters in groups of low and high WFP_1 values (i.e. higher or lower than the median of all patients) found that for AMSA, MdS, PSA and VS a significant increase with CCF≥0.6 occurred for low and high values of WFP_1, while this difference did not occur for either low or high values in the CCF<0.6 group. For MAA, the low values of WFP_1 showed a significant increase ($p<0.01$) in the CCF≥0.6 group, while high values of WFP_1 did not result in an increase. However, low values of WFP_1 in the CCF<0.6 group did not lead to an increase, therefore it is expected that with comparable WFP_1 values the increase with CCF≥0.6 will still occur.

Furthermore, the higher WFP_1 in the CCF<0.6 group could be the result of a perfusing rhythm in between the two shocks in this groups. When the circulation is restored, the application of chest compressions is not indicated. This will lead to a lower CCF in the patients where shock success with perfusing rhythm occurred. Since a perfusing rhythm restores blood flow to the myocardium, its metabolic state is expected to improve. Therefore, when the rhythm returns to VF, the VF waveform parameters may be improved without the application of CPR. That still no overall increase is detected in the CCF<0.6 group suggests that either the perfusing rhythms did not occur often, or the decrease in parameters during VF without CPR dominates the overall change. In further research, groups should be selected based on the same distribution of the initial waveform parameter, and in-field assessment of perfusing rhythm should be collected to discriminate between (un)justified pauses in chest compressions.

3.4.4 Implications

Firstly, the results support the suggestion that the VF waveform is favourably affected by CPR, correspondingly to findings of animal studies, as well as the results from the human study by Eftestøl et al. Moreover, this study shows that this also applies in the common situation during OHCA, where chest compressions need to be interrupted for rhythm analysis, shock delivery or application of ventilations. That this increase in VF waveform characteristics was only found in patients where CCF was 0.6 or higher once more emphasizes the importance of good quality CPR, i.e. with a minimum duration of CPR interruptions. Additionally, the change in VF waveform characteristics can provide a method to monitor the quality of CPR. Furthermore, more evidence that CPR favourably affects the VF waveform in combination with findings that higher VF waveform parameters are associated with more defibrillation success supports the possible benefit of VF waveform guided initial therapy, i.e. using the VF waveform to decide whether defibrillation should be delayed to apply CPR to increase the chance of defibrillation success.

Secondly, this is the first human study investigating the response of VF waveform characteristics to CPR in the presence of an acute coronary occlusion. This is of particular importance since myocardial ischemia is a common etiology of cardiac arrest, but identification of this cause during the resuscitation is very difficult. An altered response of VF waveform characteristics to CPR in the presence of an ACO may provide a tool to identify patients who are having an ACO as underlying cause of the OHCA early in the resuscitation. The waveform evolution therefore may give additional information to ensure correct and early triage of patients to the cardiac catheterization laboratory, potentially leading to an increase in survival after OHCA.

3.4.5 Limitations

The most important limitation is the relatively small number of patients included in this study. To be able to analyze more data, we could have included the change in waveform characteristics between all the shocks in patients with more than 2 shocks. However, since it is suggested that the change in waveform characteristics is dependent on the duration of untreated VF [103], it may also be dependent on the length and quality of the preceding resuscitation. Therefore, we chose to only investigate the change between the first and second defibrillation attempt, to (as much as possible) eliminate these possible influences. Furthermore, since the analyses in the subgroup are performed on an even more limited sample-size, these should be considered only hypothesis generating.

Another limitation in this study is the difference in initial values of the waveform parameters (WFP_1) between the groups. The height of this initial value may influence the amount of in- or decrease that the waveform parameter can show. We performed additional analysis by subdividing patients with low and high initial values within the groups (as discussed above), and by investigating the relative change in VF characteristics (WFP_2/WFP_1), which gave similar results as the absolute differences. Therefore, we expect that similar results will be found when groups have comparable WFP_1 values, but this should be confirmed in future studies.

Lastly, even though the analysis of ECG data can tell us whether the rhythm during the cardiac arrest is organized or non-organized, this cannot tell us if this rhythm resulted in a sufficient cardiac output. However, given that the return of a spontaneous circulation does not occur immediately after defibrillation [11], short periods of organized rhythm will (most likely) not have led to perfusion. In this study, 15% of the patients had more than 2 minutes of organized rhythm between the first two defibrillations, and when these patients are excluded the results remain the same. Additionally, analysis of only patients without organized rhythm in between the first two defibrillations (84/138) also revealed an increase in VF amplitude characteristics for patients with CCF$\geq$0.6, while this increase did not occur in patients with CCF<0.6. This suggests that return of spontaneous circulation may not have a large impact in this study. However, in further studies information about the presence or absence of a perfusing rhythm should be collected, so that the chest compression fraction can be calculated over the time that chest compressions are indicated.

3.5 Conclusion

In OHCA-patients with VF, VF waveform amplitude characteristics were significantly increased when CCF was 0.6 or higher, while no increase was seen when CCF was lower than 0.6. These differences were also seen in a sub analysis in patients without ACO, while these differences were not found in patients with ACO. Further studies are warranted to confirm these findings in larger (preferably prospective) studies and to determine if changes in VF waveform characteristics can help in developing a decision tool for early treatment strategy, and/or may help in the early identification of patients with an underlying ACO during OHCA.

4 Differentiating between patients with and without acute coronary occlusion in out-of-hospital cardiac arrests based on ventricular fibrillation waveform measures

4.1 Introduction

A leading cause of death in Europe and the United States is out-of-hospital cardiac arrest (OHCA), with ventricular fibrillation (VF) the first observed cardiac rhythm in about 40% [1, 2, 5]. The only therapy to establish the return of spontaneous circulation (ROSC) from VF is electrical defibrillation [8]. Nevertheless, success rates are poor if the myocardial metabolic state is compromised, which also increases the likelihood of inducing asystole after defibrillation [10]. A method of interest to give information about arrest duration and myocardial metabolic state is VF waveform analysis [75, 79]. In several studies, different amplitude and frequency characteristics of the VF waveform have been shown to correlate with defibrillation success and long-term outcome [20–23].

However, several animal and human studies indicate that VF characteristics are also influenced by the presence of myocardial infarction (MI) [24–27, 29]. In addition, animal studies suggest that the change in VF waveform characteristics in reaction to CPR may also be altered in the presence of acute coronary occlusion (ACO) [30, 101]. Our human study on difference in change in VF waveform parameters as response to CPR between patients with and without ACO (Chapter 3) also indicates that VF amplitude characteristics increase in patients with and without ACO, but this increase is significantly higher in patients without ACO.

These VF waveform differences between patients with and without ischemic aetiology may provide a method to discriminate between these patients in the field. Since ACO is a common and reversible cause of OHCA [57, 86], early identification of these patients during resuscitation could be beneficial.

While the described studies found differences in individual VF characteristics between the groups, they did not investigate the capability of using these differences to actually discriminate an ACO in the field. Therefore, this study aims to determine the ability of the individual waveform parameters to discriminate between patients with and without ACO during OHCA. Furthermore, this study aims to determine the ability of the waveform parameters combined with their change in response to CPR to discriminate between these patients.

4.2 Methods

4.2.1 Patient population

All consecutive out-of-hospital cardiac arrest patients who where resuscitated by the emergency medical services (EMS) in the region of Nijmegen (Gelderland-Zuid, the Netherlands) between November 2005 and January 2011 are identified. For the present study inclusion criteria are: available paddle ECG tracings, VF as first observed cardiac rhythm and transportation to the Radboud University Medical Center. Exclusion criteria are: age < 18 years, traumatic arrest (including hanging and drowning), AED shocks before EMS arrival and prematurely stopped resuscitations (due to 'do not resuscitate order' or terminal illness). Given the observational design of the study, written informed consent is not necessary to obtain according to the Dutch Act on Medical Research involving Human Subjects.

Gelderland-Zuid has a population of about 540,000 residents and covers 1,040 square kilometers, including urban, suburban and rural areas. The EMS system in Gelderland-Zuid is a one-tier system that is activated by calling 112. Paramedics will give instructions to the caller to initiate basic life support (BLS), and at least one, but usually two ambulances are dispatched to the location of the emergency. A mechanical chest compression device (Autopulse) was part of the standard EMS-equipment, but not routinely used. During the study period, CPR was performed according to the guidelines of the European Resuscitation Council of 2005. EMS staff were not instructed to withhold chest compressions in order to acquire artefact-free ECG recordings.

4.2.2 Data collection

Demographic, clinical and arrest characteristics were defined according to the Utstein style definitions [60] and collected using EMS and hospital records. During resuscitation, ECG tracings and transthoracic impedance (TTI) data were recorded with the two paddles of the LIFEPAK Biphasic Defibrillator (Physio-Control, Redmond, WA, USA) at a sample frequency of 125 Hz and 61 Hz respectively. A MATLAB (version 2014b, Mathworks, Natick, MA, USA) programmed Graphical User Interface was used for the annotation of chest compressions in the tracings, in order to identify chest compression free periods.

4.2.3 VF waveform characteristics

Analysis of the VF waveform was performed using MATLAB. The ECG recordings were processed by twice applying a fourth-order Butterworth bandpass filter with cut-off frequencies of 2 and 48 Hz for elimination of non-physiological low and high frequency noise. Three-second chest compression free segments of pre-shock VF (i.e. the chest compression free segment of the ECG tracing closest before the shock) before the first and second shock were selected for further analysis.

From the selected ECG signal in the time domain, the mean absolute amplitude (MAA) was computed as the mean absolute deviation (i.e. amplitude) from the mean of the waveform and the median slope (MdS) was computed as the median value of all amplitude differences, describing the median steepness of the waveform [25, 65]. The variance of the slope (VS) gives an indication about the diversity of the slope in the segment, and is computed as the variance of all amplitude differences. The VF segment was then transformed to the frequency domain using the Fast Fourier Transform (FFT). From this signal the amplitude spectrum area (AMSA) is computed as the summed product of individual frequencies and their corresponding amplitudes [19, 64, 65, 69]. From the signal's power spectrum (estimated by squaring the Fourier transform of the original VF signal) we calculated the dominant frequency, which is the frequency where the power spectrum attains its maximum [22, 75] and the median frequency, the frequency at which the power spectrum is divided into two regions with equal power [29, 75]. Furthermore, we calculated the power spectrum area

(PSA) as the summed product of individual frequencies and corresponding powers [65]. A detailed description and mathematical formulation of these characteristics was presented in Chapter 2.

In addition, two parameters were determined using a scaling analysis approach. The first is detrended fluctuation analysis (DFA), which is used to describe the underlying structure of non-stationary data [78]. DFA is calculated to give information about the complexity of the VF waveform morphology [78, 79]. The method of DFA and an extensive investigation on applying this method to different kinds of signals is presented in Appendix A. The other scaling analysis approach is wavelet analysis, based on continuous wavelet transform. The scale distribution width (SDW) is the width of the distribution of wavelet energy among scales, and gives a measure for the degree of organization of the signal [87, 88]. A more extensive explanation of the use of wavelet analysis to calculate SDW was given in Chapter 2.

The reaction of the waveform parameters on CPR was determined as the change in the parameter between the first and second shock, calculated as ΔWFP = WFP_2 - WFP_1. The WFP_1 is the investigated waveform parameter before the first shock and WFP_2 before the second shock. Since some patients received resuscitation according to an old protocol, where up to three stacked shocks were given [89], these delta characteristics were only taken into account if the period between the two segments was more than 30 seconds.

4.2.4 Study groups

The presence or absence of a localised myocardial infarction related to an ACO as underlying cause of VF was determined on a case-by-case basis. For each patient, records of symptoms, cardiac biomarkers, 12-leads ECG in the emergency department (ED), echocardiography, coronary angiography (CAG) and autopsy reports were investigated. Categorization was based on the criteria of the third universal definition of myocardial infarction and criteria for ACO (i.e. ACO on CAG or autopsy and/or ST-segment elevation in accordance with an acute localized MI) [41]. Subjects without sufficient clinical information were excluded. Patients that met both the universal definition of MI as well as the criteria for ACO were categorised in the ACO group. Patients that did not meet the universal definition of MI and/or the criteria for ACO, were categorised in the non-ACO group. An extensive description of study group categorisation regarding ACO can be found in Appendix B.

4.2.5 Statistical analysis

Statistical analysis was performed using IBM SPSS Statistics software (version 22, IBM Corp., Armon, NY, USA). Baseline characteristics, waveform parameters and change in waveform parameters were compared between the two study groups. Categorical data were expressed as frequencies (percentages) and continuous data as medians (interquartile ranges). In case of missing data, proportions were calculated using the available data as denominator. The difference between groups was determined with the Chi-square test for categorical data and the Mann-Whitney U test for continuous data. A p-value of <0.05 was considered statistically significant for all tests.

Receiver operating characteristic (ROC) curve analysis was used to determine the evaluate the discriminative ability. The area under the curve (AUC) gives an overall measure of the discriminative ability of the waveform parameter, and is displayed with 95% confidence interval (CI).

Combination of parameters in a prediction model

The combination of multiple parameters into one is done with binary logistic regression, which estimates

$$P_{ACO} = \frac{1}{1 + e^{-(\beta_0 + \beta_1 \cdot X_1 + \beta_2 \cdot X_2 + \cdots + \beta_n \cdot X_n)}} ,$$

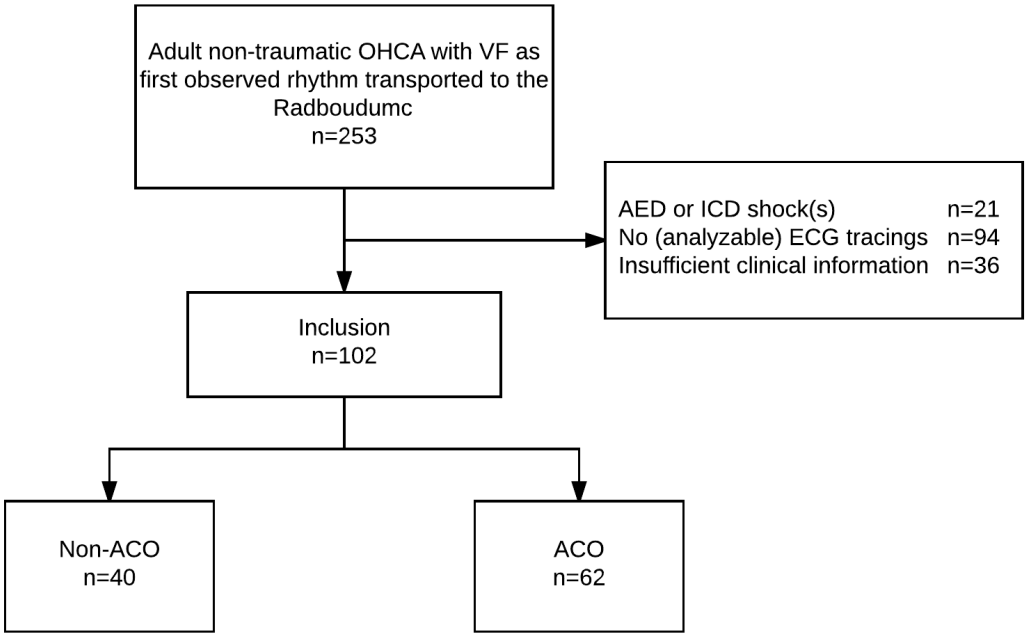

FIGURE 4.1: Flowchart of patient inclusion. OHCA = Out-of-hospital cardiac arrest, VF = Ventricular fibrillation, AED = Automated external defibrillator, ICD = Implantable cardioverter defibrillator, ECG = Electrocardiogram, ACO = Acute coronary occlusion.

where β_0 is the regression constant, β_1 to β_n are the regression coefficients and X_1 to X_n are the variables entered in the regression model. This method gives a predicted probability, i.e. the probability that the patient belongs to the ACO-group.

First, the single waveform parameters that were significantly different between the ACO and non-ACO group were investigated for their individual discriminative ability. Since there was a high level of multicollinearity between the waveform parameters, combination of two different waveform parameters calculated from the same segment of VF was not attempted. Secondly, the waveform parameter is combined with the change in that parameter in response to CPR. In order to do so, the application of adequate CPR (measured as a categorical variable determining whether the chest compression fraction (CCF) is greater than or equal to 0.6) also has to be entered in the regression model as interaction term. Therefore, the model then consists of four variables: WFP_1, ΔWFP, CCF and ΔWFP*CCF. Since this model can only be applied to those patients for which a ΔWFP could be determined (i.e. patients receiving more than one shock), the discriminative ability of this model is only determined for those patients. Lastly, it will be determined whether clinical characteristics can further improve the model. Univariate logistic regression analysis was carried out to identify clinical variables associated with the presence of an ACO. Factors that were found to be significant ($p<0.1$) in this univariate analysis were separately included in a multivariate logistic regression model with the single waveform parameters. If the inclusion of the clinical characteristic led to a higher AUC than for the single waveform parameter, the clinical characteristic was combined with the WFP_1, ΔWFP, CCF and ΔWFP*CCF into a new model.

4.3 Results

4.3.1 Study population

In the study period of November 2005 and January 2011, 102 patients were included. Main reasons for exclusion were AED shocks before EMS arrival (8%), no available or analyzable ECG tracing (37%) and insufficient clinical information to determine the underlying etiology (14%). Details regarding in- and exclusion can be found in Figure 4.1.

Of these included patients, median age was 61.5 years (51 – 71) and 72% was male. 87% of patients had a witnessed arrest, either by bystanders (85%) or EMS (2%). Bystander CPR was delivered in 67% of the patients. The median EMS response time was 8 minutes (6-10) and median number of shocks delivered by the EMS was 3 (1-6). In total, 79% of the patients had ROSC at ED arrival, and 48% survived until hospital discharge.

TABLE 4.1: Baseline characteristics of OHCA patients with or without an underlying ACO

Variable	All (n=102)	ACO (n=62)	Non-ACO (n=40)	p-value
Age	61.5 (51 – 71.3)	60.5 (49 – 71.3)	62 (53.5 – 71.8)	0.641
Male gender	73 (71.6)	47 (75.8)	26 (65)	0.237
		Pre-hospital		
Previous MI (n=92)	25 (27.2)	12 (22.2)	13 (34.2)	0.203
Public location arrest	44 (43.1)	27 (43.5)	17 (42.5)	0.917
Witnessed arrest: (n=99)	86 (86.9)	53 (88.3)	33 (84.6)	0.593
- Bystander witnessed	84 (84.8)	51 (85.0)	33 (84.6)	0.958
- EMS witnessed	2 (2.0)	2 (3.3)	0 (0)	0.518
Bystander CPR (n=99)	66 (66.7)	41 (68.3)	25 (64.1)	0.669
Autopulse used (n=99)	31 (63.3)	17 (56.7)	14 (73.7)	0.428
Response time (min) (n=92)	8 (6 – 10)	8 (6 – 10.8)	7 (5 – 9)	0.038
Shocks delivered by EMS	3 (1 – 6)	3 (1 – 6)	2.5 (1 – 4)	0.272
Amiodarone (n=98)	64 (65.3)	43 (71.7)	21 (55.3)	0.096
Epinephrine (n=99)	79 (79.8)	49 (81.7)	30 (76.9)	0.566
Atropine (n=98)	24 (24.5)	17 (28.3)	7 (18.4)	0.266
		In-hospital		
12-leads ECG	97 (95.1)	59 (95.2)	38 (95)	1.00
Coronary angiography	74 (72.5)	50 (80.6)	24 (60)	0.023
- Immediate CAG	63 (61.8)	48 (77.4)	15 (37.5)	<0.001
- Delayed CAG	11 (10.8)	2 (3.2)	9 (22.5)	0.006
PCI	54 (52.9)	44 (71)	10 (25)	<0.001
CABG	2 (2)	1 (1.6)	1 (2.5)	1.00
Troponin I max (n=98)	19.5 (1.1 – 94.2)	41.7 (3.7 – 100)	3.4 (0.6 – 27.6)	<0.001
Autopsy	14 (13.7)	10 (16.1)	4 (10)	0.557
		Clinical outcomes		
First shock success (n=101)	50 (49.5)	26 (42.6)	24 (60)	0.090
ROSC at arrival ED	81 (79.4)	45 (72.6)	36 (90)	0.034
Survival 24 hrs (n=101)	77 (76.2)	43 (70.5)	34 (85)	0.094
Survival at discharge	49 (48.0)	28 (45.2)	21 (52.5)	0.469

Values are given in numbers (%) or medians (interquartile ranges). Age is given in years, response time in minutes and troponin I in μg/L (measured with the (no longer available) Immulite 2000, DPC cardiac troponin I immunoassay). OHCA = Out-of-hospital cardiac arrest, ACO = Acute coronary occlusion, MI = Myocardial infarction, EMS = Emergency medical services, ECG = Electrocardiogram, CPR = Cardiopulmonary resuscitation, PCI = Percutaneous coronary intervention, CABG = Coronary artery bypass grafting, ROSC = Return of spontaneous circulation, ED = Emergency department.

A total of 61% of the included patients had an underlying ACO. EMS response time was significantly longer in the ACO group compared to the non-ACO group. Furthermore, maximum troponin I was significantly higher and more patients underwent CAG and percutaneous coronary intervention (PCI) in the ACO group. In the ACO group a significantly lower proportion had ROSC at ED arrival and there was a trend towards less 24-hour survival, but the survival to discharge did not differ significantly between the ACO and non-ACO study groups. The baseline characteristics for all patients and comparisons between the groups are presented in Table 4.1.

TABLE 4.2: VF waveform characteristics before the first defibrillation of OHCA-patients with or without an underlying ACO

Waveform parameters	ACO (n=62)	Non-ACO (n=40)	p-value
Amplitude characteristics			
Amplitude spectrum area (AMSA)	7.86 (5.28– 11.14)	12.95 (6.60 – 15.61)	0.009
Mean absolute amplitude (MAA)	0.10 (0.06 – 0.13)	0.13 (0.08 – 0.16)	0.040
Median slope (MdS)	2.87 (1.83 – 4.41)	4.40 (2.40 – 5.67)	0.013
Power spectrum area (PSA)	0.05 (0.02 – 0.14)	0.15 (0.04 – 0.22)	0.009
Variance of slope (VS)	0.05 (0.03 – 0.13)	0.15 (0.04 – 0.22)	0.008
Frequency characteristics			
Dominant frequency (DF)	4.16 (2.99 – 5.73)	4.65 (3.66 – 6.98)	0.118
Median frequency (MdF)	4.32 (3.66 – 5.40)	4.99 (3.99 – 6.32)	0.058
Frequency ratio (FR)	0.22 (0.12 – 0.60)	0.38 (0.15 – 0.68)	0.220
Scaling analysis characteristics			
Detrended Fluctuation Analysis (DFA) α_1	1.41 (1.31 – 1.52)	1.34 (1.23 – 1.46)	0.033
Detrended Fluctuation Analysis (DFA) α_2	0.01 (0.05 – 0.09)	0.08 (0.05 – 0.11)	0.225
Scale distribution width (SDW)	23.3 (18.1 – 29.0)	22.4 (17.3 – 27.3)	0.317

Values are given in medians (interquartile ranges). VF = Ventricular fibrillation, OHCA = Out-of-hospital cardiac arrest, ACO = Acute coronary occlusion.

4.3.2 VF waveform characteristics

All calculated VF amplitude characteristics (i.e. AMSA, MAA, MDS, PSA and VS) were significantly lower in patients in the ACO group than in patients in the non-ACO group (Table 4.2). Of the frequency characteristics, none showed a significant difference between patients in the ACO and non-ACO group, although MDF showed a trend towards lower values in the ACO-group (p=0.058). In the scaling analysis characteristics, DFAα_1 values were significantly higher in the ACO-group compared to the non-ACO group.

In Chapter 3, we found that the increase in amplitude waveform characteristics between the first and the second shock in patients without ACO was significantly higher for CCF$\geq$0.6 than for CCF<0.6, but this difference did not occur in patients with underlying ACO. Therefore, even though the changes were not different between patients with and without ACO (Appendix D), combination of the single waveform parameter with the change in that parameter interacted with the CCF is expected to increase the discriminative ability of the model. From our study population of 102 patients, the change between the first and the second shock could be determined in 60 patients (38 ACO; 22 non-ACO).

4.3.3 Discriminating ACO and non-ACO

Firstly, the waveform characteristics that significantly differed between the study groups are individually investigated for their ability to discriminate between ACO and non-ACO patients. The areas under the curve of the ROC curves of the waveform characteristics with corresponding 95% confidence interval are given in the left side of Table 4.3. All waveform parameters show a similar limited discriminative ability, with AMSA and VS showing the best discriminative ability with an AUC of 0.66. With a cut-off value for AMSA of 10.00 mVHz, this resulted in a sensitivity of 67.7% with a sensitivity of 65%.

Secondly, logistic regression was used to combine the single waveform parameters with the change in that parameter in response to CPR. This was applied to the 60 patients from which the change in waveform parameter between the first and second shock could be determined. The areas under the curve of the ROC curves of the waveform characteristics with corresponding 95% confidence interval are given in the right side of Table 4.3. From these models, the model with MdS+ΔMdS performed the best with an AUC of 0.75, and

MAA+ΔMAA performed second best with an AUC of 0.72. The other combined models did not show improvement compared to the single waveform parameter model, or even a decreased discriminative ability for VS+ΔVS and DFAα_1+ΔDFAα_1.

Lastly, we combined the best performing models with clinical patients characteristics. After univariate analysis, first shock success and administration of amiodarone and EMS response time were associated with ACO status (p<0.1). Separately combining these characteristics with the waveform parameters did not lead to an increase in AUC for administration of amiodarone and first shock success, but combination of WFP_1 with EMS response time did lead to a (slight) increase in AUC (see Table 4.4). Combining the EMS response time with the WFP_1, ΔWFP, CCF and ΔWFP*CCF into a new model leads to an even further increase in AUC, with the highest AUC of 0.79 for the model with MAA and the model with MdS (see Table 4.5).

4.4 Discussion

This is the first human study describing the discriminative ability of the VF waveform characteristics during OHCA to discriminate between patients with and without an underlying ACO. We found the VF amplitude characteristics before the first defibrillation to be lower in OHCA patients with than without ACO, with a limited discriminative ability (AUC=0.66). Combining the VF waveform parameter before the first shock with the change in that parameter in response to CPR led to an improved discriminative ability (AUC=0.75). Combination of this model with the response time led to a small further improvement (AUC=0.79). These findings indicate that the VF waveform might offer a method to discriminate between patients with and without an underlying ACO. This may be used as additional information to ensure correct and early triage of patients to the cardiac catheterization laboratory. Further research is needed to confirm these results in a larger cohort.

4.4.1 Previous studies

Several animal and human studies have investigated differences in VF waveform characteristics in the presence of cardiac ischemia. Animal studies mainly found lowered frequency characteristics in animals with previous and acute coronary occlusion [25, 73], while animal studies investigating amplitude characteristics sometimes do and sometimes do not describe differences between animals with and without ACO [25, 26, 101, 104].

Results from human studies regarding cardiac ischemia and VF waveform characteristics also describe some discrepancies. One study found lower VF amplitude characteristics in patients with MI compared to patients without MI [27], another study found lower AMSA

TABLE 4.3: AUCs with corresponding 95% confidence intervals of the single waveform parameters and of the combined models.

Individual waveform parameters	**AUC [95% CI] (n=102)**	**Combined models**	**AUC [95% CI] (n=60)**
Amplitude spectrum area (AMSA)	0.66 [0.54; 0.77]	AMSA+ΔAMSA	0.69 [0.55; 0.82]
Mean absolute amplitude (MAA)	0.62 [0.51; 0.74]	MAA+ΔMAA	0.72 [0.59; 0.86]
Median slope (MdS)	0.65 [0.53; 0.76]	MdS+ΔMdS	0.75 [0.61; 0.88]
Power spectrum area (PSA)	0.65 [0.54; 0.77]	PSA+ΔPSA	0.67 [0.53; 0.81]
Variance of slope (VS)	0.66 [0.54; 0.77]	VS+ΔVS	0.64 [0.50; 0.79]
Detrended Fluctuation Analysis (DFA) α_1	0.63 [0.52; 0.74]	DFAα_1+ΔDFAα_1	0.60 [0.45; 0.75]

The combined models consist of the waveform parameter before the first shock, the change in that parameter between first and second shock, the chest compression fraction (categorical $\geq$ or < 0.6) and an interaction term of ΔWFP*CCF. CCF = Chest compression fraction, AUC = Area under the curve, CI = Confidence interval.

values in patients with a STEMI vs. patients without MI [105], while a third study found no differences in VF waveform characteristics between STEMI, non-STEMI and non-ischemic patients [102]. In our study, differences in frequency characteristics between the ACO and non-ACO group were not found, while the amplitude characteristics did show these differences, with lower characteristics in patient with ACO compared to patients without ACO.

It is difficult to provide a clear explanation for the discrepancies between the previously reported studies and our study, but one contributing factor may be a difference in the definition of study groups. In the investigations categorising MI or STEMI, the presence of global arrest- and CPR-induced ischemia and subsequent cardiac biomarker release might have led to categorisation of patients with type II MI (MI secondary to ischemia due to either increased oxygen demand or decreased supply) instead of localised type I MI. Another contributing factor may be a difference in study population, as in one study, survival to hospital discharge was very high (73%). Furthermore, the same study had a significant difference in the number of EMS witnessed cases between STEMI and non-ischemic patients (11% vs. 1%, respectively) [102]. Since EMS witnessed OHCA typically results in VF of short duration with corresponding higher VF characteristics, differences between study groups may be masked. Accordingly, the study applying a correction for response time revealed a lower AMSA in patients with MI [105].

In addition to these differences in VF waveform parameters, animal studies suggested that the change in these parameters in response to CPR may be altered in the presence of an ACO. A swine study of Ristagno et al. showed that when the left anterior descending coronary artery (LAD) was completely occluded, no increase in VF characteristics after CPR was seen, while an increase did occur with an unoccluded LAD [30]. A study of Indik et al. on swine with AMI shows lower VF characteristics after 2 minutes of CPR in swine with ACO than in swine with VF without ACO [101]. In our human study on difference in change in VF waveform parameters as response to CPR between patients with and without ACO (Chapter 3), we found that VF amplitude characteristics differed significantly between CCF$\geq$0.6 and CCF<0.6 in patients without ACO, while this difference did not occur in patients with ACO.

Although the above described studies provide an insight in the differences in VF waveform characteristics between patients with and without ACO, studies describing the actual discriminative ability of these characteristics are scarce. As mentioned in one of the human studies, this may be due to the inability of these characteristics to provide a well defined cut-off value for clinical use. This is due to a relatively large overlap in waveform parameter values. The highest AUC of 0.66 in our study confirms this statement.

One animal study describing the discriminative ability of the VF waveform in relation to ACO found comparable values for AMSA and slope in the VF segment before the first defibrillation, but before the second defibrillation a significant difference was found between swine with ACO and control swine [101]. After the first defibrillation, 2 minutes of uninterrupted CPR at a metronome-guided rate of 100/min was administered, therefore the

TABLE 4.4: AUCs of single waveform parameters combined with clinical characteristics

WFP_1 + Amiodarone	**AUC [95%CI] n=98**	**WFP_1 + SS**	**AUC [95%CI] n=101**	**WFP_1 + EMS response time**	**AUC [95%CI] n=92**
AMSA	0.64 [0.53; 0.75]	AMSA	0.65 [0.54; 0.76]	AMSA	0.69 [0.58; 0.81]
MAA	0.62 [0.50; 0.73]	MAA	0.63 [0.51; 0.74]	MAA	0.66 [0.54; 0.77]
MdS	0.63 [0.52; 0.75]	MdS	0.64 [0.53; 0.76]	MdS	0.68 [0.57; 0.79]
PSA	0.62 [0.51; 0.74]	PSA	0.64 [0.53; 0.76]	PSA	0.67 [0.56; 0.78]
VS	0.62 [0.51; 0.74]	VS	0.64 [0.53; 0.76]	VS	0.68 [0.57; 0.79]
DFAα_1	0.64 [0.53; 0.75]	DFAα_1	0.63 [0.52; 0.74]	DFAα_1	0.69 [0.59; 0.80]

AUC = Area under the curve, WFP = Waveform parameter, CI = Confidence interval, SS = Shock success, EMS = Emergency medical services, AMSA = Amplitude spectrum area, MAA = Mean absolute amplitude, MdS = Median slope, PSA = Power spectrum area, VS = Variance of slope, DFA = Detrended Fluctuation Analysis.

TABLE 4.5: AUCs with 95% CI of combined models (i.e. WFP+ΔWFP+CCF+ΔWFP*CCF) with EMS response time

Waveform parameter	**AUC [95%CI] n=55**
Amplitude spectrum area (AMSA)	0.76 [0.64; 0.89]
Mean absolute amplitude (MAA)	0.79 [0.66; 0.93]
Median slope (MdS)	0.79 [0.67; 0.91]
Power spectrum area (PSA)	0.75 [0.62; 0.89]
Variance of slope (VS)	0.73 [0.58; 0.87]
Detrended Fluctuation Analysis (DFA) α_1	0.73 [0.60; 0.87]

AUC = Area under the curve, CI = Confidence interval, WFP = Waveform parameter, CCF = Chest compression fraction, EMS = Emergency medical services.

parameters before the second shock indirectly include the change in waveform parameters in response to CPR. From these values before the second shock, they found that AMSA and slope were predictive of ACO with AUCs of 0.85 and 0.75 respectively [101]. In the predictive models including the change in waveform parameters, we found the best discriminative ability to be for the model combining MdS with ΔMds, CCF and CCF*ΔMdS, with an AUC of 0.75. This is lower than the best discriminative ability described in the animal study, however the experimental setting of animal studies provides for controlled conditions of the resuscitation. In all the swine in their study, CPR of good quality was achieved, while in our study we had to take the CCF into account with regard to the change in VF waveform parameters. Furthermore, induction of ACO in the animal study was all done according to the same protocol, by placement of a plug in the mid LAD artery, causing an occlusion in the arteries that supply the anterior wall. A previous study investigating the VF waveform characteristics with regards to localisation of a previous MI found that VF amplitude characteristics were lowest in the ECG leads adjacent to the region of previous infarction [29]. Since in our study localisation of ACO was not controlled, this could also contribute to the difference in discriminative ability between our study and the animal study.

Given this difference in VF amplitude characteristics according to ACO localisation, we investigated the influence of ACO localisation in a sub analysis. Since the recording direction during OHCA roughly corresponds to lead II in the 12 leads ECG (the area adjacent to the inferior wall), inferior coronary occlusions may show even lower VF characteristics than anterior or posterior coronary occlusions. Therefore, in the sub analysis patients with an inferior ACO were classified in one group, whereas patients with anterior and posterior ACO and patients without ACO were classified in the other group. The single waveform parameters and the combination with change in waveform parameters resulted in AUCs of 0.67 and 0.74, respectively, to identify an inferior ACO, similar to AUCs discriminating between ACO and non-ACO. Therefore, we conclude that the predictive model combining waveform parameters with their change performs equally well for different localisations of the ACO. A more extensive description of this sub analysis can be found in Appendix E.

4.4.2 Response time

In this study, response time differed between the two study groups and was therefore included as an explanatory variable. This led to a slight improvement of the discriminative ability when compared to the model of waveform parameters combined with their change in response to CPR without response time included (AUC=0.79 vs. AUC=0.75). However, response time only gives an indication of the actual arrest duration, and is often unknown. Given that VF waveform parameters are investigated as a proxy for arrest duration, inclusion of response time in the prediction model might not have clinical implication. Nonetheless, we tried to identify all variables that might offer an increase in discriminative ability for scientific purposes, to offer a theoretical discriminative ability.

4.4.3 Implications

Acute coronary occlusion is an important etiology for cardiac arrest [57]. Patients with VF based on an underlying coronary occlusion are advised to be taken to the catheterization laboratory as soon as possible [106], therefore early recognition of an underlying ACO is of significant importance. Even percutaneous coronary intervention (PCI) during mechanical CPR may be considered as a treatment option in patients with shock resistant VF. Considering that this is costly and resource consuming [107], identification of patients expected to benefit from this treatment (i.e. patients with ACO) is of great importance.

In this study, we have shown that in patients requiring more than 1 shock, providing the possibility to analyze the change in VF waveform parameters in response to CPR, analysis of the VF waveform may provide a method to identify patients with ACO early in the resuscitation. Furthermore, given that patients with acute MI resuscitated from cardiac arrest caused by ventricular fibrillation do not always show ST-segment elevation on a postresuscitation ECG [57, 108], VF waveform parameters might also provide additional information to discriminate between patients with and without ACO after the restoration of a normal, perfusing rhythm is acquired. Thus, the VF waveform may be used to ensure correct and early triage of patients to the cardiac catheterization laboratory, both in the field during resuscitation as early in the emergency department, potentially leading to an increase in survival after OHCA.

4.4.4 Limitations

The most important limitation is the patient selection in this retrospective study. Patients were excluded if insufficient information was available for group classification, and therefore only patients that are admitted to the hospital are included in this study. As a result, included patients have relatively favourable arrest characteristics.

Another limitation is the relatively small number of patients included in this study. Although 102 patients were selected with VF waveform parameters before the first shock, from only 60 patients the change in VF waveform parameters in response to CPR could be determined. Therefore the prediction model is based and tested on the same patients. For better testing of the discriminative ability of a logistic regression model, it would be better to divide the patients in a training set for developing of the model parameters, and a testing set to determine the discriminative ability of the model. However, dividing a group of 60 patients into a training and testing set would lead to an even smaller number of patients on which the model is be based.

4.5 Conclusion

Individual VF waveform characteristics offered a modest ability to discriminate between patients with and without ACO, with an AUC of 0.66. Combining this with the change in VF waveform characteristics in response to CPR led to a more clinically relevant discriminative ability, with an AUC of 0.75. Therefore, analysing VF waveform parameters and their change in response to CPR might provide a method to ensure distinction of these patients even before a perfusing rhythm is acquired, possibly leading to earlier revascularization. Further studies are needed to determine if the combination of waveform parameters and their change in response to CPR can predict the presence of an ACO in a prospective fashion, and whether this leads to improved survival after OHCA.

5 Discussion

This study first aimed to investigate the change in VF waveform measures in relation to CPR quality, and the difference in this between patients with and without underlying ACO. Secondly, this study aimed to assess the predictive ability of single waveform measures, and of the waveform measures combined with their change in response to CPR. Both study aims have (to our knowledge) never been described before in human OHCA based on VF.

Chapter 3 outlines the first study aim, by investigating the difference in change in VF waveform characteristics between patients with and without adequate CPR (i.e. chest compression fraction $\geq$ or < 0.6). This way the common situation during OHCA is investigated, where chest compressions need to be interrupted for rhythm analysis, intubation attempts or shock delivery. In patients with adequate CPR, an increase in all amplitude characteristics (AMSA, MAA, MdS, PSA and VS) was detected, while a decrease in most scaling analysis characteristics was detected (DFAα_1 and SDW). For the amplitude characteristics MAA, PSA and AMSA, this numeric increase was significantly higher in patients with CCF$\geq$0.6 compared to patients with CCF<0.6. Secondary analysis also revealed a difference in the response of VF characteristics to CPR between patients with and without an ACO, with a larger increase in VF amplitude characteristics in patients without ACO compared to patients with ACO after adequate CPR. These findings support the suggestion that the VF waveform is favourably affected by CPR, and show that this also applies in common situation with interruptions of chest compressions, as long as these interruptions are kept to a minimum. Furthermore, the difference in response of VF characteristics to CPR between patients with and without myocardial substrate may offer a method for early distinction of acute coronary occlusion. This is further investigated in Chapter 4.

In Chapter 4, we investigated the discriminative ability of the VF waveform to discriminate between patients with and without an underlying ACO during OHCA. The VF waveform characteristics were lower in OHCA patients with than without ACO, showing a limited discriminative ability with an AUC of 0.66. Combining the VF waveform parameter before the first shock with the change in that parameter in response to CPR led to an improved discriminative ability (AUC = 0.75). These findings suggests that the VF waveform may provide additional information to identify patients with underlying ACO, to ensure correct and early triage of these patients to the cardiac catheterization laboratory. Further studies are warranted to confirm these results in a larger population, and prospective studies are needed to determine if this will lead to an increase in survival after OHCA.

Furthermore, this is the first study investigating the difference in VF waveform between patients with and without ACO using scaling analysis characteristics. These characteristics have been used before to predict shock success or monitor CPR quality, but have never been investigated in relation to underlying heart disease. Even though DFAα_1 shows a difference between patients with and without ACO, performance of this parameter in differentiating these patients is not better when compared to other (more conventional) parameters.

6 Conclusion

This study showed that VF waveform amplitude characteristics were significantly increased when CCF was 0.6 or higher, while no increase was seen when CCF was lower than 0.6. These differences were also seen in a sub analysis in patients without ACO, while these differences were not found in patients with ACO. Including the change in VF waveform characteristics in response to CPR led to an improved predictive ability of the presence of an underlying ACO compared to using a single value of the VF waveform parameter. These findings suggest that electrocardiographic measures during VF OHCA in combination with CPR quality can provide a tool for early identification of patients with underlying ACO. Further studies are needed to determine if the combination of waveform parameters and their change in response to CPR can predict the presence of an ACO in a prospective fashion, and whether this results in an improved survival after OHCA.

A Detrended Fluctuation analysis

A.1 Introduction

Time series analysis comprises methods for analysing time series in order to extract meaningful statistics and other characteristics of the data. Descriptions of the time series can help in obtaining an understanding of the underlying forces and structure that produced the observed signal [109]. One often-used method is describing the frequency-content of the signal. This is done by Fourier transforming the signal, to display periodic-like behaviour in the time-domain as a peak in the frequency-domain. The squared absolute value of the Fourier transform represents the power spectrum of the signal [110].

One of the main issues in applying Fourier analysis is that this method is established for stationary signals. Stationarity means that the signal is roughly similar in different time windows, i.e. the mean, variance, power and standard deviation do not change over time [109]. Applying Fourier transformation on a signal that is non-stationary can lead to varying results, because the resulting power spectrum is dependent of the sampling frequency and the chosen length of the signal segment wished to be analyzed [111, 112].

This problem with stationarity was also noted by Peng et al. [80]. They were dealing with applying analysis on cardiac interbeat intervals, which is often highly nonstationary. They questioned whether this nonstationarity arises from changes in environmental conditions or from a complex nonlinear dynamical system. Only the fluctuations arising from the dynamics of the complex, multiple-component system should show long-range correlations. They introduced a modified root mean square analysis of an integrated signal - detrended fluctuation analysis - to detect the presence of these long-range correlation [80].

Computation of detrended fluctuation analysis is as follows: First the global trend of the original time series is eliminated by subtracting the mean of the signal. This signal is integrated by taking the cumulative sum of the signal (Figure A.1a). The resulting signal is divided into equal boxes of length n, for various values of n. In each box the local linear trend is calculated and subtracted from the integrated time series. Of this detrended signal the root mean square (RMS) is calculated representing the fluctuation in that box size (Figure A.1b). This is repeated for several box sizes n (different scales) (Figure A.1c). A relationship between $F(n)$, the fluctuation as a function of box size, and the box size n (i.e. the number of samples in a box which is the size of the window of observation) is plotted on logarithmic axes. The DFA scaling exponent α is the slope of the trend line of this function estimated using linear regression (see Figure A.2).

A.2 Example of DFA on mathematical signals

A.2.1 Linear function

First, we take a linear function, say $y = 2x$, which is symmetrically around zero (see Figure A.3a). This function has an equal number or negative and positive samples, therefore the mean is zero. The integral of a discrete signal can be determined by taking the cumulative sum of the signal, which for a linear function gives us a parabola (see Figure A.3b). The

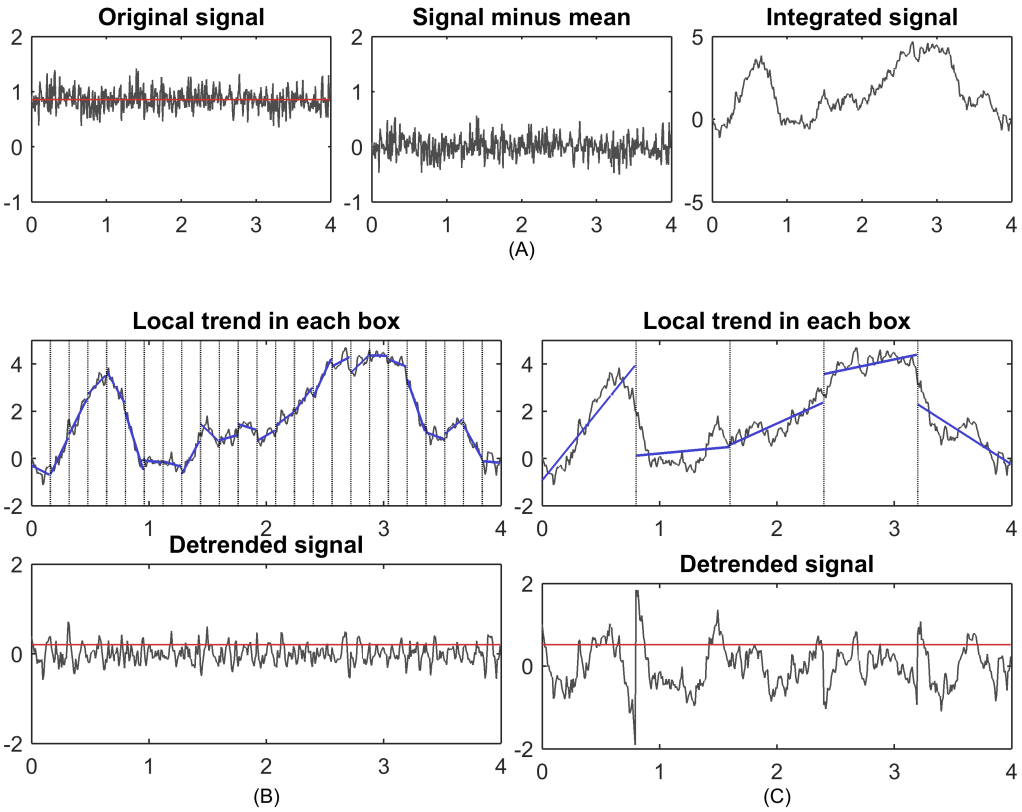

FIGURE A.1: Step-wise explanation of Detrended Fluctuation Analysis. In panel A, the mean is subtracted from an example signal sampled at 125 Hz with a duration of 4 seconds (left and middle plot). The right plot shows the resulting integrated signal. In panel B, the local trends of the integrated signal from panel A are calculated (blue lines) and subtracted (bottom figure) for box size≈0.2 s (20 samples). In panel C this is shown for box size=0.8 s (100 samples). In the bottom plots of B and C, the root-mean-square of the detrended signal is presented as the red line.

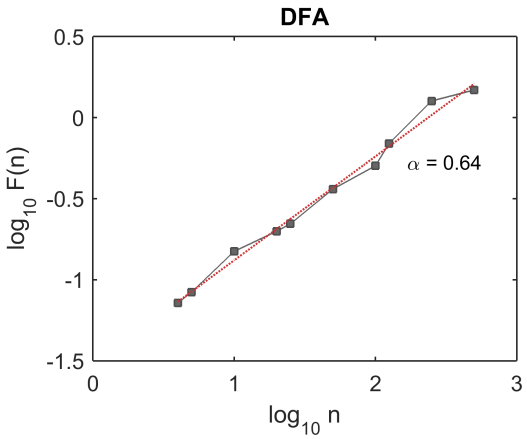

FIGURE A.2: DFA on the example signal of Figure A.1.

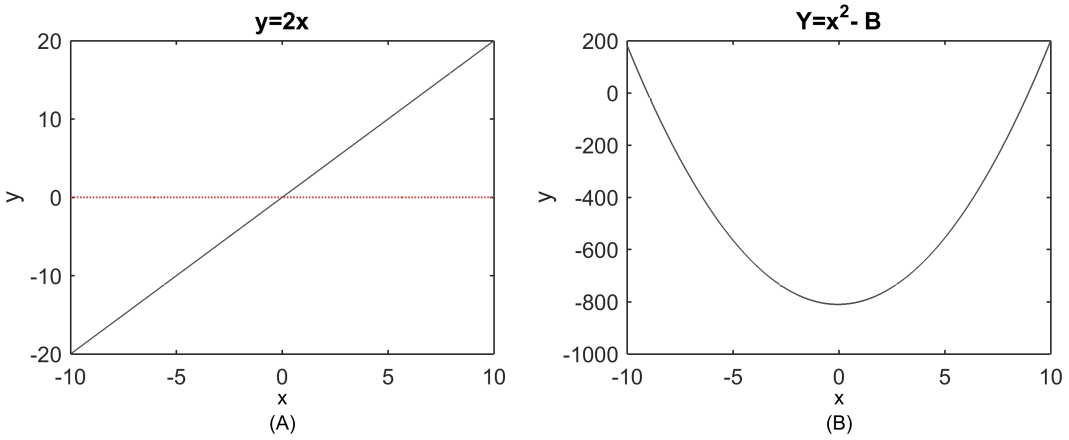

FIGURE A.3: The linear function $y = 2x$ (A) - with in red the mean of the signal - and its integral $y = x^2 - B$ (B).

mathematical integral of this function is given in Equation (A.1):

$$\int 2x\, dx = x^2 - B, \tag{A.1}$$

with the constant *B* determining the horizontal translation of the parabola.

The next step of DFA is dividing the signal into boxes of equal length and subsequently calculating and subtracting the local linear trend. An example of a segment of signal divided in box length A is given in Figure A.4a. This segment contains the same amplitude-properties when it is moved along the x-axis to center around zero, so the beginning and end points of the signal can be stated as $-\frac{A}{2}$ and $\frac{A}{2}$ (see Figure A.4b). The linear trend in this segment can be seen in Figure A.4c, and the remaining signal after subtracting this trend is shown in Figure A.4d. The translation of the signal will change the function y to a function shaped like $y-(ax+b)$. Subtracting the linear trend will result in removal of the ax term. Therefore, detrending a segment of a parabola will result in a new parabola.

This parabola can be described with the formula:

$$y_A = x^2 - B_A, \tag{A.2}$$

with constant B_A and therefore y_A dependent on the box length A. Note: in discrete samples, this is only true for box sizes that contain more than 3 samples.

The value for B_A represents the horizontal displacement of the graph, and it's value can be expressed as a function of A by solving Equation (A.3):

$$\int_{-\frac{A}{2}}^{\frac{A}{2}} x^2 - B_A\, dx = 0. \tag{A.3}$$

Calculating this integral and solving it over the interval $\left[-\frac{A}{2}, \frac{A}{2}\right]$ gives:

$$\begin{aligned}
\left[\frac{1}{3}x^3 - B_A x + C\right]_{-\frac{A}{2}}^{\frac{A}{2}} &= 0 \\
\frac{1}{3}\left(\frac{A}{2}\right)^3 - B_A\frac{A}{2} + C - \left(\frac{1}{3}\left(\frac{-A}{2}\right)^3 - B_A\frac{-A}{2} + C\right) &= 0 \\
\frac{1}{24}A^3 - \frac{B_A A}{2} + C - \left(-\frac{1}{24}A^3 + \frac{B_A A}{2} + C\right) &= 0 \\
\frac{2}{24}A^3 - B_A A &= 0 \\
B_A A &= \frac{1}{12}A^3 \\
B_A &= \frac{1}{12}A^2. \qquad \text{(A.4)}
\end{aligned}$$

The last step of DFA is calculating the root-mean-square for each box length A. The general formula to calculate root mean square is:

$$RMS = \sqrt{\frac{1}{n}\sum_{n=1}^{n} x_n^2}. \qquad \text{(A.5)}$$

The summation of all samples on a segment $\left(\sum_{n=1}^{n} x_n^2\right)$ can be calculated by taking the integral over the length of this segment $\left[-\frac{A}{2}, \frac{A}{2}\right]$, and the formula for the specific segment

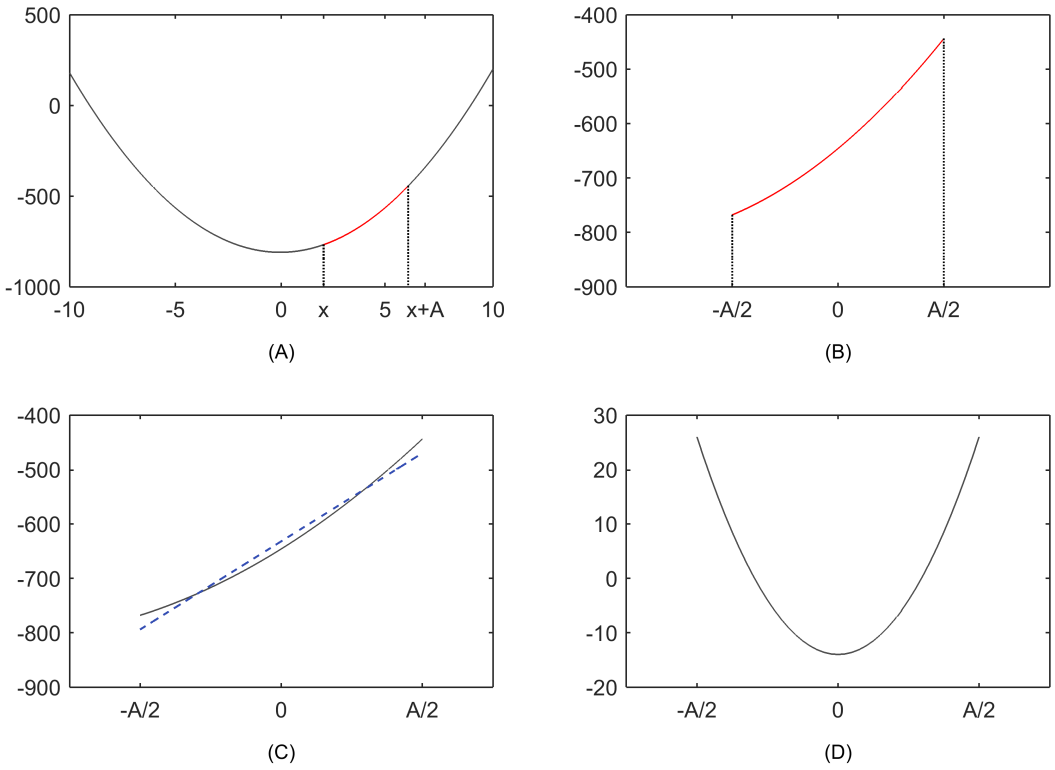

FIGURE A.4: Example of detrending a segment of $y = x^2 - B$ for box length A. (A) A segment of the integrated signal $y = x^2 - B$ with box size A. (B) The segment of (A) moved along the x-axis. (C) The segment of (A) with its local linear trend in blue. (D) The segment of (A) with its linear trend subtracted.

given in Equation (A.4) can be substituted to form the following equation for RMS:

$$RMS(A) = \sqrt{\frac{1}{A}\int_{-\frac{A}{2}}^{\frac{A}{2}} \left(x^2 - B_A\right)^2 \, dx}. \tag{A.6}$$

This can be simplified by calculating a value for the integral over $\left(x^2 - B_A\right)^2$, with the substitution of B_A for the value found in Equation (A.4). The solution of the integral in terms of box length A is given by:

$$\begin{aligned}
\int_{-\frac{A}{2}}^{\frac{A}{2}} \left(x^2 - B_A\right)^2 \, dx &= \int_{-\frac{A}{2}}^{\frac{A}{2}} \left(x^2 - \frac{1}{12}A^2\right)^2 \, dx \\
&= \int_{-\frac{A}{2}}^{\frac{A}{2}} x^4 - \frac{1}{6}A^2x^2 + \frac{1}{144}A^4 \, dx \\
&= \left[\frac{1}{5}x^5 - \frac{1}{18}A^2x^3 + \frac{1}{144}A^4x + C\right]_{-\frac{A}{2}}^{\frac{A}{2}} \\
&= \frac{1}{5}\left(\frac{A}{2}\right)^5 - \frac{1}{18}\left(\frac{A}{2}\right)^3 A^2 + \frac{1}{144}\left(\frac{A}{2}\right)A^4 + C - \\
&\qquad \left(\frac{1}{5}\left(\frac{-A}{2}\right)^5 - \frac{1}{18}\left(\frac{-A}{2}\right)^3 A^2 + \frac{1}{144}\left(\frac{-A}{2}\right)A^4 + C\right) \\
&= \frac{1}{5}\frac{A^5}{32} - \frac{1}{18}\frac{A^5}{8} + \frac{1}{144}\frac{A^5}{2} + C - \left(-\frac{1}{5}\frac{A^5}{32} + \frac{1}{18}\frac{A^5}{8} - \frac{1}{144}\frac{A^5}{2} + C\right) \\
&= \frac{1}{5}\frac{A^5}{16} - \frac{2}{144}A^5 + \frac{1}{144}A^5 \\
&= \frac{1}{80}A^5 - \frac{1}{144}A^5 \\
&= \frac{1}{180}A^5.
\end{aligned} \tag{A.7}$$

Substituting the integral with this value in the formula for RMS as a function of box size A given in Equation (A.6) leads to:

$$\begin{aligned}
RMS(A) &= \sqrt{\frac{1}{A}\frac{1}{180}A^5} \\
&= \sqrt{\frac{1}{180}A^4} \\
&= \sqrt{\frac{1}{180}}A^2 \\
&= \frac{1}{6\sqrt{5}}A^2.
\end{aligned} \tag{A.8}$$

This equation shows that the root mean square increases quadratically with increasing box size A. Plotting this on a double logarithmic scale would result in a linear graph that increases with a slope of exactly 2.

An example of detrended fluctuation analysis calculated on a discrete signal with the function $y = 2x$ in MATLAB is shown in Figure A.5. The calculated slope is 2.02, which deviates slightly from the theorized value of exactly 2. This difference is caused by the effect of discretization of the signal. Therefore it may be concluded that a linear signal will have a slope of 2 in detrended fluctuation analysis. This has been shown for $y = 2x$, but with logical reasoning one can conclude that this is true for all for all linear functions. Take for instance the function $y = 200x$, a linear function that is much steeper than the function from Figure A.3a.

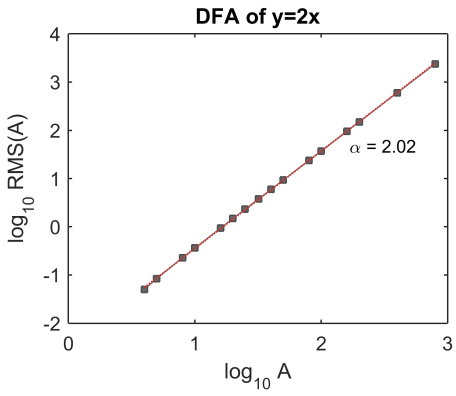

FIGURE A.5: DFA of the linear signal $y = 2x$.

However, in the detrending step of DFA, the calculated trend will also be 100 times as steep, and subtracting this will lead to the same detrended signal.

A.2.2 Quadratic function

As a next step we want to show a function that is still a smooth function but is somewhat more complex, therefore we chose the quadratic function $y = x^2$. This is the same parabola as the integrated version of $y = 2x$.Mathematically we expect the integral of this function to look like the function $\frac{1}{3}x^3$. However, before integrating we subtract the signal mean. The mean being a constant, this introduces another factor in the original function that needs to be integrated, which can be seen in the following equation:

$$\int x^2 - M \, dx = \frac{1}{3}x^3 - Mx - C. \tag{A.9}$$

The extra factor Mx is a linear factor, and therefore will disappear in linear detrending. Thus, introducing a constant factor does not change the slope of the DFA curve. Since Peng et al. introduced DFA to investigate relationships in cardiac interbeat intervals [80], we expect that subtracting the mean is a step implemented for near-oscillatory data. Without subtracting the mean, integrating the signal would lead to a signal that has an increasing trend. However, since this does not influence the slope of the DFA curve because of linear detrending, this step seems unnecessary. Therefore in this example we ignore this step and integrate the signal without subtracting the mean, which can be seen in Figure A.6 and the mathematical representation in the following equation:

$$\int x^2 \, dx = \frac{1}{3}x^3 - C. \tag{A.10}$$

Similar to with the integral of the linear function, we can look at the detrended segment for different box sizes. For a box size that is small, the line will look smooth and subtraction of the linear trend will result in a detrended signal that is similar to a parabola, see Figure A.7a and A.7b. However, for a box size that is larger, the segment will contain some sort of different curve. This affects the local linear trend that is calculated and as a result, the detrended signal will not be an exact parabola like in the other segments, see Figure A.7c and A.7d. This causes the RMS of the detrended signal to not increase quadratically as shown in Section A.2.1. This can be seen in Figure A.8, where the increase in RMS for the last two box sizes starts to deviate from the slope of 2.

Theoretically, when the box size is made infinitely small, every signal will display linear behaviour, therefore the slope over these boxsizes will be exactly two. However, in most physiological measurements the minimal boxsize is limited by the sample frequency of the

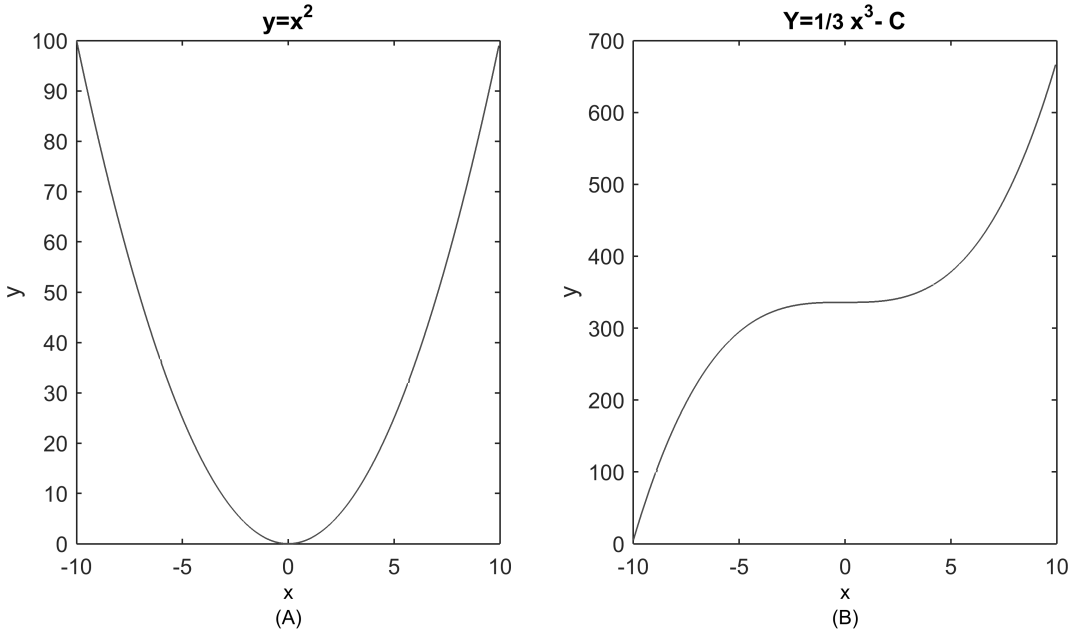

FIGURE A.6: Quadratic function $y = x^2$ (A) and its integral $Y = \frac{1}{3}x^3 - C$ (B).

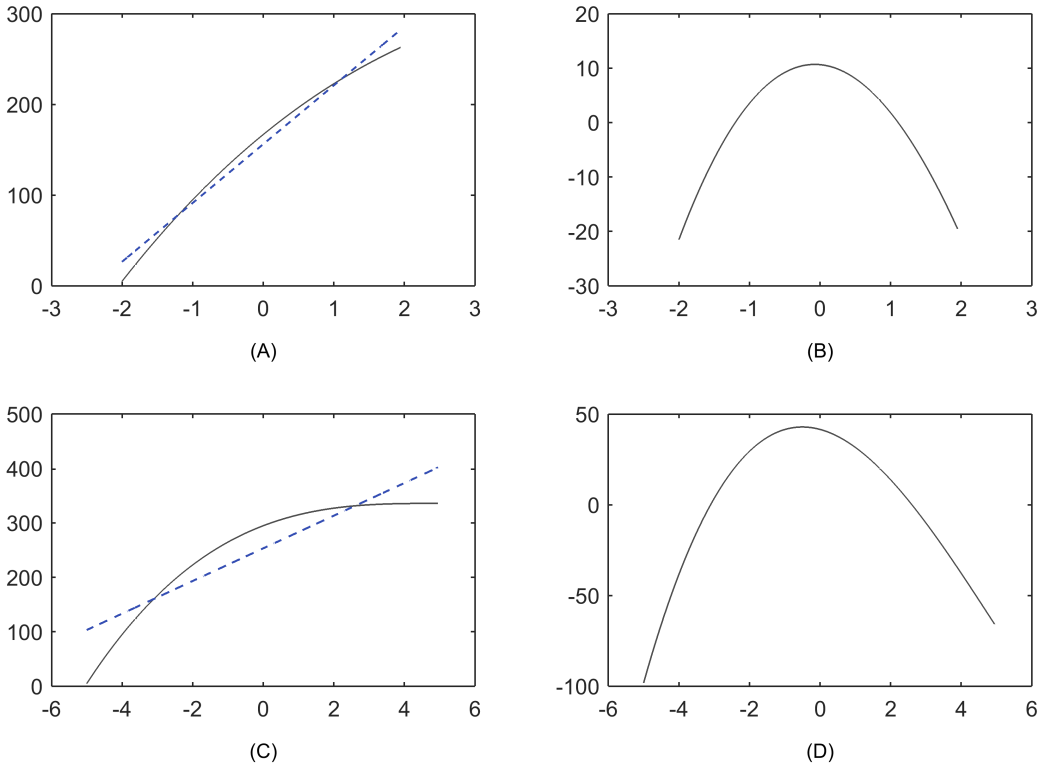

FIGURE A.7: Detrending of different segments of $y = \frac{1}{3}x^3$. (A) Segment of the integrated quadratic signal and its linear trend for small box size (i.e., the signal is divided into 5 segments). (B) Detrended segment for small box size. (C) Segment of the integrated quadratic signal and its linear trend for large box size (i.e., the signal is divided into 2 segments). (D) Detrended segment for large box size.

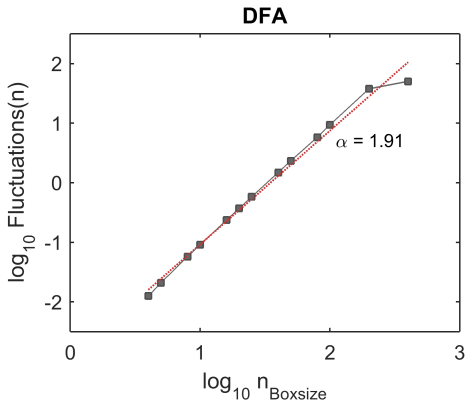

FIGURE A.8: DFA of $y = x^2$.

recording device. A linear trend can only be calculated over a signal of more than two samples, therefore the lower limit for box size was set at 4 samples. This means that the smallest box size possible in seconds is 4 divided by the sample frequency. For a very disorganized or high-frequent signal, this may be not small enough to represent the parabola pattern and will therefore not exhibit the scaling exponent of 2 for the (relatively) small box sizes.

A.2.3 Sinusoidal signal

We saw that DFA gave a slope of (theoretically) exactly 2 for a linear signal, but that the slope deviates slightly when the function becomes less linear.

A different kind of function is a repetitive waveform, e.g. a sine function. Subtracting the mean from this signal would result in a function oscillating around zero. In this example, the calculation and subtraction of the local trend is most deviant from the linear signal. See Figure A.9. For very small box sizes, the subtraction of local trends will lead to parabolic segments, and therefore the root-mean-square will increase exponentially with box size. However, this will not be true when the box size increases to a size where it captures more of the signal than just the linear increasing or decreasing part. Moreover, when the box sizes equals one period of the sine wave, the direction of the signal is as much negative as positive, therefore the local trend is a flat line (see Figure A.9a). The root mean square of the detrended signal is therefore equal to the root-mean-square of the sine function itself. The same is true if the box size is a multiple of one period of the sine wave, e.g. as in Figure A.9b. A different situation occurs when the box size is not equal to (a multiple of) one period of the sine wave. Dependent on which segment of signal looked at, it will contain more positive or more negative numbers, and therefore the local trend will not be zero. This can be seen in Figure A.9c. The detrended signal for the box size shown in Figure A.9c can be seen in Figure A.9d. This will lead to a RMS that is smaller than the RMS of the signal itself. If the box size becomes bigger, the amount of extra positive or negative numbers becomes smaller in proportion to the rest of the segment, therefore the local trend is less affected. This leads to the local trend approaching zero, and the RMS approximating the RMS of the original signal. Applying this logic, the RMS will slightly increase with increasing box size, until the maximum of the RMS of the original signal. An exception occurs when one box size exactly equals one period of the sine wave, in which case the RMS will be highest and will remain equally high or lower for a bigger box size. Therefore, after a certain tipping point, i.e. when box size becomes larger than one period of the sine wave, the slope of the RMS as a function of box size will decrease and approximate zero. The deviation from zero is (in discrete signals) dependent on the frequency and the total length of the signal. An example of a sine wave of the same frequency but for a different signal length can be seen in Figure A.10a.

Another factor influencing the shape of the DFA curve of a sine wave is the frequency. As mentioned previously, once the box size is larger than one period of sine, the RMS of the detrended signal will stop increasing with box size. Since one period of a sine wave (T)

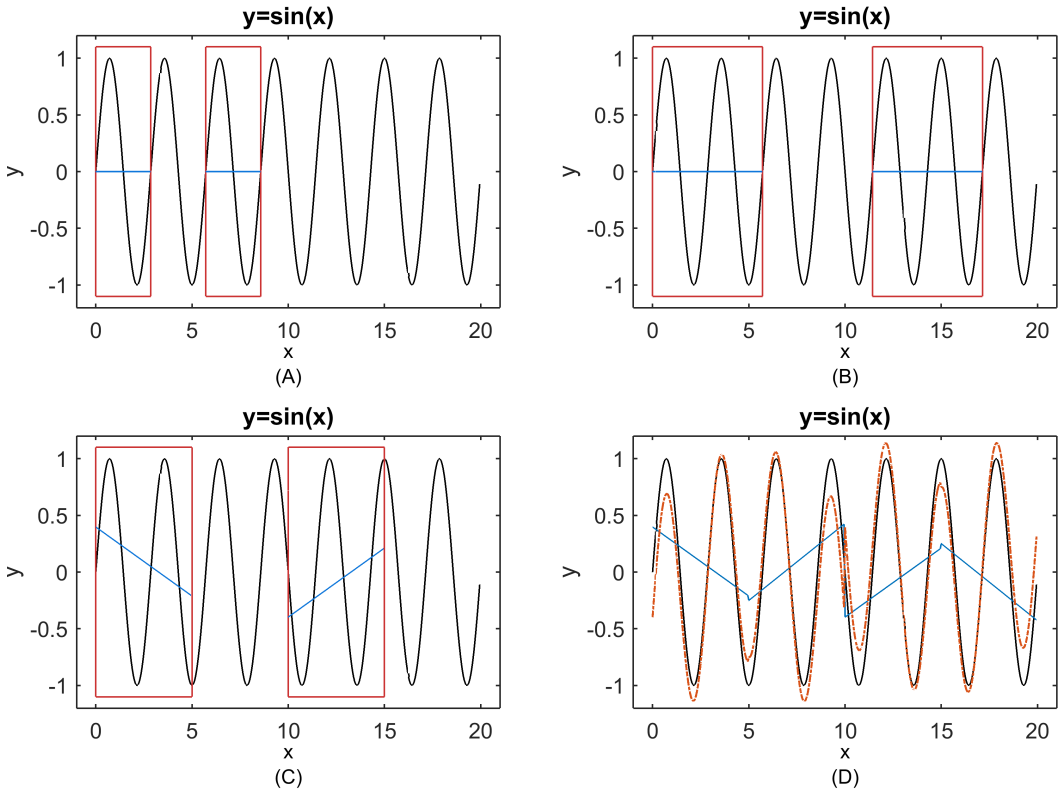

FIGURE A.9: Detrending of the sine function for different box lengths. (A) Sine with local trend for one period of the wave. (B) Sine with local trend for two periods of the wave. (C) Sine with local trend for a segment longer than one period of the wave. (D) Sine wave detrended for a box length that is not exactly one period of the sine wave.

is dependent on the frequency ($T = \frac{1}{f}$), the box size after which the increase of RMS will stagnate is smaller for a sine wave of a higher frequency. An example of this can be seen in Figure A.10b.

Because of the different shape of the DFA curve for sinusoidal signals, when describing such a signal it would be best to report two slope coefficients, i.e. α_1 for the slope of the smaller box sizes and α_2 for the slope of the larger box sizes (larger than one period of the sine wave).

A.3 Example of DFA on white noise

In a white noise signal x_t there is no correlation between subsequent samples. The odds of one sample being higher than the previous one is just as big as the odds of it being lower, without correlation to the previous samples. Integrating this signal, i.e. taking the cumulative sum ($Y_t = x_1 + \cdots + x_t$), results in a signal that in mathematics is known as a random walk (see Figure A.11b).

In all signals, the variance at a certain time t can be found by taking the variance of the summation of all point until that time t:

$$\text{var}(Y_t) = \text{var}(x_1 + x_2 + \cdots + x_t).$$

When there is no correlation between subsequent samples, as is the case in a random walk, the variance at time t can be calculated by summing the variance of each individual point:

$$\text{var}(Y_t) = \text{var}(x_1) + \text{var}(x_2) + \cdots + \text{var}(x_t) = \sum_{i=1}^{t} \text{var}\, x_i. \tag{A.11}$$

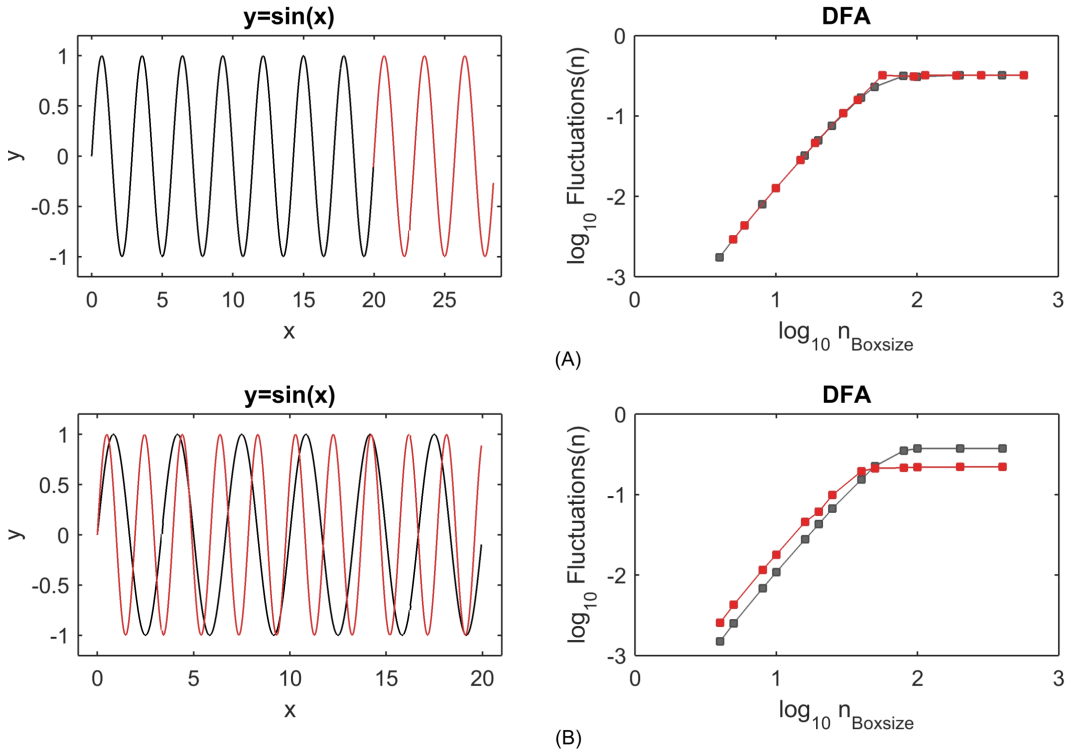

FIGURE A.10: (A) DFA of sine waves of different signal lengths, with in red the longer signal. (B) DFA of sine waves of different frequencies, with in red the signal with a higher frequency.

Since the number of variances added to calculate the variance at time t is dependent on t, Equation (A.11) can also be written as:

$$\text{var}(Y_t) = t \sum_{i=1}^{t} \text{var}\, x_i. \tag{A.12}$$

The variance can be estimated (when $x_1, x_2, \ldots, x_N$ are known) as:

$$\text{var}(x) = \frac{1}{N} \sum_{i=1}^{N} (x_i - \bar{x})^2, \tag{A.13}$$

with $\bar{x}$ the mean of x. Since we subtract the mean in DFA, we can derive that the equation for RMS (Equation (A.5)) equals the square root of the variance (i.e. standard deviation). Therefore it seems prudent to assume that the RMS is expected to increase in time with $\sqrt{t}$. An increase with a square root factor is equal to an exponential factor of 0.5, which will result in a slope of 0.5 on a double logarithmic scale. This is shown in Figure A.11c.

A.4 How to interpret α

When investigating DFA exponents for physiological measurements, one should consider the type of signal that is measured. If no clear relation is expected and the measured signal is not expected to be oscillatory, the slope of the DFA curve (α) will give information about the smoothness of the signal (i.e. if α approximates 2, the signal is a smooth function and if α approximates 0.5 the signal may be a random distribution of values). If the signal is expected to be oscillating, one should consider reporting separate slopes for the smaller and larger box sizes, i.e. α_1 for the smaller and α_2 for the larger box sizes.

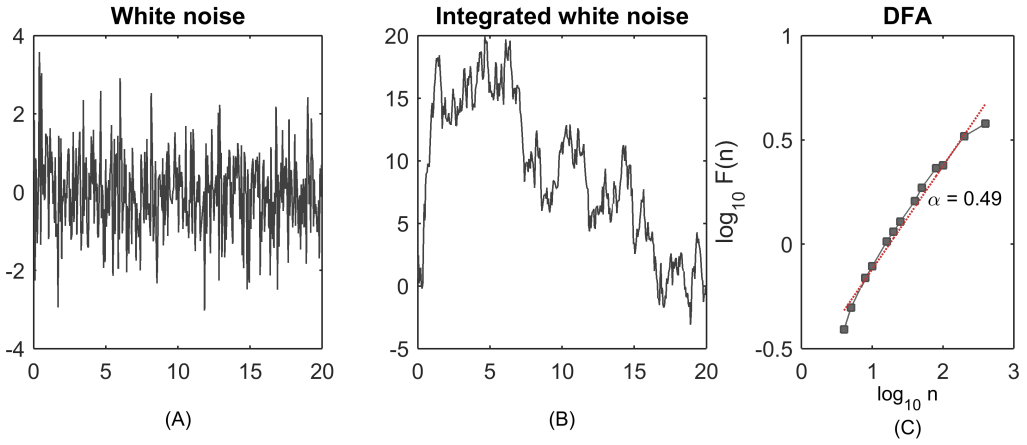

FIGURE A.11: Integration and Detrended Fluctuation Analysis of white noise. (A) Example of white noise, sampled at 20 Hz for 20 seconds. (B) Integration of the same white noise signal. (C) Detrended Fluctuation Analysis of white noise, which shows an α of approximately 0.5.

The first DFA exponent, α_1, gives information about the signal for the smaller box sizes. When this signal is a relatively smooth function, it will resemble a parabola and therefore the α_1 will be almost two. If the signal is more noisy or is more complex on a smaller level, the α_1 will be lower than two. The second DFA exponent, α_2, gives information about the signal for the larger box sizes, i.e. when the box size becomes larger than one period of the oscillating signal. If the signal is more complex, e.g. changing amplitude per period, the α_2 will not decrease so much towards zero, and will be higher than for more homogeneous signals.

A.5 Use of DFA in VF analysis

Several studies show that changes in VF waveform parameters give information about the myocardial state and survival [15, 68, 96, 98], suggesting that it is a dynamical system [77]. Therefore the VF signal measured during the resuscitation period will most likely be a non-stationary signal. Therefore the stationarity-assumption of Fourier transformation is not met. Therefore the application of DFA on VF signals might give more information.

How unorganized ventricular fibrillation may seem, there is still some organization in the signal; some sort of oscillation. Therefore, we expect the DFA-slope to decrease after a certain box size, similar to the sine signal. However, even if the box size covers exactly one period of this oscillation, since VF is so unorganized the next period will be different in length, amplitude or other factors. Therefore, the RMS will still increase with box length and the slope will not totally decrease to zero. It is expected that for VF signals with more organization, the slope will decrease more towards zero than for signals that are more unorganized.

As an example two VF signals are shown in Figure A.12, one of which has a (relatively) high AMSA (21.6 mVHz) and the other a (relatively) low AMSA (4.5 mVHz). Since VF is an oscillatory signal, the DFA curves of Figure A.12c indeed show a decrease of the slope after a certain box size. Therefore α_1 is determined for smaller box sizes (4 - 47 samples, i.e. 0.032 - 0.4 seconds) and α_2 is determined for larger box sizes (47-376 samples, i.e. 0.4 - 3.0 seconds). In the DFA analysis of Figure A.12c, it can be seen that the curves have a different height, a different slope in the first part of the graph (α_1 is 1.18 and 1.47) but a similar slope in the second part of the graph (α_2 is 0.069 and 0.084).

A possible explanation for the large difference in AMSA and not-so-large difference in DFA slopes between the two signals is that the AMSA is very dependent on the signal amplitude, since it is a combination measure of amplitude and frequency. In DFA the slope of the curve is investigated, therefore this measure is not so much dependent on the amplitude of the

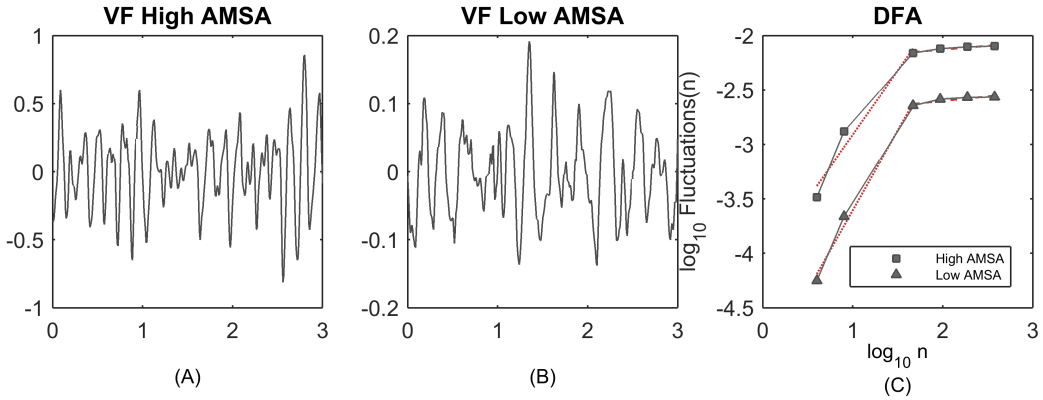

FIGURE A.12: (A) VF with high AMSA (21.6 mVHz), (B) VF with low AMSA (4.5 mVHz), with both time in seconds on the x-axis and voltage in millivolts on the y-axis, C) DFA of both signals, the squares indicating the DFA of the high AMSA VF and the triangles indicating the DFA of the low AMSA VF. The high AMSA VF has a α_1 of 1.18 and a α_2 of 0.069, the low AMSA VF has a α_1 of 1.47 and a α_2 of 0.083

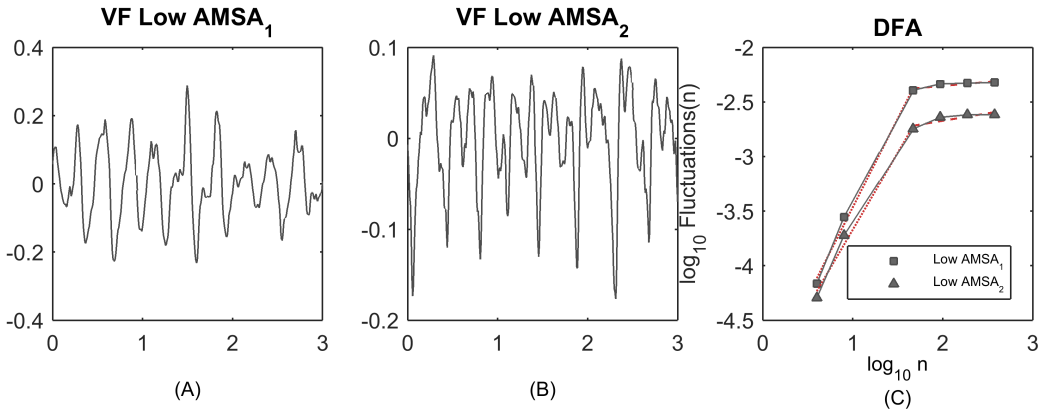

FIGURE A.13: (A) VF with low AMSA (4.4 mVHz), but relatively organized, (B) VF with low AMSA (4.1 mVHz) but relatively unorganized (C) DFA of both signals, the squares indicating the DFA of the VF in the left figure and the triangles indicating the DFA of the VF in the middle figure. The VF of (A) has a α_1 of 1.63 and a α_2 of 0.073, the VF of (B) has a α_1 of 1.41 and a α_2 of 0.137.

signal. The DFA most likely gives more information about the morphology of the signal. When visually inspecting the two VF signals it indeed appears that the two signals do not differ much in organization.

In another example, we look at two VF segments that have a similar value in AMSA, but different signal morphology. This is shown in Figure A.13.The VF signal of Figure A.13a appears visually more organized, or less complex, than the VF signal of Figure A.13b. The DFA analysis shows similar values for α_1 (1.63 and 1.41), but different values for α_2 (α_2 for left figure is 0.073, α_2 for middle figure is 0.137). The lower value for α_2 in the left figure indicates a more organized signal, which agrees with our visual examination.

A.6 Discussion and conclusion

In this chapter we investigated characteristic behaviour of detrended fluctuation analysis on different signals. We have shown that linear functions have a scaling exponent of exactly 2. On smaller box sizes, smooth functions also approximate this scaling exponent. When the signal contains more noise and/or is more complex on the smaller scales, the scaling exponent will be lower. For a complete white noise signal, the scaling exponent will

approximate 0.5. For a sine signal the DFA curve reaches a plateau after a certain box size, i.e. a box size larger than the period of the sine wave. For sinusoidal signal with noise or a combination of sines, the second slope of the DFA curve (i.e. the slope of the plateau) shows how similar the signal is to a single sine wave.

Detrended fluctuation analysis has been used for VF waveform analysis in a few studies. A study of Lin et al. in 2010 showed lower values of α_2 in subjects with successful defibrillation, but no difference in α_1 [78]. They found a similar discriminative ability for DFAα_2 and AMSA to identify the presence of a successful defibrillation. Similarly to what is described here, they conclude that the second slope of DFA describes how similar a signal is to a sinusoidal wave. In a study by Endoh et al. in 2011, a different approach was used where no difference was made between the slope of the first and second part of the graph. They found a lower value of DFA in successful defibrillation episodes, after which they conclude that a more irregular, unpredictable and complex VF waveform is strongly associated with increased possibility of successful defibrillation [113]. Lower DFAα_2 values indicate more similarity to a sinusoidal wave, meaning less complex signals, therefore the conclusion of Endoh does not correspond to the results of Lin. A study not directly investigating defibrillation success is done by Hall et al. in 2011. They found lower values for DFA (similarly to Endoh et al., no α_1 or α_2 is shown) in patients with primary VF compared to patients with secondary VF, but did not find differences in the rate of shock success between these groups. They did find differences in long-term outcome, with 42% discharged alive in primary VF group versus no survivors in secondary VF group [114].

Unfortunately, the studies by Lin and Endoh do not report baseline characteristics and differences between patient population, while Hall only reports characteristics of the primary and secondary VF groups, and not differences between patients with successful and unsuccessful defibrillation within the primary VF group. Furthermore, the study by Lin reported the separate DFA α_1 and α_2 values, while Endoh and Hall did not make this distinction. Therefore it is difficult to compare these studies.

Given the limitations of these studies, DFA may not yet be suitable for clinical application in VF waveform analysis. However, since this method investigates the slope of a curve, it is not so much affected by the amplitude of the signal. Considering that the presence of an underlying inferior infarction greatly influences mainly the amplitude of the signal [25–27, 29, 104], it may be worthwhile to further investigate this parameter in terms of prediction of for example shock success or arrest duration. Also in prediction of acute myocardial infarction it may be useful to combine DFA with established parameters as AMSA in an effort to further improve discriminative ability of the VF waveform.

B Acute coronary occlusion categorisation criteria

Included patients were firstly categorised according to the presence of a myocardial infarction (MI), following the criteria of the 3rd universal definition of myocardial infarction [41]:

- Detection of a rise and/or fall of cardiac troponin with at least one value above the 99th percentile upper reference limit and with at least one of the following:
  - Symptoms suggestive of ischaemia, as determined using the ambulance or emergency department (ED) notes.
  - New or presumed new ST segment or T wave changes in two contiguous leads or new left bundle branch block (LBBB), as determined on the ambulance or ED ECG.
  - Development of pathological Q waves on the ECG.
  - Imaging evidence of new loss of viable myocardium, as determined on echocardiography or coronary angiography (CAG).
  - Identification of an intracoronary thrombus by acute angiography or on autopsy.
- Cardiac death with symptoms suggestive of myocardial ischaemia or presumed new ischaemic ECG changes or new LBBB, but death occurred before cardiac biomarkers were obtained, or before cardiac biomarker values would be increased.

Subsequently, we assessed whether a patient had evidence of an acute coronary occlusion (ACO), according to the following criteria, of which one had to be present to be categorised in the ACO group:

- ST-segment elevation according to current guidelines: new ST-elevation at the J-point in two contiguous leads with the cut-points: $\geq$0.1 mV in all leads other than leads V2–V3 where the following cut points apply: $\geq$0.2 mV in men $\geq$40 years; $\geq$0.25 mV in men <40 years, or $\geq$0.15 mV in women) as determined on ambulance or ED ECG.
- Identification of an intracoronary thrombus or acute occlusion, as identified by an experienced interventional cardiologist on acute CAG or by a pathologist on autopsy.

All patients meeting the criteria for MI as well as the criteria for ACO were assigned to the ACO group, whereas all other patients were assigned to the patient group without ACO.

C Flowchart sub-analysis acute coronary occlusion

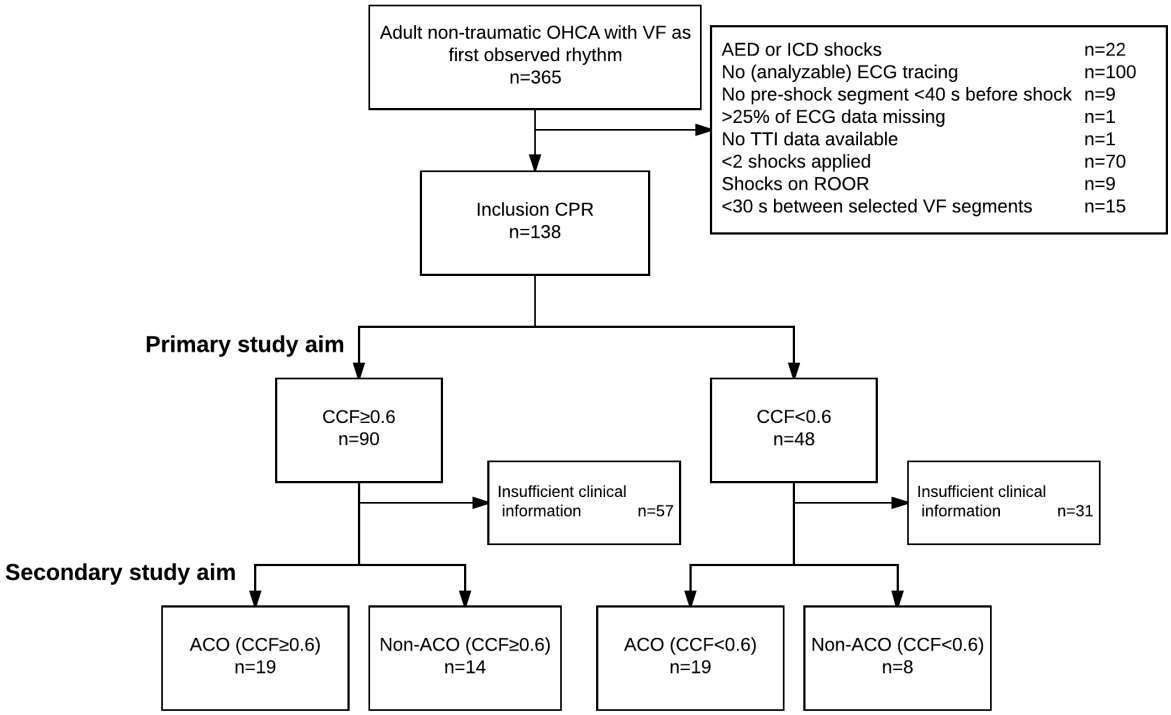

FIGURE C.1: Flowchart patient inclusion. OHCA = Out-of-hospital cardiac arrest, VF = Ventricular fibrillation, AED = Automated external defibrillator, ICD = Implantable cardioverter defibrillator, ECG = Electrocardiogram, TTI = Transthoracic impedance, ROOR = Return of organized rhythm, CPR = Cardiopulmonary Resuscitation, CCF = Chest compression fraction, ACO = Acute coronary occlusion.

D Change in VF waveform characteristics of OHCA-patients with or without an underlying acute coronary occlusion

TABLE D.1: Change in VF waveform characteristics of OHCA-patients with or without an underlying ACO

ΔWFP	**ACO (n=38)**	**Non-ACO (n=22)**	**p-value**
	Amplitude characteristics		
ΔAMSA	1.29 (-0.56 – 4.04)	1.34 (-0.38 – 5.09)	0.937
ΔMAA	0.01 (-0.01 – 0.03)	0.02 (-0.01 – 0.06)	0.284
ΔMDS	0.57 (-0.26 – 1.16)	0.86 (-0.12 – 2.45)	0.250
ΔPSA	0.02 (-0.01 – 0.07)	0.02 (-0.02 – 0.14)	0.547
ΔVS	0.02 (-0.01 – 0.09)	0.04 (-0.01 – 0.10)	0.448
	Frequency characteristics		
ΔDF	0.33 (-0.33 – 1.66)	0.50 (-0.66 – 1.58)	0.660
ΔMDF	0.33 (-0.66 – 1.00)	0.33 (-0.33 – 1.33)	0.674
ΔFR	0.05 (-0.34 – 0.30)	0.08 (-0.21 – 0.90)	0.255
	Scaling analysis characteristics		
Δ$DFA\alpha$	-0.03 (-0.09 – 0.04)	-0.04 (-0.09 – 0.03)	0.844
Δ$DFA\alpha_1$	-0.05 (-0.16 – 0.09)	-0.05 (-0.13 – 0.02)	0.764
Δ$DFA\alpha_2$	-0.01 (-0.04 – 0.01)	-0.01 (-0.03 – 0.01)	0.896
ΔSDW	-2.00 (-8.57 – 0.96)	-5.27 (-10.51 – 0.01)	0.158

Values are given in medians (interquartile ranges). VF = Ventricular fibrillation, OHCA = Out-of-hospital cardiac arrest, ACO = Acute coronary occlusion. AMSA = Amplitude spectrum area, MAA = Mean absolute amplitude, MdS = Median slope, PSA = Power spectrum area, VS = Variance of slope, DF = Dominant frequency, MdF = Median frequency, FR = Frequency ratio, DFA = Detrended fluctuation analysis, SDW = Scale distribution width.

E Discrimination of inferior coronary occlusion

In Chapter 4, we investigated the discriminative ability of (a combination of) VF waveform parameters to identify an underlying ACO in OHCA. This was based on several studies showing that VF waveform parameters were altered in the presence of an ACO [27, 30, 101]. However, these parameters are also dependent on the ECG lead direction [115]. Since the recording direction during OHCA roughly corresponds to lead II in the 12 leads ECG (the area adjacent to the inferior wall), inferior coronary occlusions may show even more alteration in VF characteristics than anterior or posterior coronary occlusions. Therefore, we performed an additional analysis for the same 102 patients, where in the ACO group the patients were subdivided according to the localisation of the occlusion. Patients with an inferior ACO were classified in one group, whereas patients with anterior and posterior ACO and patients without ACO were classified in the other group. Similar analysis as in Chapter 4 were used to determine whether (a combination of) VF waveform parameters could discriminate between inferior ACO and no inferior ACO. In this sub analysis, the results will be briefly discussed and will be regarded in relation to the results from Chapter 4 without extensively discussing all details and clinical implications.

The baseline characteristics of patients with an inferior ACO versus patients with anterior and posterior ACO together with patients without ACO can be found in Table E.1. Between patients with and without an inferior ACO, no differences occurred in EMS response time. In the patients without inferior ACO, a higher rate of first shock success, ROSC at arrival ED and 24 hour survival was found when compared to patients with inferior ACO.

The waveform parameters of patients with an inferior ACO versus patients with anterior and posterior ACO together with patients without ACO are shown in Table E.2. Similar to the difference between ACO and non-ACO patients, all the amplitude differences are significantly lower in patients with inferior ACO compared to patients without an inferior ACO. The frequency and scaling analysis characteristics show no significant differences between the groups.

Regarding the change in waveform parameters in response to CPR, a significant difference in increase in VF amplitude characteristics occurred between CCF$\geq$0.6 and CCF<0.6 in patients without inferior ACO, whereas this difference was not seen in patients with inferior ACO. These results are also similar to the differences between ACO and non-ACO patients.

The areas under the curve of the ROC curves of the single waveform parameters and the waveform parameters combined with change and CPR with corresponding 95% confidence interval can be found in Table E.3. Although the DFAα_1 did not differ between patients with and without inferior ACO, this parameter was still investigated to be able to compare the results with the original results from Chapter 4. All amplitude characteristics show a similar limited predictive ability, with PSA and VS showing the best predictive ability with an AUC of 0.67. The combination of the single waveform parameters with the change in that parameter in response to CPR was applied to the 60 patients from which the change in waveform parameter between the first and second shock could be determined (18 inferior ACO vs. 42 no inferior ACO). For all parameters, the combined model showed a higher AUC than the single WFP. Similar to the discrimination between ACO and non-ACO, the highest AUC is found for the combined model with MdS. This is slightly lower than the AUC of the same model for predicting ACO (0.75). Therefore the combination of a single waveform parameter with the change in that parameter in response to CPR is not better

in discriminating inferior ACO from no inferior ACO than discriminating ACO from non-ACO.

In the baseline characteristics of the patients in Chapter 4, a significant difference was found in EMS response time between patients with and without ACO. In this sub-analysis, no significant difference was found between patients with an inferior ACO compared to patients with anterior and patients without ACO. However, to be able to compare this sub analysis with the analysis in Chapter 4, here we also added the response time to the combined models to see whether this leads to an improved (theoretical) discriminative ability. The results are displayed in Table E.4. Similar to the discrimination of ACO and non-ACO, adding response time to the combined models leads to an improved discriminative ability for all waveform parameters. Furthermore, the AUCs of MdS, PSA and DFAα_1 are slightly higher than the AUCs of the model with response time discriminating ACO and non-ACO. However, as discussed in Chapter 4 (Section 4.4.2), using response time in the discrimination model might not be clinically relevant.

TABLE E.1: Baseline characteristics of patients with an inferior ACO versus patients with anterior and posterior ACO together with patients without ACO.

Variable	**All (n=102)**	**Inferior ACO (n=25)**	**No inferior ACO (n=77)**	**p-value**
Age (years)	61.5 (51 – 71.3)	66.0 (55.5 – 71.5)	61.0 (50.5 – 71.5)	0.228
Male gender (n=102)	73 (71.6)	19 (76.0)	54 (70.1)	0.572
		Pre-hospital		
Previous MI (n=92)	25 (27.2)	5 (25.0)	20 (27.8)	0.805
Public location arrest n=102	44 (43.1)	9 (36.0)	6 (45.5)	0.407
Witnessed arrest: n=99	86 (86.9)	20 (83.3)	66 (88.0)	0.510
- Bystander witnessed	84 (84.8)	20 (83.3)	64 (85.3)	0.754
- EMS witnessed	2 (2.0)	0 (0)	2 (2.7)	1.000
Bystander CPR n=99	66 (66.7)	16 (64.0)	50 (67.6)	0.744
Autopulse used n=99	31 (63.3)	7 (28.0)	24 (32.4)	0.679
Response time (min) n=92	8 (6 – 10)	8 (6 – 11.75)	8 (6 – 10)	0.419
Shocks delivered by EMS	3 (1 – 6)	4 (2 – 8)	3 (1 – 5)	0.101
Amiodarone n=98	64 (65.3)	17 (70.8)	47 (63.5)	0.513
Epinephrine n=99	79 (79.8)	21 (87.5)	58 (77.3)	0.386
Atropine n=98	24 (24.5)	11 (45.8)	13 (17.6)	0.005
		In-hospital		
12-leads ECG n=102	97 (95.1)	23 (92.0)	74 (96.1)	0.594
Coronary angiography n=102	74 (72.5)	16 (64.0)	58 (75.3)	0.270
Immediate CAG n=102	63 (61.8)	14 (56.0)	49 (63.6)	0.495
Delayed CAG n=102	11 (10.8)	2 (8.0)	9 (11.7)	1.000
PCI n=102	54 (52.9)	14 (56.0)	40 (51.9)	0.724
CABG n=102	2 (2)	0 (0)	2 (2.6)	1.000
Troponin I max n=98	19.5 (1.1 – 94.2)	20.3 (0.25 – 100)	15.6 (1.83 – 92.3)	0.873
Autopsy n=102	14 (13.7)	6 (24.0)	8 (10.4)	0.101
		Clinical outcomes		
First shock success n=101	50 (49.5)	7 (30.4)	43 (57.3)	0.024
ROSC at arrival ED n=102	81 (79.4)	13 (52.0)	68 (88.3)	0.000
Survival 24 hrs n=101	77 (76.2)	13 (52.0)	64 (84.2)	0.001
Survival at discharge n=102	49 (48.0)	10 (40.0)	39 (50.6)	0.354

Values are given in numbers (%) or medians (interquartile ranges). Troponin I is given in μg/L (measured with the (no longer available) Immulite 2000, DPC cardiac troponin I immunoassay). OHCA = Out-of-hospital cardiac arrest, ACO = Acute coronary occlusion, MI = Myocardial infarction, EMS = Emergency medical services, ECG = Electrocardiogram, CPR = Cardiopulmonary resuscitation, PCI = Percutaneous coronary intervention, CABG = Coronary artery bypass grafting, ROSC = Return of spontaneous circulation, ED = Emergency department.

TABLE E.2: Waveform parameters of patients with an inferior ACO versus patients with anterior and posterior ACO together with patients without ACO.

Waveform parameter	Inferior ACO (n=25)	No inferior ACO (n=77)	p-value
	Amplitude characteristics		
Amplitude spectrum area (AMSA)	7.83 (4.65 – 9.45)	10.81 (5.91 – 14.16)	0.014
Mean absolute amplitude (MAA)	0.09 (0.05 – 0.12)	0.11 (0.08 – 0.15)	0.023
Median slope (MdS)	2.52 (1.74 – 3.42)	4.06 (2.17 – 5.36)	0.014
Power spectrum area (PSA)	0.04 (0.02 – 0.07)	0.10 (0.03 – 0.19)	0.009
Variance of slope (VS)	0.05 (0.02 – 0.08)	0.09 (0.04 – 0.19)	0.012
	Frequency characteristics		
Dominant frequency (DF)	3.66 (2.99 – 5.15)	4.65 (3.32 – 6.15)	0.064
Median frequency (MdF)	4.32 (3.66 – 5.49)	4.65 (3.99 – 5.98)	0.261
Frequency ratio (FR)	0.26 (0.11 – 1.01)	0.26 (0.14 – 0.60)	0.776
	Scaling analysis characteristics		
Detrended Fluctuation Analysis (DFA) α_1	1.42 (1.30 – 1.53)	1.39 (1.26 – 1.48)	0.235
Detrended Fluctuation Analysis (DFA) α_2	0.07 (0.04 – 0.10)	0.07 (0.05 – 0.10)	0.759
Scale distribution width (SDW)	24.81 (19.80 – 30.12)	22.55 (17.40 – 27.54)	0.163

Values are given in medians (interquartile ranges). ACO = Acute coronary occlusion.

TABLE E.3: AUCs with corresponding 95% confidence intervals of the single waveform parameters and of the combined models.

Single WFP	AUC [95% CI] (n=102)	WFP+ΔWFP+CCF	AUC [95% CI] (n=60)
AMSA	0.66 [0.55; 0.78]	AMSA	0.73 [0.59; 0.86]
MAA	0.65 [0.53; 0.77]	MAA	0.68 [0.52; 0.83]
MdS	0.66 [0.55; 0.76]	MdS	0.74 [0.60; 0.87]
PSA	0.67 [0.56; 0.78]	PSA	0.70 [0.56; 0.85]
VS	0.67 [0.55; 0.78]	VS	0.70 [0.56; 0.84]
DFAα_1	0.58 [0.44; 0.71]	DFAα_1	0.70 [0.57; 0.84]

The combined models consist of the waveform parameter before the first shock, the change in that parameter between first and second shock, the chest compression fraction (categorical $\geq$ or < 0.6) and an interaction term of ΔWFP*CCF. WFP = Waveform parameter, AUC = Area under the curve, CI = Confidence interval, CCF = Chest compression fraction, AMSA = Amplitude spectrum area, MAA = Mean absolute amplitude, MdS = Median slope, PSA = Power spectrum area, VS = Variance of slope, DFA = Detrended fluctuation analysis.

TABLE E.4: AUCs with 95% CI of combined models (i.e. WFP+ΔWFP+CCF+ ΔWFP*CCF) with EMS response time

Waveform parameter	AUC [95%CI] n=55
Amplitude spectrum area (AMSA)	0.77 [0.64; 0.91]
Mean absolute amplitude (MAA)	0.76 [0.63; 0.90]
Median slope (MdS)	0.83 [0.73; 0.94]
Power spectrum area (PSA)	0.79 [0.68; 0.91]
Variance of slope (VS)	0.74 [0.61; 0.88]
Detrended Fluctuation Analysis (DFA) α_1	0.77 [0.65; 0.89]

AUC = Area under the curve, CI = Confidence interval, WFP = Waveform parameter, CCF = Chest compression fraction, EMS = Emergency medical services.

Bibliography

[1] D. Mozaffarian et al. "Heart disease and stroke statistics–2015 update: a report from the American Heart Association". In: *Circulation* 131.4 (2015), e29–322.

[2] C. Atwood et al. "Incidence of EMS-treated out-of-hospital cardiac arrest in Europe". In: *Resuscitation* 67.1 (2005), pp. 75–80.

[3] J. Berdowski et al. "Global incidences of out-of-hospital cardiac arrest and survival rates: Systematic review of 67 prospective studies". In: *Resuscitation* 81.11 (2010), pp. 1479–87.

[4] M. T. Blom et al. "Improved survival after out-of-hospital cardiac arrest and use of automated external defibrillators". In: *Circulation* 130.21 (2014), pp. 1868–75.

[5] M. R. Daya et al. "Out-of-hospital cardiac arrest survival improving over time: Results from the Resuscitation Outcomes Consortium (ROC)". In: *Resuscitation* 91 (2015), pp. 108–15.

[6] W. D. Weaver et al. "Amplitude of ventricular fibrillation waveform and outcome after cardiac arrest". In: *Ann Intern Med* 102.1 (1985), pp. 53–5.

[7] Daniel R. Martin, Charles G. Brown, and Roger Dzwonczyka. "Frequency analysis of the human and swine electrocardiogram during ventricular fibrillation". In: *Resuscitation* 22.1 (1991), pp. 85–91.

[8] T.E. Auble, J.J. Menegazzi, and P.M. Paris. "Effect of out-of-hospital defibrillation by basic life support providers on cardiac arrest mortality: a meta-analysis". In: *Ann Emerg Med.* 25.5 (1995), pp. 642–48.

[9] G. D. Perkins et al. "European Resuscitation Council Guidelines for Resuscitation 2015: Section 2. Adult basic life support and automated external defibrillation". In: *Resuscitation* 95 (2015), pp. 81–99.

[10] H. Yamaguchi et al. "Myocardial dysfunction after electrical defibrillation". In: *Resuscitation* 54.3 (2002), pp. 289–96.

[11] Ava E. Pierce et al. "The need to resume chest compressions immediately after defibrillation attempts: An analysis of post-shock rhythms and duration of pulselessness following out-of-hospital cardiac arrest". In: *Resuscitation* 89 (2015), pp. 162–68.

[12] Reinier A. Waalewijn et al. "Prevention of deterioration of ventricular fibrillation by basic life support during out-of-hospital cardiac arrest". In: *Resuscitation* 54 (2002), pp. 31–36.

[13] J. Christenson et al. "Chest Compression Fraction Determines Survival in Patients With Out-of-Hospital Ventricular Fibrillation". In: *Circulation* 120.13 (2009), pp. 1241–47.

[14] M. L. Weisfeldt and L. B. Becker. "Resuscitation after cardiac arrest: a 3-phase time-sensitive model". In: *JAMA* 288.23 (2002), pp. 3035–8.

[15] T. Eftestøl et al. "Effects of cardiopulmonary resuscitation on predictors of ventricular fibrillation defibrillation success during out-of-hospital cardiac arrest". In: *Circulation* 110.1 (2004), pp. 10–5.

[16] L. A. Cobb et al. "Influence of cardiopulmonary resuscitation prior to defibrillation in patients with out-of-hospital ventricular fibrillation". In: *JAMA* 281.13 (1999), pp. 1182–8.

[17] L. Wik et al. "Delaying defibrillation to give basic cardiopulmonary resuscitation to patients with out-of-hospital ventricular fibrillation: a randomized trial". In: *JAMA* 289.11 (2003), pp. 1389–95.

[18] T. Eftestøl, K. Sunde, and P. A. Steen. "Effects of interrupting precordial compressions on the calculated probability of defibrillation success during out-of-hospital cardiac arrest". In: *Circulation* 105.1 (2002), pp. 2270–73.

[19] G. Ristagno et al. "Amplitude spectrum area to guide resuscitation-a retrospective analysis during out-of-hospital cardiopulmonary resuscitation in 609 patients with ventricular fibrillation cardiac arrest". In: *Resuscitation* 84.12 (2013), pp. 1697–703.

[20] J. H. Indik et al. "Association of amplitude spectral area of the ventricular fibrillation waveform with survival of out-of-hospital ventricular fibrillation cardiac arrest". In: *J Am Coll Cardiol* 64.13 (2014), pp. 1362–9.

[21] G. Ristagno et al. "Amplitude spectrum area to guide defibrillation: a validation on 1617 patients with ventricular fibrillation". In: *Circulation* 131.5 (2015), pp. 478–87.

[22] A. Scapigliati, G. Ristagno, and F. Cavaliere. "The best timing for defibrillation in shockable cardiac arrest". In: *Minerva Anestesiol* 79.1 (2013), pp. 92–101.

[23] C. Young et al. "Amplitude spectrum area: measuring the probability of successful defibrillation as applied to human data". In: *Crit Care Med* 32.9 Suppl (2004), S356–8.

[24] J. H. Indik et al. "Ventricular fibrillation frequency characteristics are altered in acute myocardial infarction". In: *Crit Care Med* 35.4 (2007), pp. 1133–38.

[25] J. H. Indik et al. "The influence of myocardial substrate on ventricular fibrillation waveform: a swine model of acute and postmyocardial infarction". In: *Crit Care Med* 36.7 (2008), pp. 2136–42.

[26] J. H. Indik et al. "Predictors of resuscitation outcome in a swine model of VF cardiac arrest: A comparison of VF duration, presence of acute myocardial infarction and VF waveform". In: *Resuscitation* 80.12 (2009), pp. 1420–3.

[27] T. M. Olasveengen et al. "Acute ischemic heart disease alters ventricular fibrillation waveform characteristics in out-of hospital cardiac arrest". In: *Resuscitation* 80.4 (2009), pp. 412–7.

[28] J. L. Bonnes et al. "Characteristics of ventricular fibrillation in relation to cardiac aetiology and shock success: A waveform analysis study in ICD-patients". In: *Resuscitation* 86 (2015), pp. 95–9.

[29] J. L. Bonnes et al. "Ventricular fibrillation waveform characteristics differ according to the presence of a previous myocardial infarction: A surface ECG study in ICD-patients". In: *Resuscitation* 96 (2015), pp. 239–45.

[30] G. Ristagno et al. "Outcomes of CPR in the presence of partial occlusion of left anterior descending coronary artery". In: *Resuscitation* 75.2 (2007), pp. 357–65.

[31] Walter F. Boron and Emile L. Boulpaep. *Medical physiology: a cellular and molecular approach*. 2nd. Philadelphia, PA: Saunders/Elsevier, 2009.

[32] Richard E. Klabunde. *Cardiovascular physiology concepts.* 2nd. Philadelphia, PA: Lippincot Williams & Wilkins / Wolters Kluwer, 2012, 243 p.

[33] Children's Health Stanford. *Blood Circulation in the Fetus and Newborn*. Website. [cited 19 October 2017]. URL: http://www.stanfordchildrens.org/en/topic/default?id=blood-circulation-in-the-fetus-and-newborn-90-P02362.

[34] A. M. R. Agur and Arthur F. Dalley. *Grant's atlas of anatomy*. 12th. Philadelphia: Wolters Kluwer Health/Lippincott Williams & Wilkins, 2009, xvi, 864 p.

[35] Richard N. Fogoros. *Electrophysiologic testing*. 5th. Chichester, West Sussex, UK: Wiley-Blackwell, 2009, 304 p.

[36] E. Robles de Medina, N.M. van Hemel, and A.A.M. Wilde. *Klinische electrocardiografie*. 4th. Houten, Netherlands: Bohn Stafleu van Loghum, 2000, 280 p.

[37] Dale Dubin. *Rapid interpretation of EKG's : an interactive course*. 6th. Tampa, Fla.: Cover Pub. Co., 2000, x, 368 p.

[38] Keith L. Moore, Arthur F. Dalley, and A. M. R. Agur. *Clinically oriented anatomy*. 6th. Philadelphia: Wolters Kluwer/Lippincott Williams & Wilkins, 2010, xxix, 1134 p.

[39] John Sandham. *Electrical signals of the heart*. Website. [cited 24 October 2017]. URL: http://www.ebme.co.uk/articles/clinical-engineering/1081-electrical-signals-of-the-heart.

[40] Greg Ikonnikov and Dominique Yelle. *Physiology of cardiac conduction and contractility*. Website. [cited 25 October 2017]. URL: http://www.pathophys.org/physiology-of-cardiac-conduction-and-contractility/.

[41] K. Thygesen on behalf of the Joint ESC/ACCF/AHA/WHF Task Force. "Third Universal Definition of Myocardial Infarction". In: *Circulation* 126.16 (2012), pp. 2020–35.

[42] H.M. Bolooki and A. Askari. *Acute myocardial infarction*. Website. 2010. [cited 17 October 2017]. URL: http://www.clevelandclinicmeded.com/medicalpubs/diseasemanagement/cardiology/acute-myocardial-infarction/.

[43] L.H. Arroyo and R.T. Lee. "Mechanisms of plaque rupture: mechanical and biologic interactions". In: *Cardiovasc Res.* 41.2 (1999), pp. 369–75.

[44] P.K. Shah. "Mechanisms of plaque vulnerability and rupture". In: *J Am Coll Cardiol* 41.4 Supplement (2003), 15s–22s.

[45] R. Virmani et al. "Lessons from sudden coronary death: a comprehensive morphological classification scheme for atherosclerotic lesions". In: *Arterioscler Thromb Vasc Biol.* 20.5 (2000), pp. 1262–75.

[46] P.T. O'Gara et al. "2013 ACCF/AHA guideline for the management of ST-elevation myocardial infarction: a report of the American College of Cardiology Foundation / American Heart Association Task Force on Practice Guidelines." In: *Circulation* 127.4 (2013), pp. 362–425.

[47] Douglas L. Mann et al. *Braunwald's heart disease: a textbook of cardiovascular medicine*. 9th. Philadelphia, PA: Elsevier/Saunders, 2011, 2048 p.

[48] Faramarz H. Samie and José Jalife. "Mechanisms underlying ventricular tachycardia and its transition to ventricular fibrillation in the structurally normal heart". In: *Cardiovascular research* 50.2 (2001), pp. 242–50.

[49] D.J. Rebergen. "Identification of a Previous Myocardial Infarction During Ventricular Fibrillation: a Machine Learning Based Approach Using the 12-Lead Electrocardiogram". Graduation thesis Technical Medicine. University of Twente, 2017.

[50] José Jalife. "Mechanisms underlying ventricular tachycardia and its transition to ventricular fibrillation in the structurally normal heart". In: *Cardiovascular research* 50.2 (2001), pp. 242–50.

[51] Paul B. Tabereaux, Derek J. Dosdall, and Raymond E. Ideker. "Mechanisms of VF maintenance: Wandering wavelets, mother rotors, or foci". In: *Heart Rhythm* 6.3 (2009), pp. 405–15.

[52] Sandeep V. Pandit and José Jalife. "Rotors and the Dynamics of Cardiac Fibrillation". In: *Circulation Research* 112.5 (2013), pp. 849–62.

[53] José Jalife. "Rotors And Turbulence In Ventricular Fibrillation - Role Of Inward Rectifier Potassium Channels". In: *US Cardiovascular Disease* 4.2 (2007), pp. 85–88.

[54] Martyn P. Nash et al. "Evidence for Multiple Mechanisms in Human Ventricular Fibrillation". In: *Circulation* 114.6 (2006), pp. 536–42.

[55] K. Nanthakumar et al. "Epicardial organization of human ventricular fibrillation". In: *Heart Rhythm* 1.1 (2004), pp. 14–23.

[56] Alan Garfinkel et al. "Preventing ventricular fibrillation by flattening cardiac restitution". In: *PNAS* 97.11 (2000), pp. 6061–66.

[57] F. Dumas et al. "Immediate percutaneous coronary intervention is associated with better survival after out-of-hospital cardiac arrest: insights from the PROCAT (Parisian Region Out of hospital Cardiac ArresT) registry". In: *Circ cardiovasc interv* 3.3 (2010), pp. 200–07.

[58] M.J. Davies. "Anatomic features in victims of sudden coronary death: Coronary artery pathology". In: *Circulation* 85.1 (1992), pp. 19–24.

[59] Nazar Luqman et al. "Myocardial ischemia and ventricular fibrillation: Pathophysiology and clinical implications". In: *Int J Card* (2007), pp. 283–90.

[60] I. Jacobs et al. "Cardiac arrest and cardiopulmonary resuscitation outcome reports: update and simplification of the Utstein templates for resuscitation registries: a statement for healthcare professionals from a task force of the International Liaison Committee on Resuscitation (American Heart Association, European Resuscitation Council, Australian Resuscitation Council, New Zealand Resuscitation Council, Heart and Stroke Foundation of Canada, InterAmerican Heart Foundation, Resuscitation Councils of Southern Africa)". In: *Circulation* 110.21 (2004), pp. 3385–97.

[61] Graham Nichol et al. "Defibrillation for ventricular fibrillation: a shocking update". In: *JACC* 70.12 (2017), pp. 1496–1509.

[62] I. Hasselqvist-Ax et al. "Early cardiopulmonary resuscitation in out-of-hospital cardiac arrest". In: *N Engl J Med* 372.24 (2015), pp. 2307–15.

[63] A. Neurauter et al. “Estimation of the duration of ventricular fibrillation using ECG single feature analysis”. In: *Resuscitation* 73.2 (2007), pp. 246–52.
[64] M. He et al. “Prediction of Defibrillation Outcome by Ventricular Fibrillation Waveform Analysis: A Clinical Review”. In: *J Clinic Experiment Cardiol* 810.9 (2013), pp. 1–8.
[65] A. Neurauter et al. “Prediction of countershock success using single features from multiple ventricular fibrillation frequency bands and feature combinations using neural networks”. In: *Resuscitation* 73.2 (2007), pp. 253–63.
[66] H. U. Strohmenger, K. H. Lindner, and C. G. Brown. “Analysis of the ventricular fibrillation ECG signal amplitude and frequency parameters as predictors of countershock success in humans”. In: *Chest* 111.3 (1997), pp. 584–9.
[67] C. G. Brown and R. Dzwonczyk. “Signal analysis of the human electrocardiogram during ventricular fibrillation: frequency and amplitude parameters as predictors of successful countershock”. In: *Ann Emerg Med* 27.2 (1996), pp. 184–8.
[68] D. D. Salcido et al. “Association of intramyocardial high energy phosphate concentrations with quantitative measures of the ventricular fibrillation electrocardiogram waveform”. In: *Resuscitation* 80.8 (2009), pp. 946–50.
[69] H. P. Povoas et al. “Predicting the success of defibrillation by electrocardiographic analysis”. In: *Resuscitation* 53.1 (2002), pp. 77–82.
[70] M. He et al. “Combining Amplitude Spectrum Area with Previous Shock Information Using Neural Networks Improves Prediction Performance of Defibrillation Outcome for Subsequent Shocks in Out-Of-Hospital Cardiac Arrest Patients”. In: *PLoS One* 11.2 (2016), e0149115.
[71] P. Schoene et al. “Course of quantitative ventricular fibrillation waveform measure and outcome following out-of-hospital cardiac arrest”. In: *Heart Rhythm* 11.2 (2014), pp. 230–6.
[72] J.P. Freese et al. “Waveform analysis-guided treatment versus a standard shock-first protocol for the treatment of out-of-hospital cardiac arrest presenting in ventricular fibrillation: results of an international randomized, controlled trial”. In: *Circulation* 128.9 (2013), pp. 995–1002.
[73] J. H. Indik et al. “Ventricular fibrillation waveform characteristics are different in ischemic heart failure compared with structurally normal hearts”. In: *Resuscitation* 69.3 (2006), pp. 471–7.
[74] A. Marn-Pernat et al. “Optimizing timing of ventricular defibrillation”. In: *Crit Care Med.* 29.12 (2001), pp. 2360–65.
[75] M. J. Reed, G. R. Clegg, and C. E. Robertson. “Analysing the ventricular fibrillation waveform”. In: *Resuscitation* 57.1 (2003), pp. 11–20.
[76] L. D. Sherman. “The frequency ratio: an improved method to estimate ventricular fibrillation duration based on Fourier analysis of the waveform”. In: *Resuscitation* 69.3 (2006), pp. 479–86.
[77] H. M. Hastings et al. “Nonlinear dynamics in ventricular fibrillation”. In: *Proc Natl Acad Sci U S A* 93.19 (1996), pp. 10495–9.
[78] L. Y. Lin et al. “Detrended fluctuation analysis predicts successful defibrillation for out-of-hospital ventricular fibrillation cardiac arrest”. In: *Resuscitation* 81.3 (2010), pp. 297–301.
[79] Clifton W. Callaway et al. “Scaling Exponent Predicts Defibrillation Success for Out-of-Hospital Ventricular Fibrillation Cardiac Arrest”. In: *Circulation* 103 (2001), pp. 1656–61.
[80] C. K. Peng et al. “Quantification of scaling exponents and crossover phenomena in nonstationary heartbeat time series”. In: *Chaos* 5.1 (1995), pp. 82–7.
[81] K. Umapathy et al. “Optimizing cardiac resuscitation outcomes using wavelet analysis”. In: *Conf Proc IEEE Eng Med Biol Soc* 2009 (2009), pp. 6761–4.
[82] T. D. Rea et al. “Incidence of EMS-treated out-of-hospital cardiac arrest in the United States”. In: *Resuscitation* 63.1 (2004), pp. 17–24.
[83] J. H. Indik et al. “Amplitude-spectral area and chest compression release velocity independently predict hospital discharge and good neurological outcome in ventricular fibrillation out-of-hospital cardiac arrest”. In: *Resuscitation* 92 (2015), pp. 122–8.

[84] M. Callaham et al. "Prehospital cardiac arrest treated by urban first-responders: profile of patient response and prediction of outcome by ventricular fibrillation waveform". In: *Ann Emerg Med* 22.11 (1993), pp. 1664–77.

[85] Y. Nakagawa et al. "Novel CPR system that predicts return of spontaneous circulation from amplitude spectral area before electric shock in ventricular fibrillation". In: *Resuscitation* 113 (2017), pp. 8–12.

[86] C.M. Spaulding et al. "Immediate coronary angiography in survivors of out-of-hospital cardiac arrest". In: *N Engl J Med* 336.23 (1997), pp. 1629–33.

[87] K. Umapathy et al. "Real-time electrogram analysis for monitoring coronary blood flow during human ventricular fibrillation: implications for CPR". In: *Heart Rhythm* 8.5 (2011), pp. 740–9.

[88] F. H. Foomany et al. "Wavelet-based markers of ventricular fibrillation in optimizing human cardiac resuscitation". In: *Conf Proc IEEE Eng Med Biol Soc* 2010 (2010), pp. 2001–4.

[89] Anthony J. Handley, Koenraad G. Monsieurs, and Leo L. Bossaert. "European Resuscitation Council Guidelines 2000 for Adult Basic Life Support: A statement from the Basic Life Support and Automated External Defibrillation Working Group". In: *Resuscitation* 48.3 (2001), pp. 199–205.

[90] B.S. Abella et al. "Quality of cardiopulmonary resuscitation during in-hospital cardiac arrest". In: *JAMA* 293.3 (2005), pp. 305–310.

[91] Jo Kramer-Johansen et al. "Uniform reporting of measured quality of cardiopulmonary resuscitation". In: *Rescuscitation* 74 (2007), pp. 406–17.

[92] L. Wik et al. "Quality of cardiopulmonary resuscitation during out-of-hospital cardiac arrest". In: *JAMA* 293.3 (2005), pp. 299–304.

[93] C. Vaillancourt et al. "The impact of increased chest compression fraction on return of spontaneous circulation for out-of-hospital cardiac arrest patients not in ventricular fibrillation." In: *Resuscitation* 82.12 (2011), pp. 1501–07.

[94] J. Kolarova et al. "Optimal timing for electrical defibrillation after prolonged untreated ventricular fibrillation". In: *Crit Care Med* 31.7 (2003), pp. 2022–28.

[95] U. Achleitner et al. "The beneficial effect of basic life support on ventricular fibrillation mean frequency and coronary perfusion pressure". In: *Resuscitation* 51.2 (2001), pp. 151–58.

[96] R. A. Berg et al. "Precountershock cardiopulmonary resuscitation improves ventricular fibrillation median frequency and myocardial readiness for successful defibrillation from prolonged ventricular fibrillation: a randomized, controlled swine study". In: *Ann Emerg Med* 40.6 (2002), pp. 563–70.

[97] R. A. Berg et al. "Precountershock cardiopulmonary resuscitation improves initial response to defibrillation from prolonged ventricular fibrillation: A randomized, controlled swine study". In: *Crit care Med* 32.6 (2004), pp. 1352–57.

[98] Y. Li et al. "Electrocardiogram waveforms for monitoring effectiveness of chest compression during cardiopulmonary resuscitation". In: *Crit Care Med* 36.1 (2008), pp. 211–15.

[99] E. Alonso et al. "Can thoracic impedance monitor the depth of chest compressions during out-of-hospital cardiopulmonary resuscitation?" In: *Resuscitation* 85.5 (2014), pp. 637–43.

[100] M.S. Box et al. "Shock outcome prediction before and after CPR: a comparative study of manual and automated active compression-decompression CPR". In: *Resuscitation* 78.3 (2008), pp. 265–74.

[101] J. H. Indik et al. "Utility of the ventricular fibrillation waveform to predict a return of spontaneous circulation and distinguish acute from post myocardial infarction or normal Swine in ventricular fibrillation cardiac arrest". In: *Circ Arrhythm Electrophysiol* 4.3 (2011), pp. 337–43.

[102] D. Hidano et al. "Ventricular fibrillation waveform measures and the etiology of cardiac arrest." In: *Resuscitation* 109 (2016), pp. 71–75.

[103] D.D. Salcido et al. "Quantitative Waveform Measures of the Electrocardiogram as Continuous Physiologic Feedback During Resuscitation with Cardiopulmonary Bypass". In: *Resuscitation* 83.4 (2012), pp. 505–10.

[104] J. H. Indik et al. "Predictors of resuscitation in a swine model of ischemic and non-ischemic ventricular fibrillation cardiac arrest: superiority of amplitude spectral area and slope to predict a return of spontaneous circulation when resuscitation efforts are prolonged". In: *Crit Care Med* 38.12 (2010), pp. 2352–7.

[105] Michiel Hulleman et al. "Predictive value of amplitude spectrum area of ventricular fibrillation waveform in patients with acute or previous myocardial infarction in out-of-hospital cardiac arrest". In: *Resuscitation* 120.Supplement C (2017), pp. 125–131.

[106] B.J. Bobrow and K.B. Kern. "Regionalization of postcardiac arrest care". In: *Curr Opin Crit Care* 15.3 (2009), pp. 221–27.

[107] Alf Inge Larsen et al. "Cardiac arrest with continuous mechanical chest compression during percutaneous coronary intervention: A report on the use of the LUCAS device". In: *Resuscitation* 75.3 (2007), pp. 454–59.

[108] Henrik Stær-Jensen et al. "Post-Resuscitation ECG for Selection of Patients for Immediate Coronary Angiography in Out-of-Hospital Cardiac Arrest". In: *Circ cardiovasc interv* 8.10 (2015).

[109] NIST/SEMATECH. *e-Handbook of Statistical Methods*. Electronic Book. Aug. 2017. URL: `http://www.itl.nist.gov/div898/handbook/`.

[110] G. Meinsma, C. Heida, and M. van Putten. "Advanced Techniques for Signal Analysis". Course book. University of Twente, 2016.

[111] B. Boashash. "Estimating and interpreting the instantaneous frequency of a signal". In: *Proceedings of the IEEE* 80.4 (1992).

[112] P. Singh et al. "The Fourier decomposition method for nonlinear and non-stationary time series analysis". In: *Proc Math Phys Eng Sci* 473.2199 (2017).

[113] H. Endoh et al. "Prompt prediction of successful defibrillation from 1-s ventricular fibrillation waveform in patients with out-of-hospital sudden cardiac arrest". In: *J Anesth* 25.1 (2011), pp. 34–41.

[114] M. Hall et al. "Myocardial substrate in secondary ventricular fibrillation: insights from quantitative waveform measures". In: *Prehosp Emerg Care* 15.3 (2011), pp. 388–92.

[115] J. H. Indik et al. "Direction of signal recording affects waveform characteristics of ventricular fibrillation in humans undergoing defibrillation testing during ICD implantation". In: *Resuscitation* 78.1 (2008), pp. 38–45.